AZOBENZENE-FUNCTIONALIZED MOLECULAR GLASSES FOR HOLOGRAPHIC APPLICATIONS

DISSERTATION

zur Erlangung des akademischen Grades eines
Doktors der Naturwissenschaften (Dr. rer. nat.) im Fach Chemie
der Fakultät für Biologie, Chemie und Geowissenschaften der
Universität Bayreuth

vorgelegt von

Roland Walker

geboren in Illertissen

Bayreuth, 2010

Die vorliegende Arbeit wurde in der Zeit von Dezember 2006 bis Mai 2010 am Lehrstuhl Makromolekulare Chemie I der Universität Bayreuth unter der Betreuung von Herrn Prof. Dr. Hans-Werner Schmidt angefertigt.

Vollständiger Abdruck der von der Fakultät für Biologie, Chemie und Geowissenschaften der Universität Bayreuth genehmigten Dissertation zur Erlangung des akademischen Grades Doktor der Naturwissenschaften (Dr. rer. nat.).

Amtierender Dekan:	Prof. Dr. Stephan Clemens
Tag des Einreichens der Dissertation:	17. September 2010
Tag des wissenschaftlichen Kolloquiums:	07. Dezember 2010

Prüfungsausschuß:

Prof. Dr. Hans-Werner Schmidt	(Erstgutachter)
Prof. Dr. Axel H. E. Müller	(Zweitgutachter)
Prof. Dr. Andreas Fery	(Vorsitzender)
Prof. Dr. Lothar Kador	

„Die haben viel gemacht, die letzten Jahre!“

Würdigung des Alumnivereins
der Chemie CSG e. V.,
Die Chemiker Spass Gesellschaft
(Orginalzitat übernommen
von Dr. Marc Claudius Schrinner)

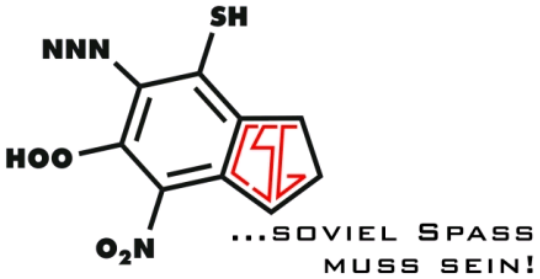

Abbreviations and symbols

45°	electric field vector at an angle of 45° to the plane of incidence
AFM	atomic force microscopy
BS	beam splitter
CCD	charge-coupled device
CD	compact disc
CD-R	CD-recordable
CD-RW	CD-rewritable
d	doublet
dd	doublet of a doublet
d_0	thickness of the film
Δd	maximum SRG height
DMF	N,N-dimethylformamide
DSC	differential scanning calorimetry
DVD	digital versatile disc
δ	chemical shift in ppm
$\vec{E}$	electric field vector of the incident light
f	gradient force
GPC	gel permeation chromatography
GPM	general preparation method
h	Plank constant
HOE	holographic optical element
I	intensity
I_1	intensity of the first order diffracted beam
I_0	intensity of the transmitted beam before writing a hologram
J	coupling constant in Hz
J_1	Bessel function of 1st kind and 1st order
k	absorption coefficient
k_b	Boltzmann constant
λ	wavelength of laser beam
lcp	left circular polarized light
m	multiplet
M	molar
M_n	number average molecular weight
M_w	weight average molecular weight
η	diffraction efficiency
n	refractive index of the sample
n.d.	not detected
n_1	refractive index modulation

$n_{1,\,max}$	maximum refractive index modulation
Δn	amplitude of the refractive index change between sample and air
NMR	nuclear magnetic resonance
ν	frequency
OD	optical density
p	electric field vector parallel to the plane of incidence
P	polarizer
P	polarization induced by the electric light field
PDI	polydispersity index
PDMS	poly(dimethyl)siloxane
POLMIC	polarizing light microscopy
PS	polystyrene
rcp	right circular polarized light
ROM	read-only memory
RT	room temperature
s	electric field vector perpendicular to the plane of incidence
s	singulet
S	sensitivity
S_{max}	maximum sensitivity
SRG	surface relief grating
τ_1	time constants of the build-up of the volume grating
τ_2	time constants of the build-up of the surface relief grating
t_{max}	writing time to the maximum of n_1
t	triplet
T	temperature
T_g	glass transition temperature
T_m	melting point
T_{cryst}	crystallization temperature
TGA	thermogravimetric analysis
THF	tetrahydrofuran
UV/Vis	ultraviolet/visible
WORM	write-once read-many
θ	angle of incidence of the laser beam
$\Delta\varphi$	phase difference between volume and surface relief grating
χ	electrical susceptibility

TABLE OF CONTENTS

SUMMARY

Holography is an optical imaging technique, with which an authentic copy of the original object can be created, even in the absence of the object itself. This means, that in contrast to conventional photography, the information of depth is not lost. Holography is based on writing an interference grating in a photosensitive volume element. Hereby two light sources are generating an interference pattern, which causes chemical or physical changes in the photosensitive material. By illumination of the stored diffraction grating, the original information can be reconstructed. One of the most important classes of photoaddressable chromophores utilized in holography are azobenzene compounds. Owing to the rich photochemistry of these chromophores, materials incorporating azobenzenes can be used as photoswitches, allowing fast and reversible control over the chemical, physical or optical properties of the entire system. Therefore, azobenzene-containing compounds are envisioned as smart light-responsive materials for various holographic applications.

This thesis describes the synthesis and characterization of azobenzene-containing molecular glasses as well as their application as functional materials in specific holographic experiments. By utilizing a modular design principle, we were able to fine-tune their physical and photo-physical properties and optimize the molecular structure in view of the formation of *surface relief nanostructures* as well as inscription of *holographic volume gratings*.

Understanding the formation of *surface relief nanostructures* and discovering ways of controlling the process is of importance, as uniform surface relief gratings (SRGs) with adjustable spacing and amplitude are of interest. Therefore a new series of azobenzene-containing molecular glasses based on a triphenylamine core has been synthesized and photo-physically characterized. A clear relationship between the chemical structure of these molecules and SRG build-up was established: the rate of formation and the maximal achievable amplitude of SRGs strongly depend on the optical susceptibility at the wavelength of the writing laser. Furthermore, we found that different polarizations of the laser beams also have a major influence. With this knowledge we were able to efficiently form SRGs with amplitude heights of up to 600 nm by tailoring the molecular structure of the material and selecting

specific experimental conditions. Furthermore, it has been demonstrated that these surface patterns are stable enough to be transferred to a polymer surface with replica molding techniques. This concept has the potential to be practically applied for holographic optical elements.

Holography is a most promising solution for optical data storage, as in contrast to conventional optical storage media, the entire volume of the medium is used instead of only a few thin layers. Unfortunately, current rewritable materials still exhibit certain challenges, most important, sufficiently fast writing times. Therefore, material concepts especially for improving the recording time as well as the long-term stability of *holographic volume gratings* are presented. By employing azobenzene-containing molecular glasses in blends with photoaddressable polymers, we were able to merge the excellent long-term stability of the polymer systems with the higher photo-physical sensitivity of the molecular glasses, thus creating a superior holographic material which combines the advantages of both material classes. In order to find a suitable blending material, we synthesized series of photochromic azobenzene-containing molecular glasses and screened them with respect to their photo-physical properties. The best combination of structural variations was chosen for the blending experiments. Already a blend comprising as less as ten wt% of molecular glass allowed us to decrease the holographic writing time of a photoaddressable block copolymer system by a factor of three while increasing the recording sensitivity by the factor five.

In addition to molecular glasses with ordinary azobenzene chromophores we also examined low molecular weight materials functionalized with bisazobenzene moieties. This enabled us to achieve higher maximum refractive index modulations. Liquid-crystalline behaviour could be introduced with the incorporation of substituents at the bisazobenzene moiety. Subsequent investigations of the photo-physical properties revealed a long-term stable photo-orientation solely based on small molecular compounds, making such materials an interesting alternative to established systems.

In summary, this thesis demonstrates that azobenzene-containing molecular glasses are a worthwile focus for research, as they are an amazingly versatile and adaptable class of materials suitable for a large number of different applications.

ZUSAMMENFASSUNG

Holographie ist eine optische Abbildungstechnik, mit der eine authentische Kopie eines Objekts erschaffen werden kann, sogar in der Abwesenheit des Orginals. Dies bedeuted, dass im Gegensatz zur konventionellen Photographie, die Tiefeninformation nicht verloren geht. Holographie basiert auf dem Einschreiben eines Interferenzsgitters in ein photosensitives Volumenelement. Hierbei generieren zwei Lichtquellen ein Interferenzmuster, welches chemische oder physikalische Veränderungen im photosensitiven Material verursacht. Durch Beleuchtung des gespeicherten Gitters kann die ursprüngliche Information rekonstuiert werden. Eine der wichtigsten Klassen von photoaddressierbaren Chromophoren, welche in der Holographie benutzt werden, sind Azobenzoleinheiten. Aufgrund der ergiebigen Photochemie dieser Chromophore können Materialen welche Azoeinheiten enthalten, als effektive Photoschalter verwendet werden. Dies erlaubt eine schnelle und reversible lichtinduzierte Kontrolle über die chemischen, physikalischen oder optischen Eigenschaften des Gesamtsystems. Deshalb werden azobenzolhaltige molekulare Gläser potentiell als intelligente und photoschaltbare Materialen für eine Vielzahl von holographischen Anwendungen angesehen.

Diese Arbeit beschreibt die erfolgreiche Synthese und Charakterisierung von azobenzolhaltigen molekularen Gläsern sowie ihre Anwendung als Funktionsmaterialien in bestimmten holographischen Experimenten. Mit Hilfe eines Baukastensystems ist es uns möglich ihre physikalischen und photo-physikalischen Eigenschaften genau einzustellen und ihre Molekülstruktur im Hinblick auf die Bildung von *Oberflächennanostrukturen* sowie *holographische Volumengittern* zu optimieren.

Die Entstehung dieser *Oberflächennanostrukturen* zu verstehen und Wege zu finden diesen Prozess zu kontrollieren, ist von grosser Wichtigkeit, da einheitliche Oberflächengitter (SRGs) mit einstellbaren Intervallen und Amplituden von Interesse sind. Deshalb wurde eine neue Serie von azobenzolhaltigen molekularen Gläsern, basierend auf einem Triphenylamin-Kern, synthetisiert und photo-physikalisch charakterisiert. Ein klarer

Zusammenhang zwischen der chemischen Struktur dieser Moleküle und des SRG-Aufbaus wurde hergestellt: die Bildungsgeschwindigkeit und die maximal erreichbare Amplitudenhöhe des SRGs sind stark von der optischen Suszeptibilität bei der Wellenlänge des Schreiblasers abhängig. Weiterhin haben wir gefunden, dass verschiedene Polarisationen der Laserstrahlen ebenfalls einen grossen Einfluss ausüben. Mit diesem Wissen konnten wir, durch massschneidern der Molekülstruktur des Materials und durch das Auswählen von spezifischen experimentellen Bedingungen, SRGs mit Amplitudenhöhen von bis 600 nm effizient ausbilden. Weiterhin wurde demonstriert, dass diese Oberflächenmuster stabil genug sind, um sie mit Hilfe von Replika-Techniken auf eine Polymeroberfläche zu transferieren. Dieses Konzept hat das Potential, für holographische, optische Elemente, in der Praxis eingesetzt zu werden.

Die Holographie ist eine der am vielversprechensten Lösungen für die optische Datenspeicherung. Im Gegensatz zu konventionellen optischen Datenspeichern, wird hier das gesamte Volumen des Mediums ausgenutzt, anstatt nur wenige dünne Schichten. Unglücklicherweise weisen aktuelle wiederbeschreibbare Materialen noch immer Herrausforderungen auf. Die Entscheidenste ist eine ausreichend schnelle Schreibzeit zu erreichen. Aus diesem Grund, werden hier Materialkonzepte speziell für die Verbesserung der holographischen Schreibzeit sowie der Langzeitstabilität von *holographischen Volumengittern* präsentiert. Indem man azobenzolhaltige molekulare Gläser in Blends mit photoaddressierbaren Polymeren einsetzt, ist es uns möglich die exzellente Langzeitstabilität von Polymersystemen mit der höheren photo-physikalischen Sensitivität der molekularen Gläser zu verbinden. Damit schaffen wir ein optimiertes photoaddressierbares Material, dass die Vorteile beider Materialklassen kombiniert. Um ein geeignetes Blendmaterial zu finden, haben wir Serien von photochromen azobenzolhaltigen molekularen Gläsern synthetisiert und im Bezug auf ihre photo-physikalischen Eigenschaften überprüft. Die beste Kombination an strukturellen Variationen wurde für die Blend-Experimente ausgewählt. Schon ein Blend mit einem Anteil von gerade einmal zehn Gewichtsprozent von molekularem Glas, erlaubte es uns, die holographische Schreibzeit eines photoaddressierbaren Blockcopolymers um

den Faktor drei zu vergrössern und gleichzeitig die Sensitivität des Einschreibprozesses um den Faktor fünf zu erhöhen.

Zusätzlich zu molekularen Gläsern mit gewöhnlichen Azobenzol-chromophoren, haben wir auch niedermolekulare, mit Bisazobenzoleinheiten funktionalisierte Materialien untersucht. Dies ermöglichte es uns eine höhere maximal erreichbare Brechungsindexmodulation zu erhalten. Flüssigkristallines Verhalten konnte durch die Einführung von Substituenten an der Bisazobenzoleinheit induziert werden. Darauffolgende Untersuchungen der photo-physikalischen Eigenschaften haben eine stabile Photoorientierung erkennen lassen, welche nur auf niedermolekularen Verbindungen basiert. Dies macht solche Materialien zu einer interessanten Alternative für bereits etablierten Systeme.

Zusammenfassend demonstriert diese Doktorarbeit, dass azobenzolhaltige molekulare Gläser ein lohnenswerter Forschungsschwerpunkt sind, da sie eine erstaunlich vielseitige und anpassungsfähige Materialklasse darstellen, welche für eine grosse Anzahl verschiedener Anwendungen geeignet ist.

INTRODUCTION

In the past decades, the developments in computer technology have continiously improved. This progress resulted in the so-called Information Age which is characterized by the ability of individuals to transfer information freely, and to have instant access to knowledge.[1] The term Information Age is often related to cell phones, digital music, high definition television, digital cameras, the Internet, and other items that have come into common use in the past 30 years. As a consequence of these recent advances, especially in the entertainment sector, the need for data storage media with steadily increasing transfer rates and capacities has arisen. Hence, the search for new storage techniques and materials is an urgent issue.

1.1 Data storage media

Mostly, current state of the art data storage is segmenting into optical and magnetic data storage as well as transistor-based storage media. Magnetic storage devices primarily consist of *hard drives*. Concerning transistor-based systems, *solid-state drives* like USB flash sticks have become increasingly popular in the last years. Commercially available optical media are *compact discs (CDs)*, *digital versatile discs (DVDs)*, and, recently introduced, the *blu-ray disc*.

Magnetic hard drives are the most commonly utilized storage medium in modern computers. A typical magnetic hard drive is organized in several flat circular disks, called platters. These platters are usually made of aluminium or glass with a thin layer of ferromagnetic material like ferric oxide or cobalt-nickel alloys. The platters are rotated and the information is stored electromagnetically as it is passed by the so-called read-and-write head (see Figure 1). The recording is conducted by magnetizing the ferromagnetic material in different directions to represent either a 0 or a 1 binary digit. Reading the data is performed by detecting the magnetization direction of the material.

However, the rapid growth of the bit density of the magnetic storage devices might soon reach a physical limit, due to the so-called *superparamagnetic effect*.[2,3] If the storage density is progressing beyond the

limit of this effect, the magnetic domains in conventional recording media will be so small that they become unstable due to thermal fluctuations. Some approaches have been discussed, how to delay reaching this limit.[4,5]

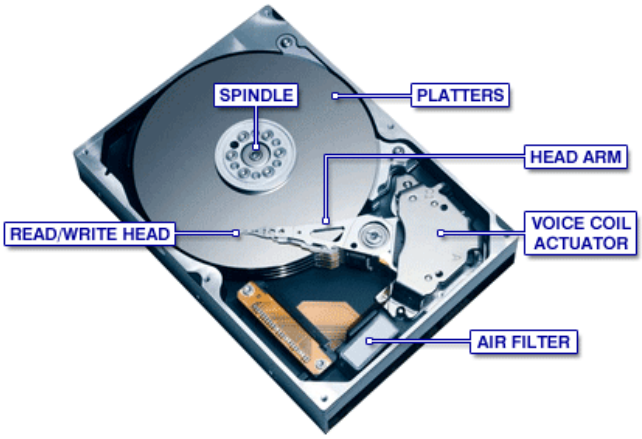

Figure 1: Schematic of a commercially available magnetic harddrive with highlighting of the most important parts.[6]

Solid state drives (SSDs), commonly known for their application in USB flash sticks and flash memory cards, are a new generation electronic storage medium using semiconductor technology. Compared to magnetic hard drives, solid-state drives have no moving parts, so they are less fragile as well as silent. Additionally, as there are no mechanical delays, they usually exhibit a very low access time. However, there are also drawbacks to SSDs. The cost per gigabyte of flash memory remains significantly higher than in common hard drives. Another limitation is the finite number of erase-write cycles accompanied by degradation of the performance of SSDs with continued use.

Typically a solid state drive stores data in an array of memory cells made from floating-gate transistors (see Figure 2). These transistors resemble standard field effect transistors, except that the transistor has two gates instead of one. A so-called floating gate is hereby interposed between the control gate and the field effect transistor channel. This floating gate is electrically isolated, consequently, trapping any charge applied to it. The charge partially screens the electric field from the control gate and thereby modifies the threshold voltage of the cell. During read-out, a certain voltage is applied to the control gate. The field effect transistor will become conducting or remain insulating,

depending on the threshold voltage of the cell. The detected resulting current forms the binary code, reproducing the stored data. So-called multi-level cell devices, can even store more than one bit per cell by choosing between multiple levels of electrical charge applied to the floating gates of its cells.[7]

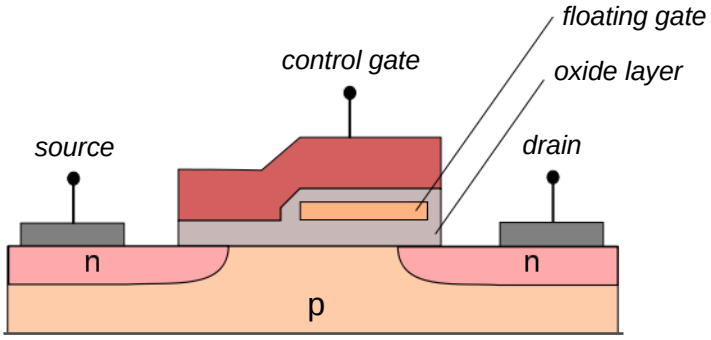

Figure 2: Schematic layout of a floating gate transistor. n and p denote the electron transport material and the hole transport material respectively. An oxide layer separates the control and the floating gate from each other.[8]

Compact discs are optical storage media in which writing and reading are performed by a laser beam. In contrast to magnetic hard drives or solid state drives, these media are very inexpensive to manufacture. In addition they can be easily interchanged or removed. For a long time they remained the standard physical storage medium, only slowly replaced in the past decade by their successor, the DVD. CDs consist of a circular piece of polycarbonate which can be rapidly reproduced by injection moulding. After the injection moulding process, the discs are sputtered with a thin reflective layer of aluminium covering the embossed structures. Additionally an acrylic lacquer is deposited on the discs by spin-coating and afterwards cured under UV light. These discs feature tiny cavities, so-called “pits”, which spiral in a single continuous track from the inside of the disc to the outside. For reading a near-infrared 780 nm laser diode is directed onto the spinning disc via an opto-electronic tracking module. The change in height due to the pits results in a difference of the intensity of the reflected light. This intensity change can be converted into the originally inscribed data.

CD-recordable (CD-R) and CD-rewritable (CD-RW) discs allow users to personally record data. The write-once media commonly have an organic dye

(e.g. phthalocyanines) embedded in a polycarbonate matrix. Upon irradiation with a laser, these dyes change their absorption spectrum irreversibly and reflect less light than areas that have not been illuminated by the laser diode. CD-RWs typically contain a recording layer composed of a phase change material, mostly an alloy of silver, indium, antimony and tellurium. The crystalline phase of this layer can be changed repeatedly to an amorphous phase and back by heating with the employed laser. The crystalline areas reflect the laser light while the amorphous areas absorb the incident light.[7]

Digital versatile discs are an optical storage medium similar to the CD, featuring the same media dimensions. They are made using mostly the same materials and manufacturing methods. A DVD is commonly composed of two layers. These are seperatly processed by injection moulding of polycarbonate. Afterwards a laquer coating, a merging and a curing step are performed. Like a CD, the data on a DVD is encoded in the form of pits in the disc, which are arranged as a single, continuous spiral track of data. For double-layer DVDs, the second (inner) layer is accessed by focusing the laser through the first semitransparent layer onto the inner data track. As opposed to 780 nm lasers for the CD technology, 650 nm wavelength lasers are employed for DVDs. Therefore, much smaller structures can be utilized to store information, in turn leading to a bigger storage capacity (about six times for a single-sided, single layer DVD). By employing multiple layers and sides, the storage capacity can be further increased.[7]

Blu-ray discs have become a rapidly growing storage medium with the spreading of high-definition audio and video. The advantage of a blu-ray disc is its high storage capacity. Unlike current DVDs, blu-ray technology uses a blue-violet laser at a shorter wavelength (405 nm). By employing further technical improvements like a larger numerical aperture of the focussing lens as well as a thinner cover layer, the laser beam can be focused to a smaller spot, enabling it to read information recorded in pits more than twice as small as the pits on a DVD (see Figure 3).[9] A single-layer disc can store up to 25 GB of data, whereas a double-layer blu-ray disc even stores up to 50 GB, which equates to 4.5 hours of high-definition video or about 20 hours of standard video.

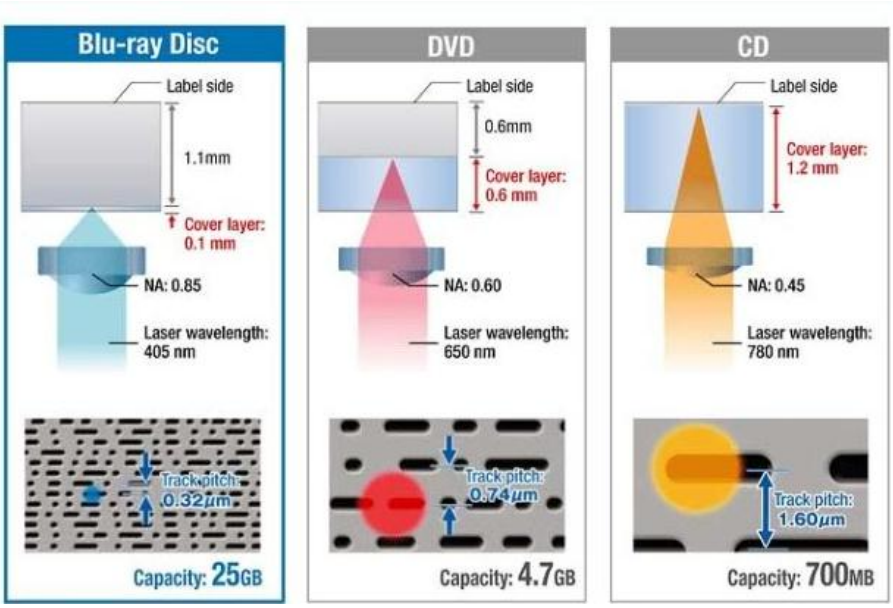

Figure 3: Comparison between blu-ray, DVD and CD technology. In the upper part, a simplified schematic of the reading process along with the corresponding technical specifications is depicted. In the lower part a schematic presentation of the corresponding discs´ surfaces and laser beam sizes is shown.[10]

These data storage technologies are commercially well established and their capacities as well as their data transfer rates have substantially increased. With the future demand for larger storage capacities and faster transfer rates, the concept of two-dimensional optical storage employing only stacked layers will eventually encounter its limits and the step to new three-dimensional data storage is required. Hereby the most promising solution in the field of optical storage media is *holographic data storage*, where, in contrast to conventional CDs or DVDs, the entire volume of the medium is used instead of only a few thin layers.[11] Data carriers with a storage capacity of 300 GB are already available.[12]

1.2 Holography

Holography is an optical imaging technique which was discovered by Dennis Gabor, a Hungarian physicist (see Figure 4), in 1948. In conventional photography only the two-dimensional irradiance distribution associated with the light wave coming from an object (the object-wave) is stored. The information of depth of the incoming light-wave is hereby lost. However, in holography, the object wave itself is recorded. This means that the light wave is stored in such a way that a subsequent illumination of the recording serves to reconstruct the original object wave, even in the absence of the object itself. With this information an authentic image of the original object can be created.[13] Gabor described the recording and reproduction of the complete optical signal coming from the object and performed experiments to illustrate his theory,[14] but the light sources available at this time were inadequate to realize the full potential of the technique. For his pioneering work in the field of holography, he was awarded the Nobel Prize of Physics in 1971.

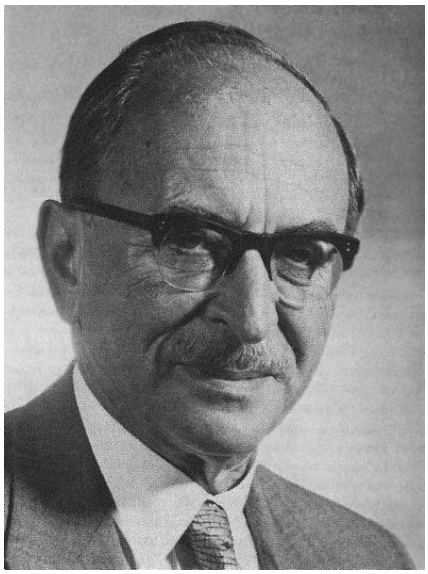

Figure 4: Dennis Gabor, Hungarian physicist, received the Nobel Prize of Physics in 1971 "for his invention and development of the holographic method"[15]

The experimental breakthrough in holography was later accomplished by Leith and Upatnieks.[16,17] Before that time, only holograms of thin transparent objects were created. By employing new experimental set-ups, like the

introduction of a reference wave or diffuse illumination of the object, as well as utilizing a gas laser as light source, they were able to record holograms of three-dimensional objects. Since these times holography has emerged to a broad scientific field with a multitude of applications for scientific[18-20] as well as commercial use.[21,22]

The *principle of holographic imaging* is shown in Figure 5. It is based on writing an interference grating in a photosensitive volume element. Hereby two light beams are incident on the material. The object beam is overlapping with a plane wave and generates an interference pattern in the photosensitive material with areas of different intensity and/or polarization (depending on laser polarization). This light pattern causes chemical or physical changes, which, for example, lead to the change of the absorption coefficient or the refractive index. By illumination of the stored diffraction grating with a reference beam, the original information can be reconstructed.[23,24]

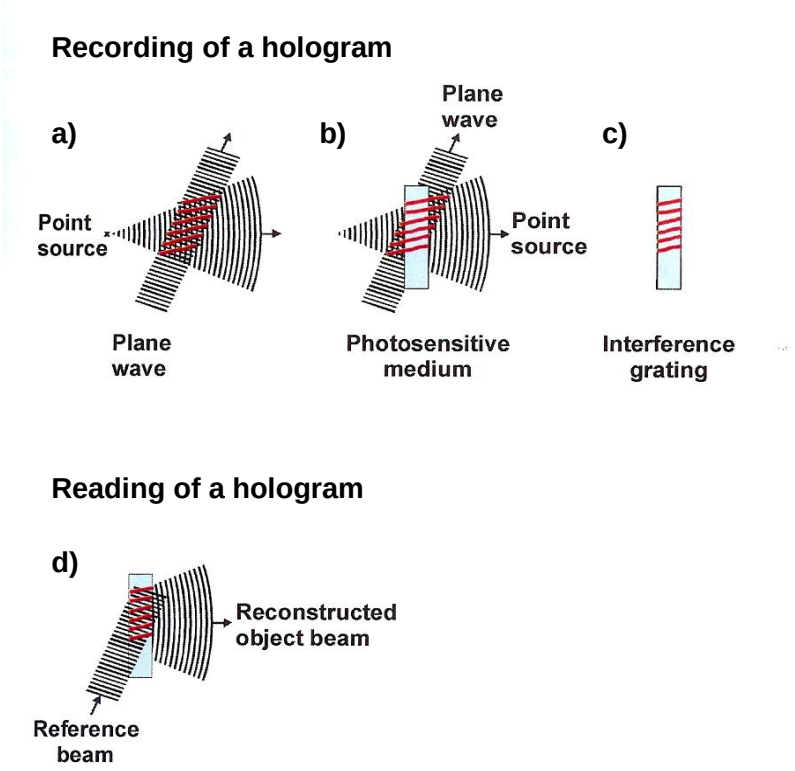

Figure 5: Writing and reading of a hologram in a photosensitive medium. a) Superposition of two beams leads to the creation of an interference pattern. b) The interference pattern can be inscribed in a photosensitive medium. c) Stored interference pattern in the photosensitive medium. d) Reconstruction of the original object beam by irradiation with the reference beam.[25]

An intriguing possibility for increasing data storage density is to use *angular multiplexing*.[26,27] When utilizing the entire volume of a medium instead of only its surface, capacities above one terabyte on a data storage medium the size of a CD are possible.[28,29] Per inscription process, millions of bits can be stored by passing the writing beam through a spatial light modulator (SLM), each pixel representing a bit by its bright/dark state (see Figure 6). This pattern is then holographically encoded in the sample and, consequently, the entire page of data is written simultaneously. Furthermore, by selecting different angles for the writing beams, new patterns can be written on the same spot without erasing previously inscribed data.[30] To read-out a page, the reference beam is set to the corresponding angle as well as position and the resulting diffraction pattern is imaged on a charge-coupled device (CCD) array. The reconstruced image from the diffracted light is identical in shape to the image resulting from the original writing beam signal. In this way, high data transfer rates can be realized since whole sets of data can be simultaneously inscribed. Moreover, expected transfer rates for holographic data storage are even higher due to the parallel nature of the writing and reading processes.[26]

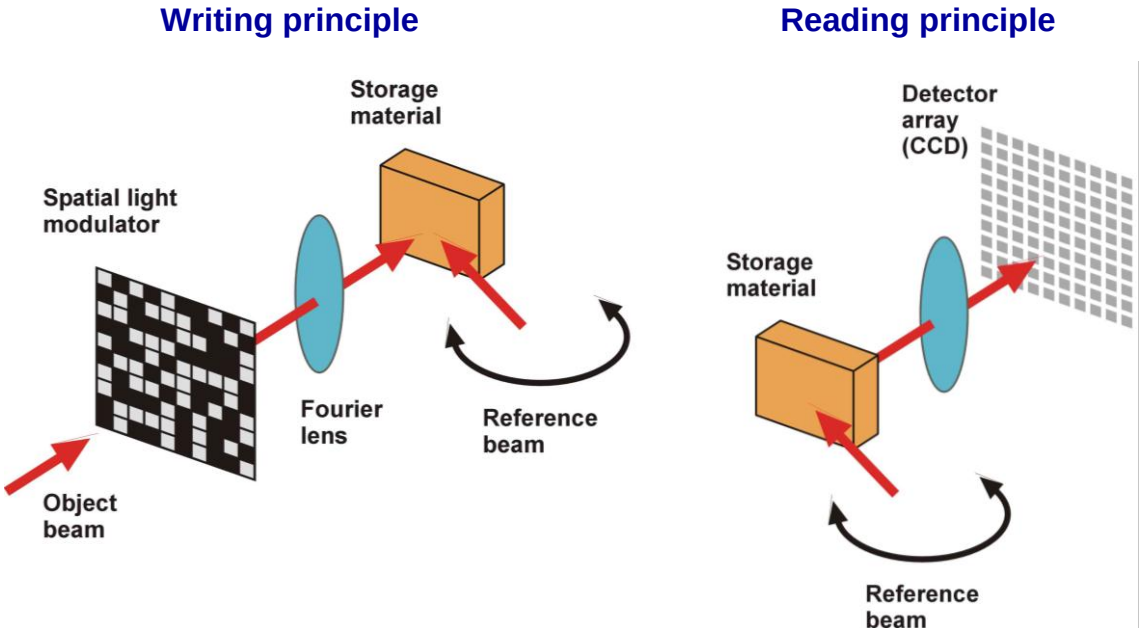

Figure 6: Principle of writing a data page in a storage material (left) and reading a complete set of inscribed data (right). By changing the angle between object and reference beam, new patterns can be written on the same spot without erasing previously inscribed data. Adopted from [25].

1.3 Materials for holographic data storage

For the application of holography as data storage technique, suitable storage materials have to be employed. Tailoring such materials is a challenging task as a good holographic storage material should fulfill a combination of required properties. Most basically the material should exhibit excellent optical quality in order to avoid scattering of the laser beams. The specimens should have a thickness in the mm-range and a sufficiently low optical density (typically 0.5-0.7) so that the laser beams can penetrate the medium. The material should be easily processable and offer high chemical and physical stability. Additional necessary requirements are a high photosensitivity to achieve a reasonable low writing time as well as high-fidelity recording in order to avoid errors at the subsequent reading process. A high dynamic range and sufficient long-term stability, ideally up to several decades, have to be guaranteed. Finally, the storage process has to be reversible if the development of rewritable storage devices is desired. It is a great challenge to satisfy all these requirements and, therefore, there are several different material approaches. Basically the developed storage materials can be classified into inorganic and organic materials.

Typical *inorganic materials* utilized as holographic media are stoichiometric lithium niobate or iron-doped lithium niobate. However, they play only a minor role in current considerations for use in holographic storage media due to their drawbacks. These are, among others, high costs as well as a low sensitivity requiring very long recording times. Moreover, difficult processablility and, especially, high error rates during writing and read-out make these materials not desirable for holographic data storage. Therefore, other inorganic storage materials have been proposed like strontium barium niobate or barium titanate.[31] Furthermore, in the last years *inorganic-organic hybrid materials* have become a topic of scientific interest.[31-33]

In the case of *organic media* for holographic data storage, reversible and irreversible systems are known. The first two systems, diffusion-amplified media as well as photopolymers are irreversible methods of data storage. Write-once media, especially those based on photopolymer systems, seem to be fairly

advanced.[34] However, their major drawback is the non-reversibility of the storage process. Once written, the information can not be overwritten or erased.

For *photopolymers*[25,34-37] the recording of a hologram is the result of a photoinduced polymerization reaction that is started in the irradiated volume element. The resulting concentration gradient causes diffusion of monomers towards the areas where polymerization was initiated. After completion of the polymerization, the holograms are permanently retained in their density and refractive index patterns with a final baking step. Although photopolymers exhibit good sensitivity and writing times, they suffer from shrinkage of the material during polymerization.

An example for *diffusion-amplified media*[38-41] is phenanthraquinone embedded in polymethylmethacrylate (PMMA). Photoexposure of this system results in writing of two periodic gratings which partially compensate each other. One of these is formed by immobilizing chromophores by photo-induced binding to the polymer matrix and the other by free chromophore molecules. After irradiation the free chromophores start to diffuse to a uniform distribution and their corresponding grating degrades. Due to this diffusion, the compensation of the gratings is decreased and the net diffraction efficiency is amplified without additional processing steps.[22,31]

In contrast, *photoaddressable materials* are a reversible method of data storage, which has the advantage of hundreds of possible read and write cycles. They are based on photoactive chromophores which are blended in a matrix or fixed to a polymer backbone or low molecular weight compound. One of the most important classes of photoaddressable chromophores are azobenzene compounds. As azobenzene-containing materials are the main focus of this thesis, an overview of the azobenzene chromophores will be given in the next section.

1.4 Azobenzene chromophores

Azobenzene chromophores are very versatile molecules, as on the one hand, their absorption behaviour can be tailored by ring substitution for a specific task and on the other hand they are relatively robust and chemically stable. Their rigid mesogenic shape is well suited to spontaneous organization

into liquid crystalline phases.[42] Azobenzenes feature a unique and rich photo-physical behaviour. According to Nathanson largely three hierarchically different categories can be distinguished: (i) on a molecular level, a *trans*-*cis*-*trans* photo-isomerization, (ii) on a domain level, a photo-induced orientation and (iii) on a macroscopic level, a mass transport to surface structures.[43] All these categories will be subsequently discussed.

On a *molecular level*, azobenzene chromophores exhibit two configuration isomers, the *trans*- and the *cis*-state. Hereby the *trans*-state is thermodynamically more stable. By irradiation with UV light, a *trans*-to-*cis* conversion is induced; with visible light, a *cis*-to-*trans* conversion occurs. Alternatively, the *cis*-state will thermally return to the *trans*-state. Thus, if stored in the dark, most azobenzene chromophores will have reverted back to the *trans*-state (see Figure 7). This photo-isomerization is highly efficient and fully reversible as well as free from side-reactions.[44]

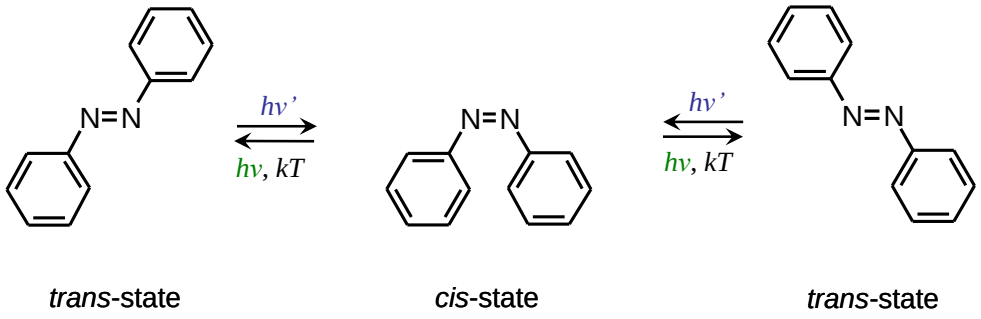

Figure 7: Schematic representation of the reversible *trans*-*cis*-*trans* photo-isomerization of azobenzene. Upon absorption of UV light, a *trans*-to-*cis* conversion is induced; with visible light, a *cis*-to-*trans* conversion occurs until a photostationary equilibrium between both isomers is reached. The thermodynamically less stable *cis* isomer can also thermally return to the *trans* isomer.

Two possible mechanisms for the isomerization are proposed in literature.[45-47] The isomerization takes place either by rotation about the nitrogen-nitrogen bond after breaking of the π-bond or through inversion with a rearrangement of a phenyl-ring leaving the π-bond intact. Both mechanisms may be competing, depending on the chromophore and the environment.[48-50] However, the dominant way of isomerization seems to be inversion, as this mechanism needs less free volume.[51]

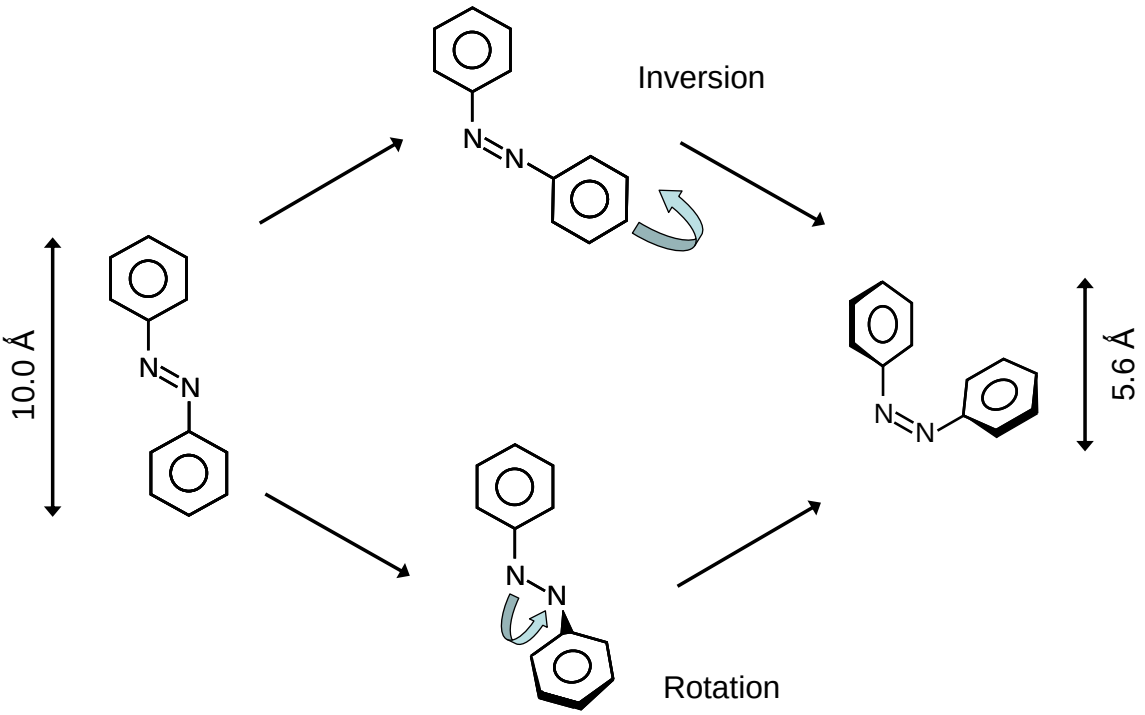

Figure 8: The isomerization of azobenzene proceeds via a rotation or inversion mechanism. Scheme adopted from literature.[42]

In addition to the molecular isomerization, the azobenzene moieties can reorient in the solid state upon light absorption on a *domain level* through multiple reversible *trans-cis-trans* photo-isomerization cycles. This orientation of the azobenzene chromophores is illustrated in Figure 9. At first, the chromophores are distributed isotropically. Upon irradiation with polarized light they start to isomerize until the azobenzene is turned perpendicular to the exciting electric field vector. This process is described later in more detail (see chapter 1.6).

Owing to the rich photochemistry of azobenzene chromophores, a large variety of small-molecular and polymeric compounds has been synthesized for use as smart light-responsive materials for various potential applications. Materials incorporating azobenzenes can be used as photoswitches, allowing fast and reversible control over the chemical, mechanical, physical or optical properties of the whole system.[42,52,53] As this thesis concentrates on holographic data storage and surface structuring with azobenzene chromophores, the next sections will focus on these two applications.

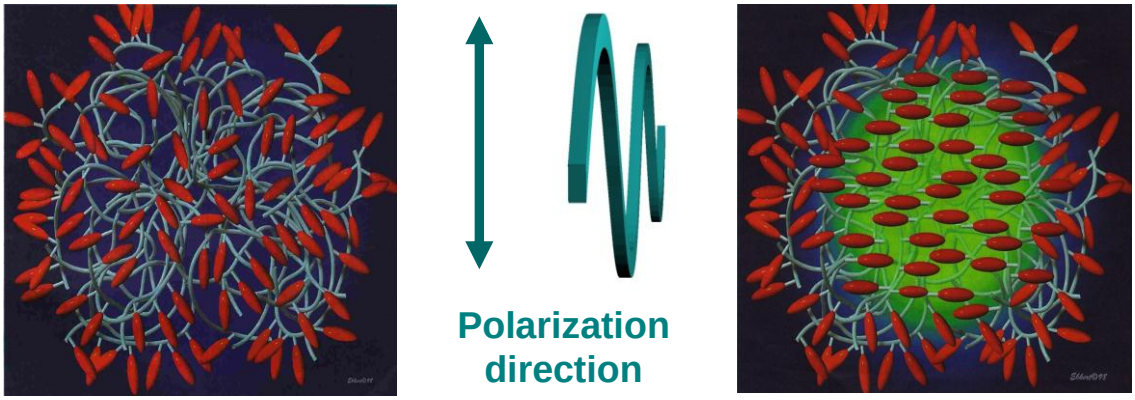

Figure 9: Orientation of azobenzene chromophores by irradiation with polarized light exemplarily shown for an azobenzene-containing side chain polymer. *Left side:* Initially, the azobenzene chromophores are isotropically distributed in the material. *Right side:* Material after irradiation with polarized light; the chromophores are oriented perpendicular to the polarization plane in the exposed area (green). Adopted from literature.[26]

1.5 Azobenzene-containing polymer systems

For holographic data storage, azobenzene-functionalized polymer materials have been recognized as promising materials. Photoaddressable homopolymers containing azobenzene side chains were first introduced by Ringsdorf and Schmidt et al.[54,55] Hereby, the azobenzene units were attached to the polymer backbone via a flexible spacer. The photoinduced isomerization of the azobenzene chromophores as well as their application in holographic data storage was investigated by Eich et al. and later by various other groups.[56-58] For example, Hvilsted et al. reported on various polyesters with liquid crystalline azobenzene side-groups[59] as well as azobenzene-containing peptide oligomers.[60] Statistical copolymers with azobenzene dyes attached to the polymer backbone were first investigated as dye-containing liquid crystalline polymers[54,61] and later in view of holographic data storage.[62] Natansohn et al. investigated different types of azobenzene-containing polymers systems.[43,63,64] Statistical methacrylate copolymers with azobenzene side-groups were studied by Zilker et al. [65,66] and by Hagen et al.[26]

However, for fully utilizing angular multiplexing, thick samples in the mm-regime are required to achieve high angular selectivity. Therefore, it is very important to adjust the optical density to a sufficiently low value, so that the

laser beam can penetrate the entire sample. This is not possible with homopolymers since their optical density is too high in thick samples. On the other hand, the azobenzene chromophores have to be close to each other to benefit from the so called “cooperative effect”. This effect makes the isomerization process more efficient, especially improving the long-term stability of inscribed holographic gratings. These cooperative motions are facilated by the azobenzene chromophores even far below T_g.[62,67] In order to decrease the optical density, diluting the chromophores by copolymerization has been investigated. However, statistical copolymerization is not a real option since the cooperative effect and, hence, the long-term stability of the gratings is lost. Moreover, homopolymer as well as statistical copolymer systems tend to develop SRGs in addition to the volume phase gratings during holographic exposure. These surface structures are detrimental to holographic data storage.

In contrast to the above mentioned systems, block copolymers composed of an amorphous majority block and an azobenzene-containing minority block are of interest because they form microphase-separated, uniform and regular morphologies below 100 nm. Hence, compared to macrophase separated homopolymer blends they do not scatter visible light. In addition, the cooperative effect is maintained in the confined geometry. Several research groups have reported on block copolymers carrying azobenzene chromophores in one block, synthesized by controlled radical polymerization techniques[68-75] or a subsequent polymeranalogous reaction on the anionic preformed polymerbackbone.[76-78] For the above mentioned reasons, block copolymers with microphase separation are the most promising class for holographic storage.[79]

1.6 Inscription of holographic gratings

One of the simplest methods for inscribing a hologram is the illumination of a photosensitive material with a light intensity pattern caused by two interfering coherent plane waves. The resulting interference pattern in the material can be described as a sinusoidal intensity gradient in the area illuminated by the incident light. The distance between the intensity maxima or

minima, the so-called grating constant Λ, can be adjusted by changing the wavelength or the angle between the writing beams (Equation 1).

$$\Lambda = \frac{\lambda_{write}}{2 \sin \Theta_{write} n} \quad \textbf{(1)}$$

***Λ*:** *grating constant*

***λ*$_{write}$:** *writing wavelength*

***Θ*$_{write}$:** *angle between writing beam and line perpendicular to the surface of the sample*

***n*:** *refractive index*

Azobenzene chromophores in a rigid matrix can be oriented by irradiation with polarized light.[80,81] In the beginning, the chromophores are distributed isotropically (Figure 10, upper part), however, upon illumination they start to isomerize. This process continues until the molecular transition dipole moment of the azobenzene, which is parallel to its long axis, is turned perpendicular to the exciting electric field vector. Chromophores which are oriented in such a way can no longer be exited, and hence, reorientation is no longer possible. Consequently, the sinusoidal gradient of intensity, leads to a locally defined orientation (Figure 10, lower part). Since the azobenzene moiety exhibits a strong anisotropy, the oriented areas have a different refractive index compared to the non-oriented areas. This way, a refractive index grating is formed, with the isotropic areas exhibiting the original refractive index n_0 and the illuminated areas exhibiting a different refractive index n*. As a consequence, the illuminated area becomes macroscopically birefringent. The achieved orientation is fully reversible either by irradiation with circularly polarized light or by heating above the system´s glass transition temperature (T_g).

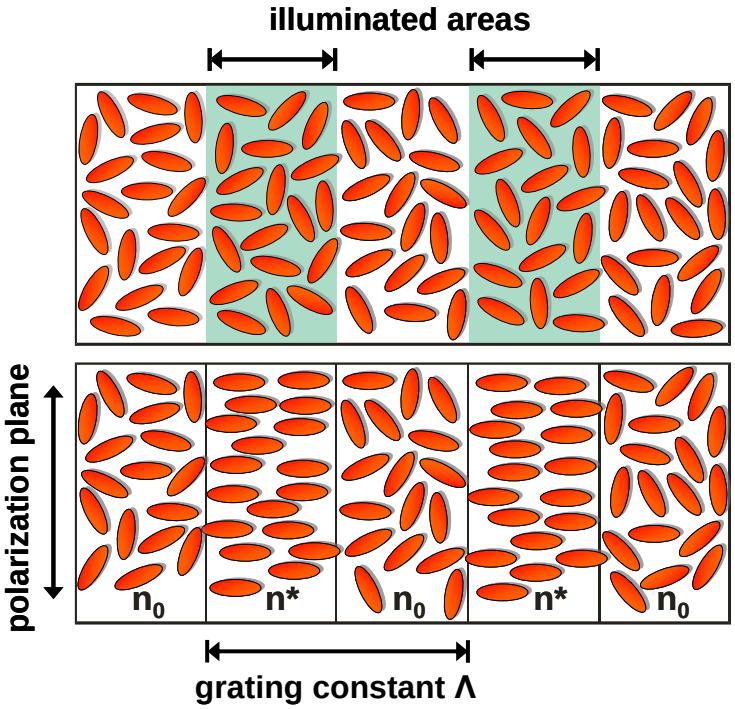

Figure 10: Orientation of the azobenzene chromophores during and after irradiation. *Upper part:* Isotropic orientation of the chromophores; the illuminated areas are highlighted (for simplification the borders of these areas are sharp and not diffuse). *Lower part:* Material after orientation; n_0 and n^* pertain to different refractive indices.

In the *read-out process*, the reading beam is focussed on the interference grating, where the beam is diffracted into several parts representing different diffraction orders. The amount of diffracted light is simultaneously measured and utilized to describe the efficiency of the inscription process. Hereby, it is important that reading is performed with a laser beam whose wavelength is well outside the absorption band of the chromophores, so the inscribed grating is not influenced.

The results of the holographic measurements in this thesis were analysed utilizing theoretical considerations made by Kogelnik in his Coupled Wave Theory.[82] Here, only the intensity of the first order diffracted beam $I_1(t)$ is considered, as it is assumed that apart from the zeroth diffraction order (the transmitted beam) only the first diffraction order occurs and the Bragg condition is not fulfilled for all higher orders. Therefore, the laser beam intensity is only divided between these two diffraction orders. This way the efficiency of the holographic inscription process can be easily determined by calculating the

diffraction efficiency η, which is given by the ratio $I_1(t)$ divided by the intensity of the transmitted beam before writing of a hologram in the sample $I_0(t_0)$.

$$\eta = \frac{I_1(t)}{I_0(t_0)} \quad \textbf{(2)}$$

η*: *diffraction efficiency

$I_1(t)$*: *intensity of the first order diffracted beam

$I_0(t_0)$*: *intensity of the transmitted beam before writing a hologram

In order to give a statement about the potential of a material utilized in holographic data storage and to compare different materials with each other, the maximum refractive index modulation n_1 has to be considered. This material property is on the one hand independent from the sample geometry and on the other it is possible to make predictions about the attainable storage capacity, as a high refractive index modulation is necessary to achieve high data storage densities by angular multiplexing. In order to calculate the refractive index modulation n_1 from the diffraction efficiency η the following equation is utilized.

$$n_1 = \frac{\lambda \cos\Theta_{write}}{\pi} \frac{\sqrt{\eta}}{d_0} \quad \textbf{(3)}$$

λ*: *wavelength of the laser

Θ_{write}*: *angle between writing beam and the surface normal of the sample

η*: *diffraction efficiency

d_0*: *thickness of the sample

A further important material characteristic is the material sensitivity S. It describes the slope of the holographic growth curve and is calculated according to Hesselink et al.[34] The sensitivity is a parameter for the photo-physical response of the whole photochromic system. Since the growth of the writing curve is not linearily increasing, the sensitivity is usually determined at the beginning of the writing process ($t \sim 0$) where it has its maximum value (S_{max}).

$$S = \frac{\frac{\partial\sqrt{\eta}}{\partial t}}{I_0 d_0} \quad \textbf{(4)}$$

η*: *diffraction efficiency

I_0*: *laser intensity

d_0*: *thickness of the sample

1.7 Surface relief gratings

In addition to the photoinduced reorientation, on a *macroscopic level*, mass transport which leads to the formation of surface relief gratings can be induced by illumination with two interfering laser beams. This phenomenon was first discovered by Kumar et al.[83] and Natansohn et al.[84] in 1995.

In Figure 11, a schematic view of a sinusoidal SRG with the grating constant Λ and the modulation height Δd (peak to valley) of a thin film with the initial thickness d_0 is shown. The grating period Λ can be adjusted according to equation 1 by the angle of incidence of the two laser beams in relation to the surface. The maximal achievable height is largely depending on the material, if the films are sufficiently thick. Within this limit the height can be easily adjusted by the beam intensity and time of illumination. If a substrate with a sinusoidal SRG is rotated by 90° and an additional SRG is superimposed, a so called egg-crate structure can be obtained. The distance from a peak to the nearest neighbouring peak corresponds to the grating period. Even more complex structures can be found in reference 85.[85]

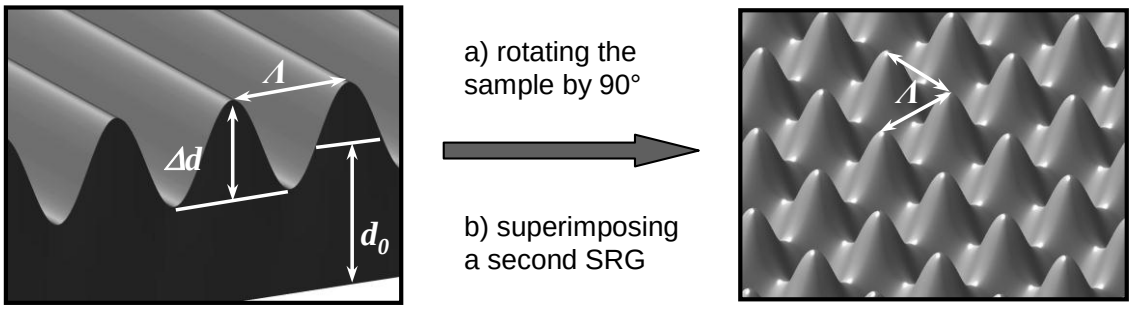

Figure 11: *Left side:* schematic representation of a sinusoidally shaped SRG with the modulation height Δd, initial film thickness d_0 and the grating constant Λ. *Right side*: rotating such a sample by 90° and superimposing a second SRG yields an egg-crate structure.

Highly uniform SRGs with adjustable spacing and amplitude can be envisioned for several application, e.g. liquid-crystal anchoring, waveguide couplers, polarization discriminators,[85] or antireflective coatings[86,87] for the visible range. In addition, SRGs might be used as channel waveguides,[88] holographical optical elements (HOEs) and in optical security devices.[89]

SRG formation was mainly investigated in photoaddressable polymers systems carrying azobenzene units.[43,64,90-94] It is remarkable that the macroscopic material transport takes place in these amorphous azobenzene-containing materials more than 100 degrees below the T_g and that SRGs with grating constants on the order of one micrometer with amplitudes of several hundred nanometers can be formed within a short time. Numerous models have been proposed to describe the process of SRG formation and substantial experimental and theoretical work was devoted to clarifying its mechanism. The theory of Yager et al.[95] explains the SRG build-up by the competition between photoexpansion and photocontraction. Henneberg and co-workers[94] introduced a viscoelastic-flow model. According to Lefin et al.,[96] the azobenzene chromophore moves like an inchworm owing to the isomerization between the stretched *trans* and the bent *cis* state resulting in a translational movement. Kumar et al.[97,98] introduced a model based on a time-averaged gradient force. Only within the latter model, the influence of different polarizations of the laser beams on the SRG formation is accounted for. Although each model describes parts of the observed effects correctly, none of them is able to reproduce all experimental results.

In addition to the above mentioned polymer-based systems, azobenzene-containing sol-gel-based systems are another material class for SRG formation. At first the group of Stumpe et al. optically generated microstructures in polymers based on ionic interactions between azobenzene units and polyelectrolytes.[99,100] Later it was shown that an efficient SRG formation can be obtained using ionic azobenzene units, which were stabilized in a polyelectrolyte matrix via an in situ sol-gel reaction.[101]

1.8 Molecular glasses

An interesting new class and an alternative to polymers are small low-molecular weight compounds which are able to form a stable amorphous phase at room temperature. These materials are called molecular glasses. At the end of the 19th century Tammann had already discovered that low molecular weight materials can vitrify on rapid cooling.[102] However, for decades only very few

molecular glasses were known.[103-107] Only as recently as the end of the 20th century, research began to intensify.[108]

The glassy state is often associated with polymers, as small molecules typically tend to readily crystallize. In contrast, molecular glasses can form a stable glassy state due to their structure and exhibit a glass transition temperature.[108] Regarding polymers, the glassy state is mostly the result of a great number of conformation possibilities and entanglement of the chains. However, this does not, for the most part, apply to molecular glasses. The formation of an amorphous phase is here often obtained by non-equilibrium processes. Such procedures include, for example, quenching of the melt, creating films by vapor deposition from the solid state or spin-coating from solution.[108,109]

Molecular glasses represent an emerging material class of great potential and hence they are the subject of intense current studies, mainly with respect to their electronic and optoelectronic properties and their application in functional electronic, optical, and electro-optical devices. They are utilized, for example, in photoconductor drums, organic light emitting devices, organic solar cells, photolithography, photorefractive materials and anti-reflective coatings.[110-118] In contrast to functional polymers used in these applications,[119-124] molecular glasses have several distinct advantages.

They feature a well-defined molecular structure, the absence of structural defects and undefined end groups as well as a uniform molecular weight. As a result, they can be highly purified with established methods of organic chemistry like absorption chromatography or recrystallization. On the other hand they can be characterized by established methods of polymer analytic like gel permeation chromatography (GPC), differential scanning calorimetry (DSC), x-ray scattering and polarizing light microscopy (POLMIC).[108]

According to literature, there are numerous strategies to obtain molecular glasses. Most commonly molceular glasses are based on spiro-compounds as well as star-shaped topologies with three or four arms (see Figure 12).[53,108,109]

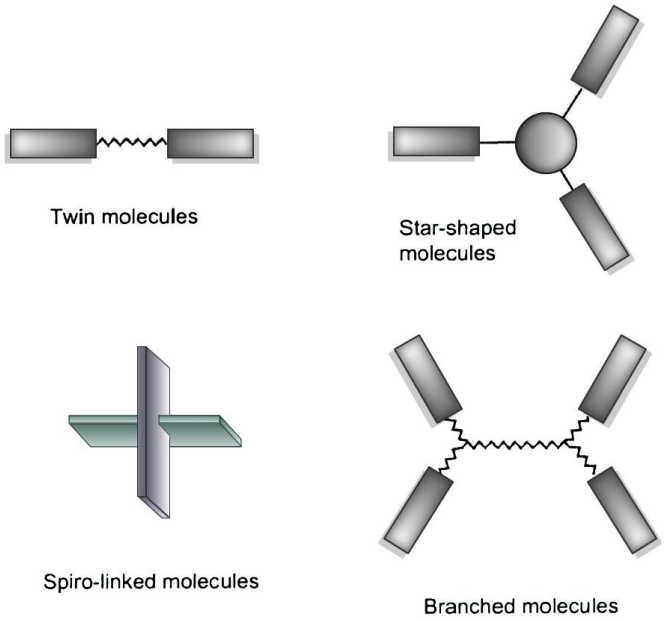

Figure 12: Typical topologies for molecular glasses. Adopted from literature.[109]

As the formation of amorphous phases commonly is fostered by bulky molecular structures, space-filling groups are often used elements for obtaining amorphous materials and tailoring their properties. Sterical demanding substituents reduce the translational and rotational motions of the molecule. This prevents dense packing of the molecules and thus hinders crystallization. Herewith the formation of a glassy state is easily reached and the long term stability of the amorphous phase is improved.[125] Another possibility to design molecular glasses is the synthesis of asymmetric molecules. Due to a high number of conformers, the tendency to crystallize is greatly reduced.[109,126]

The stability of the molecular glasses´ amorphous phase depends to a large extent on intermolecular interactions. In contrast to inorganic materials which exhibit strong covalent and/or ionic interactions in the solid state, molecular glasses consist of individual molecules featuring mostly weak intermolecular interactions, e.g. van-der-Waals interactions.[125]

Besides the vitrifying in an isotropic phase, the position of the glass transition temperature is an important factor, since high T_g materials posses a more stable amorphous phase.[127] A high T_g can be obtained by rigid substituents or strong intermolecular interactions like hydrogen bridge bonds. Examples for rigid substituents are biphenyl-, napthyl-, fluorenyl- or carbazolyl-

moieties. It is important to consider that a strong interaction between molecules can also lead to recrystallization. An enlargement in molecular weight or size of the molecule also causes an increase of the glass transition temperature.[108,125]

Azobenzene-containing molecular glasses

Photochromic molecular glasses can be envisioned for the same applications as photoaddressable polymers, but they have been studied far less extensively. Azobenzene-containing molecular glasses were first introduced by Shirota et al. in 1998.[128] One azobenzene chromophore was incorporated into arylamine-derivatives. Since then Shirota et al. reported several azobenzene-containing molecular glasses with different substitution patterns and their influence on glass forming and photochromic response.[53,129-131] Fuhrmann et al. also reported on an amorphous azobenzene-containing amorphous material which readily forms SRGs in holographic experiments.[132,133] Hereby, the SRG formation can be enhanced by utilizing electric field assisted holographic recording.[134] Ishow et al. demonstrated that fluorescence patterning and photoinduced mass migration can be combined.[135,136] There have also been reports on the influence of modifications at the azobenzene moiety on the SRG formation.[137-140] Additionally, the polarization of the laser beams is a decisive factor.[141] Up to date SRG formation is mainly performed at room temperature, and the achieved heights are often correlated to the glass transition temperature of the molecular glass.[142] Above the glass transition the surface patterns are destroyed and the initial smooth sample surface is restored.[93,143] It was demonstrated by Wendorff et al. that SRGs also formed in the glassy amorphous phase of an azobenzene-containing low molecular-weight material.[144,145] Several reports showed that the photoinduced growth of SRGs can be more efficient in thin films of a molecular glass as compared to polymers, since the mass transport is not hindered by entanglements of the polymer chains.[143,146-148] Furthermore Kim et al. reported that photoinduced birefringence can be generated in thin films of azobenzene-based molecular glasses.[146,149] Recently our group showed that such photoinduced birefringence can be long-term stable if inscribed in amorphous films of

azobenzene-functionalized low molecular weight compounds, which feature a latent liquid-crystalline phase.[150]

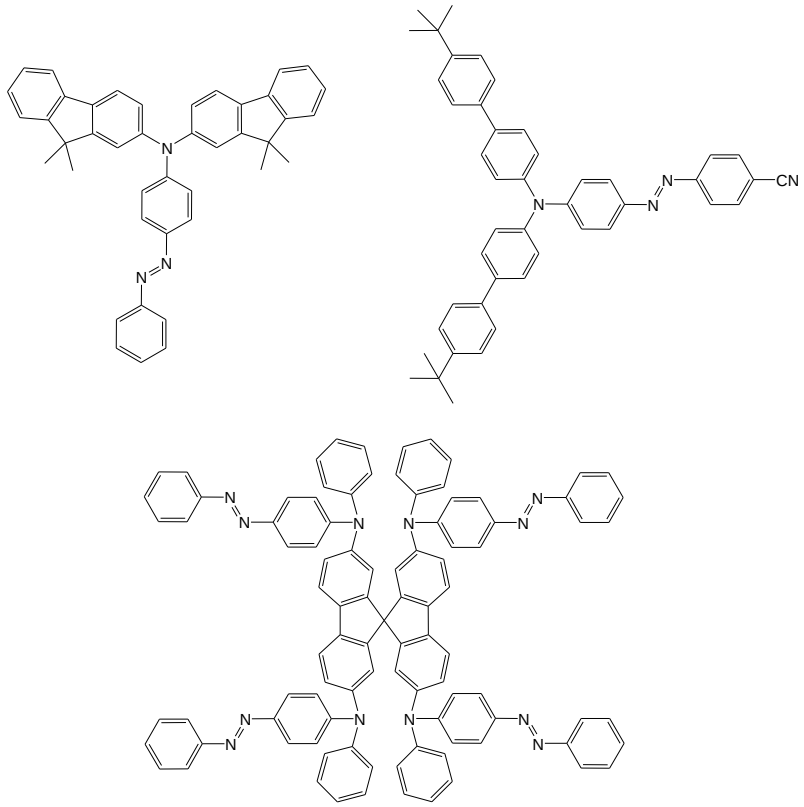

Figure 13: Molecular glasses with azobenzene chromophores by Shirota et al.[108] (*top left*), Ishow et al.[137] (*top right*) and Kim et al. (*bottomt*).[146]

References

[1] D. S. Alberts, D. S. Papp, *The Information Age: An Anthology on Its Impact and Consequences*. **1997**, published online: CCRP Publications (accessed may 2010)
[2] D. Weller, A. Moser, *IEEE Trans. Magn.* **1999**, *35*(6), 4423-4439
[3] D. A. Thompson, J. S. Best, *IBM J. Res. Dev.* **2000**, *44*(3), 311-322
[4] M. Albrecht, G. Hu, A. Moser, O. Hellwig, B. D. Terris, *J. Appl. Phys.* **2005**, *97*(10, Pt. 1), 103910/1-103910/5
[5] V. Skumryev, S. Stoyanov, Y. Zhang, G. Hadjipanayis, D. Givord, J. Nogues, *Nature* **2003**, *423*(6942), 850-853
[6] news.bbc.co.uk, *Hard disk drive*. **2007**, published online: British Broadcasting Coporation. (accessed may 2010)
[7] A. S. Tanenbaum, *Structured computer organization* **2009**, Prentice Hall International, Upper Saddle River, NJ
[8] picture adopted from: upload.wikimedia.org/wikipedia/commons/d/d3/FLASH_RAM-Cell.svg (accessed may 2010)
[9] www.blu-raydisc.com, *Blu-ray disc format*. **2004**, published online: Blu-ray white paper (accessed may 2010)
[10] picture taken from: www.highdefforum.com/blu-ray-movie-reviews/99641-real-marlowe-exclusive-maxell-blu-ray-laser-cleaner-3.html (accessed may 2010)
[11] M. Haw, *Nature* **2003**, *422*(6932), 556-558
[12] www.inphase-technologies.com, *InPhase Technologies showcases first commercial holographic storage solution*. **2007**, published online: Inphase Press Release (accessed may 2010)
[13] H. Smith, *Principles of Holography* **1975**, Wiley, New York
[14] D. Gabor, *Nature* **1948**, *161*(4098), 777
[15] www.nobel-prize.org, *Nobel Laureates in Physics*. **2010**, published online: Nobel Foundation (accessed may 2010)
[16] E. Leith, J. Upatnieks, *J. Opt. Soc. Am.* **1964**, *54*(11), 1295-1301
[17] E. Leith, J. Upatnieks, *J. Opt. Soc. Am.* **1962**, *52*(10), 1123-1130
[18] S. Benton, V. Bove, *Holographic Imaging* **2008**, Wiley, Hoboken
[19] H. Bjelkhagen, H. Caulfield, *Fundamental Techniques in Holography* **2001**, SPIE, Bellingham
[20] U. Schnars, W. Juptner, *Digital Holography* **2005**, Springer, New York
[21] J. Eichler, G. Ackermann, *Holography - A Practical Approach* **2007**, Wiley, Weinheim
[22] J. Ludman, H. Caulfield, J. Riccobono, *Holography for the New Millenium* **2002**, Springer, New York
[23] P. Hariharan, *Basics of Holography* **2002**, Cambridge University Press, Cambridge
[24] H. Kiemle, D. Röss, *Holographie* **1969**, Akademische Verlagsgesellschaft, Frankfurt am Main
[25] J. Ashley, M. P. Bernal, G. W. Burr, H. Coufal, H. Guenther, J. A. Hoffnagle, C. M. Jefferson, B. Marcus, R. M. Macfarlane, R. M. Shelby, G. T. Sincerbox, *IBM J. Res. Dev.* **2000**, *44*(3), 341-368
[26] R. Hagen, T. Bieringer, *Adv. Mater.* **2001**, *13*(23), 1805-1810
[27] G. T. Huang, *Technol. Rev.* **2005**, *108*, 64-67
[28] P. S. Ramanujam, S. Hvilsted, F. Ujhelyi, P. Koppa, E. Lorincz, G. Erdei, G. Szarvas, *Synth. Met.* **2001**, *124*(1), 145-150
[29] M. Haw, *Nature* **2003**, *422*(6932), 556-558
[30] G. Barbastathis, D. Psaltis, *Volume holographic multiplexing methods, in: Holographic data storage* **2000**, Springer-Verlag, Berlin
[31] R. M. Shelby, *Proc. SPIE-Int. Soc. Opt. Eng.* **2002**, *4659*, 344-360
[32] H. Kakiuchida, M. Takahashi, Y. Tokuda, T. Yoko, *Adv. Funct. Mater.* **2009**, *19*(16), 2569-2576
[33] G. Garnweitner, L. M. Goldenberg, O. V. Sakhno, M. Antonietti, M. Niederberger, J. Stumpe, *Small* **2007**, *3*(9), 1626-1632
[34] L. Hesselink, S. S. Orlov, M. C. Bashaw, *Proc. of IEEE* **2004**, *92*(8), 1231-1280
[35] M. L. Schilling, V. L. Colvin, L. Dhar, A. L. Harris, F. C. Schilling, H. E. Katz, T. Wysocki, A. Hale, L. L. Blyler, C. Boyd, *Chem. Mater.* **1999**, *11*(2), 247-254

[36] D. A. Waldman, C. J. Butler, D. H. Raguin, *Proc. SPIE-Int. Soc. Opt. Eng.* **2003**, *5216*, 10-25
[37] M. Schnoes, B. Ihas, L. Dhar, D. Michaels, S. Setthachayanon, G. L. Schomberger, W. L. Wilson, *Proc. SPIE-Int. Soc. Opt. Eng.* **2003**, *4988*, 68-76
[38] S. H. Lin, K. Y. Hsu, W.-Z. Chen, W. T. Whang, *Opt. Lett.* **2000**, *25*(7), 451-453
[39] G. J. Steckman, I. Solomatine, G. Zhou, D. Psaltis, *Opt. Lett.* **1998**, *23*(16), 1310-1312
[40] G. J. Steckman, I. Solomatine, G. Zhou, D. Psaltis, *Proc. SPIE-Int. Soc. Opt. Eng.* **1999**, *3623*, 234-242
[41] S.-H. Lin, K. Y. Hsu, *Proc. SPIE-Int. Soc. Opt. Eng.* **2002**, *4929*(Optical Information Processing Technology), 208-214
[42] Y. Zhao, T. Ikeda, *Smart light-responsive materials* **2009**, Wiley, Hoboken, NJ
[43] A. Natansohn, P. Rochon, *Chem. Rev.* **2002**, *102*(11), 4139-4175
[44] H. Rau, *Stud. Org. Chem.* **1990**, *40*, 165-92
[45] S. Xie, A. Natansohn, P. Rochon, *Chem. Mater.* **1993**, *5*(4), 403-11
[46] H. Rau, E. Lueddecke, *J. Am. Chem. Soc.* **1982**, *104*(6), 1616-20
[47] Z. F. Liu, K. Morigaki, T. Enomoto, K. Hashimoto, A. Fujishima, *J. Phys. Chem.* **1992**, *96*(4), 1875-80
[48] C.-H. Ho, K.-N. Yang, S.-N. Lee, *J. Polym. Sci., Part A: Polym. Chem.* **2001**, *39*(13), 2296-2307
[49] C. Angeli, R. Cimiraglia, H.-J. Hofmann, *Chem. Phys. Lett.* **1996**, *259*(3,4), 276-282
[50] B. S. Jursic, *Chem. Phys. Lett.* **1996**, *261*(1,2), 13-17
[51] T. Ikeda, O. Tsutsumi, *Science* **1995**, *268*(5219), 1873-5
[52] K. G. Yager, C. J. Barrett, *J. Photochem. Photobiol., A* **2006**, *182*(3), 250-261
[53] Y. Shirota, *J. Mater. Chem.* **2005**, *15*(1), 75-93
[54] H. Ringsdorf, H. W. Schmidt, *Makromol. Chem.* **1984**, *185*(7), 1327-34
[55] M. Eich, J. H. Wendorff, H. Ringsdorf, H. W. Schmidt, *Makromol. Chem.* **1985**, *186*(12), 2639-47
[56] M. Eich, J. H. Wendorff, B. Peck, H. Ringsdorf, *Makromol. Chem., Rapid Commun.* **1987**, *8*(1), 59-63
[57] X. Meng, A. Natansohn, P. Rochon, *Polymer* **1997**, *38*(11), 2677-2682
[58] V. Cimrova, D. Neher, S. Kostromine, T. Bieringer, *Macromolecules* **1999**, *32*(25), 8496-8503
[59] S. Hvilsted, F. Andruzzi, C. Kullia, H. W. Siesler, P. S. Ramanujam, *Macromolecules* **1995**, *28*, 2172-2183
[60] R. H. Berg, S. Hvilsted, P. S. Ramanujam, *Nature* **1996**, *383*(6600), 505-508
[61] H. Ringsdorf, H. W. Schmidt, G. Baur, R. Kiefer, F. Windscheid, *Liq. Cryst.* **1986**, *1*(4), 319-25
[62] X. Meng, A. Natansohn, C. Barrett, P. Rochon, *Macromolecules* **1996**, *29*(3), 946-52
[63] A. Natansohn, P. Rochon, J. Gosselin, S. Xie, *Macromolecules* **1992**, *25*, 2268-2273
[64] A. Natansohn, P. Rochon, *Adv. Mater.* **1999**, *11*(16), 1387-1391
[65] S. J. Zilker, M. R. Huber, T. Bieringer, D. Haarer, *Appl. Phys. B* **1999**, *68*(5), 893-897
[66] S. J. Zilker, T. Bieringer, D. Haarer, R. S. Stein, J. W. Van Egmond, S. G. Kostromine, *Adv. Mater.* **1998**, *10*(11), 855-859
[67] U. Wiesner, N. Reynolds, C. Boeffel, H. W. Spiess, *Makromol. Chem., Rapid Commun.* **1991**, *12*(8), 457-64
[68] L. Cui, Y. Zhao, A. Yavrian, T. Galstian, *Macromolecules* **2003**, *36*(22), 8246-8252
[69] Y.-K. Han, B. Dufour, W. Wu, T. Kowalewski, K. Matyjaszewski, *Macromolecules* **2004**, *37*(25), 9355-9365
[70] G. Wang, X. Tong, Y. Zhao, *Macromolecules* **2004**, *37*(24), 8911-8917
[71] P. Forcen, L. Oriol, C. Sanchez, F. J. Rodriguez, R. Alcala, S. Hvilsted, K. Jankova, *Eur. Polym. J.* **2007**, *43*(8), 3292-3300
[72] H. Yu, A. Shishido, T. Ikeda, T. Iyoda, *Macromol. Rapid Commun.* **2005**, *26*(20), 1594-1598
[73] Y. Morikawa, T. Kondo, S. Nagano, T. Seki, *Chem. Mater.* **2007**, *19*(7), 1540-1542
[74] S. Gimeno, P. Forcen, L. Oriol, M. Pinol, C. Sanchez, F. J. Rodriguez, R. Alcala, K. Jankova, S. Hvilsted, *Eur. Polym. J.* **2009**, *45*(1), 262-271
[75] H. Yu, Y. Naka, A. Shishido, T. Ikeda, *Macromolecules* **2008**, *41*(21), 7959-7966
[76] C. O. Osuji, J. T. Chen, G. Mao, C. K. Ober, E. L. Thomas, *Polymer* **2000**, *41*(25), 8897-8907

[77] T. Hayakawa, S. Horiuchi, H. Shimizu, T. Kawazoe, M. Ohtsu, *J. Polym. Sci., Part A: Polym. Chem.* **2002**, *40*(14), 2406-2414
[78] G. Mao, J. Wang, S. R. Clingman, C. K. Ober, J. T. Chen, E. L. Thomas, *Macromolecules* **1997**, *30*(9), 2556-2567
[79] M. Haeckel, L. Kador, D. Kropp, C. Frenz, H.-W. Schmidt, *Adv. Funct. Mater.* **2005**, *15*(10), 1722-1727
[80] K. Ichimura, *Chem. Rev.* **2000**, *100*(5), 1847-1873
[81] Y. Yu, T. Ikeda, *J. Photochem. Photobiol., C* **2004**, *5*(3), 247-265
[82] H. Kogelnik, *Bell System Tech. J.* **1969**, *48*(9), 2909-2947
[83] D. Y. Kim, S. K. Tripathy, L. Li, J. Kumar, *Appl. Phys. Lett.* **1995**, *66*(10), 1166-1168
[84] P. Rochon, E. Batalla, A. Natansohn, *Appl. Phys. Lett.* **1995**, *66*(2), 136-8
[85] N. K. Viswanathan, D. Y. Kim, S. Bian, J. Williams, W. Liu, L. Li, L. Samuelson, J. Kumar, S. K. Tripathy, *J. Mater. Chem.* **1999**, *9*, 1941-1955
[86] P. Rochon, A. Natansohn, C. L. Callender, L. Robitaille, *Appl. Phys. Lett.* **1997**, *71*(8), 1008-1010
[87] J. A. Delaire, K. Nakatani, *Chem. Rev.* **2000**, *100*(5), 1817-1845
[88] O. Watanabe, M. Tsuchimori, A. Okada, H. Ito, *Appl. Phys. Lett.* **1997**, *71*(6), 750-752
[89] J. Kato, I. Yamaguchi, H. Tanaka, *Opt. Lett.* **1996**, *21*(11), 767-769
[90] L. L. Carvalho, T. F. C. Borges, M. R. Cardoso, C. R. Mendonca, D. T. Balogh, *Eur. Polym. J.* **2006**, *42*(10), 2589-2595
[91] B. M. Schulz, M. R. Huber, T. Bieringer, G. Krausch, S. J. Zilker, *Synth. Met.* **2001**, *124*(1), 155-157
[92] K. G. Yager, C. J. Barrett, *Macromolecules* **2006**, *39*(26), 9320-9326
[93] C. Chun, J. Ghim, M.-J. Kim, D. Y. Kim, *J. Polym. Sci., Part A: Polym. Chem.* **2005**, *43*(16), 3525-3532
[94] O. Henneberg, T. Geue, M. Saphiannikova, U. Pietsch, P. Rochon, A. Natansohn, *Appl. Surf. Sci.* **2001**, *182*(3-4), 272-279
[95] K. G. Yager, O. M. Tanchak, C. Godbout, H. Fritzsche, C. J. Barrett, *Macromolecules* **2006**, *39*(26), 9311-9319
[96] P. Leffin, C. Fiorini, J.-M. Nunzi, *Opt. Mater.* **1998**, *9*, 323-328
[97] K. Yang, S. Yang, J. Kumar, *Phys. Rev. B* **2006**, *73*(16), 165204/1-165204/14
[98] J. Kumar, L. Li, X. L. Jiang, D. Y. Kim, T. S. Lee, S. Tripathy, *Appl. Phys. Lett.* **1998**, *72*(17), 2096-2098
[99] O. Kulikovska, L. M. Goldenberg, J. Stumpe, *Chem. Mat.* **2007**, *19*(13), 3343-3348
[100] L. M. Goldenberg, Y. Gritsai, O. Kulikovska, J. Stumpe, *Opt. Lett.* **2008**, *33*(12), 1309-1311
[101] O. Kulikovska, L. M. Goldenberg, L. Kulikovsky, J. Stumpe, *Chem. Mat.* **2008**, *20*(10), 3528-3534
[102] G. Tammann, *Zeit. Physikal. Chem.* **1898**, *25*, 441-79
[103] B. Rosenberg, *J. Chem. Phys.* **1959**, *31*, 238-46
[104] J. H. Magill, *J. Chem. Phys.* **1967**, *47*(8), 2802-7
[105] J. H. Magill, D. J. Plazek, *J. Chem. Phys.* **1967**, *46*(10), 3757-69
[106] Y. Sano, K. Kato, M. Yokoyama, Y. Shirota, H. Mikawa, *Mol. Cryst. Liq. Cryst.* **1976**, *36*(1-2), 137-41
[107] A. Fullsow, *J. Alc. Res.* **1981**, *33*(66), 99-111
[108] Y. Shirota, *J. Mater. Chem.* **2000**, *10*(1), 1-25
[109] P. Strohriegl, J. V. Grazulevicius, *Adv. Mater.* **2002**, *14*(20), 1439-1452
[110] J. Dai, S. W. Chang, A. Hamad, D. Yang, N. Felix, C. K. Ober, *Chem. Mat.* **2006**, *18*(15), 3404-3411
[111] F. Steuber, J. Staudigel, M. Stössel, J. Simmerer, A. Winnacker, H. Spreitzer, F. Weissörtel, J. Salbeck, *Adv. Mater.* **2000**, *12*, 130-133
[112] J. M. Shaw, P. F. Seidler, *IBM J. Res. Dev.* **2001**, *45*(1), 3-9
[113] M. Van der Auweraer, F. C. De Schryver, P. M. Borsenberger, H. Bassler, *Adv. Mater.* **1994**, *6*(3), 199-213
[114] C. W. Tang, S. A. VanSlyke, *Appl. Phys. Lett.* **1987**, *51*(12), 913-15
[115] M. Thelakkat, H. W. Schmidt, *Adv. Mater.* **1998**, *10*(3), 219-223
[116] U. Bach, D. Lupo, P. Comte, J. E. Moser, F. Weissortel, J. Salbeck, H. Spreitzer, M. Gratzel, *Nature* **1998**, *395*(6702), 583-585

[117] M. Thelakkat, C. Schmitz, C. Hohle, P. Strohriegl, H.-W. Schmidt, U. Hofmann, S. Schloter, D. Haarer, *Phys. Chem. Chem. Phys.* **1999**, *1*(8), 1693-1698
[118] M. Yoshiiwa, H. Kageyama, Y. Shirota, F. Wakaya, K. Gamo, M. Takai, *Appl. Phys. Lett.* **1996**, *69*(17), 2605-2607
[119] R. H. Friend, R. W. Gymer, A. B. Holmes, J. H. Burroughes, R. N. Marks, C. Taliani, D. D. C. Bradley, D. A. Dos Santos, J. L. Bredas, M. Logdlund, W. R. Salaneck, *Nature* **1999**, *397*(6715), 121-128
[120] J. H. Burroughes, D. D. C. Bradley, A. R. Brown, R. N. Marks, K. Mackay, R. H. Friend, P. L. Burns, A. B. Holmes, *Nature* **1990**, *347*(6293), 539-41
[121] C. J. Brabec, N. S. Sariciftci, J. C. Hummelen, *Adv. Funct. Mater.* **2001**, *11*(1), 15-26
[122] S. Guenes, H. Neugebauer, N. S. Sariciftci, *Chem. Rev.* **2007**, *107*(4), 1324-1338
[123] M. T. Bernius, M. Inbasekaran, J. O'Brien, W. Wu, *Adv. Mater.* **2000**, *12*(23), 1737-1750
[124] A. C. Mayer, S. R. Scully, B. E. Hardin, M. W. Rowell, M. D. McGehee, *Mat. Today* **2007**, *10*(11), 28-33
[125] K. Naito, A. Miura, *J. Phys. Chem.* **1993**, *97*(23), 6240-8
[126] B. E. Koene, D. E. Loy, M. E. Thompson, *Chem. Mater.* **1998**, *10*(8), 2235-2250
[127] G. Adam, J. H. Gibbs, *J. Chem. Phys.* **1965**, *43*(1), 139-46
[128] Y. Shirota, K. Moriwaki, S. Yoshikawa, T. Ujike, H. Nakano, *J. Mater. Chem.* **1998**, *8*(12), 2579-2581
[129] D. Nagahama, T. Ujike, K. Moriwaki, S. Yoshikawa, H. Nakano, Y. Shirota, *J. Photopolym. Sci. Technol.* **1999**, *12*(2), 277-278
[130] T. Tanino, S. Yoshikawa, T. Ujike, D. Nagahama, K. Moriwaki, T. Takahashi, Y. Kotani, H. Nakano, Y. Shirota, *J. Mater. Chem.* **2007**, *17*(47), 4953-4963
[131] H. Nakano, *J. Photopolym. Sci. Technol.* **2008**, *21*(4), 545-547
[132] T. Fuhrmann, T. Tsutsui, *Chem. Mater.* **1999**, *11*(8), 2226-2232
[133] A. Perschke, T. Fuhrmann, *Adv. Mater.* **2002**, *14*(11), 841-843
[134] N. Reinke, A. Draude, T. Fuhrmann, H. Franke, R. A. Lessard, *Appl. Phys. B* **2004**, *78*, 205-209
[135] E. Ishow, A. Brosseau, G. Clavier, K. Nakatani, R. B. Pansu, J.-J. Vachon, P. Tauc, D. Chauvat, C. R. Mendonca, E. Piovesan, *J. Am. Chem. Soc.* **2007**, *129*(29), 8970-8971
[136] L.-H. Liu, K. Nakatani, R. Pansu, J.-J. Vachon, P. Tauc, E. Ishow, *Adv. Mater.* **2007**, *19*(3), 433-436
[137] E. Ishow, B. Lebon, Y. He, X. Wang, L. Bouteiller, L. Galmiche, K. Nakatani, *Chem. Mater.* **2006**, *18*(5), 1261-1267
[138] E. Ishow, R. Camacho-Aguilera, J. Guerin, A. Brosseau, K. Nakatani, *Adv. Funct. Mater.* **2009**, *19*(5), 796-804
[139] H. Nakano, T. Takahashi, T. Tanino, Y. Shirota, *J. Photopolym. Sci. Technol.* **2007**, *20*(1), 87-89
[140] H. Nakano, T. Takahashi, Y. Shirota, *J. Photopolym. Sci. Technol.* **2009**, *22*(2), 253-255
[141] H. Nakano, T. Takahashi, T. Kadota, Y. Shirota, *Adv. Mater.* **2002**, *14*(16), 1157-1160
[142] H. Nakano, T. Tanino, T. Takahashi, H. Ando, Y. Shirota, *J. Mater. Chem.* **2008**, *18*(2), 242-246
[143] E.-M. Seo, M. J. Kim, Y.-D. Shin, J.-S. Lee, D.-Y. Kim, *Mol. Cryst. Liq. Cryst.* **2001**, *370*, 143-146
[144] A. Stracke, J. H. Wendorff, D. Goldmann, D. Janietz, B. Stiller, *Adv. Mater.* **2000**, *12*(4), 282-285
[145] A. Stracke, J. H. Wendorff, D. Goldmann, D. Janietz, *Liq. Cryst.* **2000**, *27*(8), 1049-1057
[146] M.-J. Kim, E.-M. Seo, D. Vak, D.-Y. Kim, *Chem. Mat.* **2003**, *15*(21), 4021-4027
[147] H. Ando, T. Takahashi, H. Nakano, Y. Shirota, *Chem. Lett.* **2003**, *32*(8), 710-711
[148] H. Ando, T. Tanino, H. Nakano, Y. Shirota, *Mater. Chem. Phys.* **2009**, *113*(1), 376-381
[149] C. Chun, M.-J. Kim, D. Vak, D. Y. Kim, *J. Mater. Chem.* **2003**, *13*(12), 2904-2909
[150] K. Kreger, P. Wolfer, H. Audorff, L. Kador, N. Stingelin-Stutzmann, P. Smith, H.-W. Schmidt, *J. Am. Chem. Soc.*, *132*(2), 509-516

AIM OF THE THESIS

The main research focus of this work is the synthesis and characterization of azobenzene-containing molecular glasses as functional materials for holographic applications. For this purpose, molecular glasses are an ideal class of materials as their material properties can be easily tailored following a modular design principle. The synthesized compounds will be based on several different core moieties which are functionalized with three or four azobenzene chromophores as side-arms. Moreover, these azobenzene units should contain terminal substituents which will allow us to fine-tune the physical and photo-physical properties. This way, the compounds can be developed and optimized for specific holographic applications and fundamental experiments. In this thesis, the focus is on the formation of *surface relief nanostructures* as well as on the inscription of *holographic volume gratings*. These experiments will be performed in close collaboration with Prof. Dr. Lothar Kador and Dipl. Phys. Hubert Audorff from the “Bayreuth Institute of Macromolecular Research”.

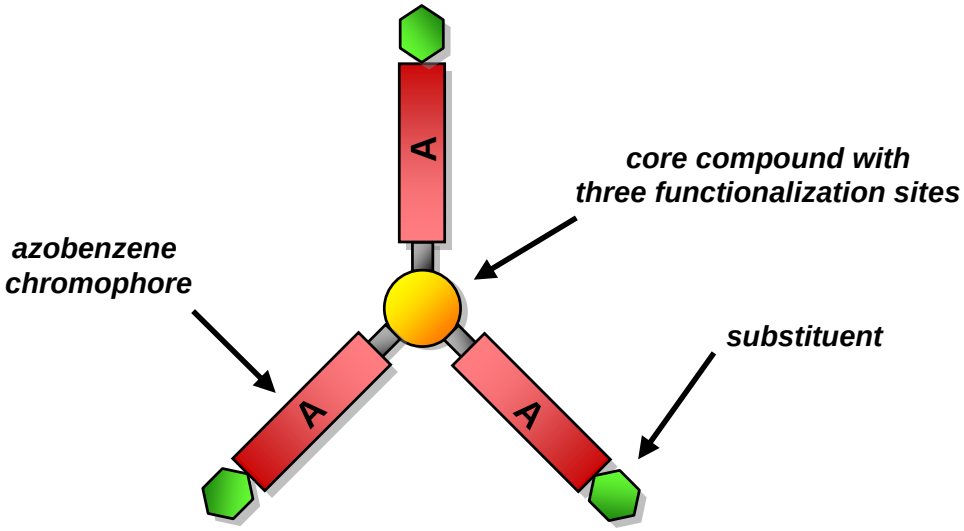

Figure 14: Schematic representation of an azobenzene-functionalized molecular glass. The three-arm starshaped topology is a typical example for compounds synthesized in this thesis.

The controlled preparation of *surface relief structures* is an important application for azobenzene-containing molecular glasses. Therefore, photochromic materials are demanded which show high SRG amplitudes as well as fast build-up behaviour. To this end, a new series of azobenzene-

containing molecular glasses with high glass transition temperatures has to be synthesized and in subsequent experiments SRGs have to be inscribed. For a profound understanding of the SRG formation process, structure-property relationships between the molecular structure and the SRG height need to be established. As the formation process could to date not been satisfactorally explained, the experimental results should be correlated with theoretical considerations. Finally the fabricated SRGs will be examined in terms of possible applications as holographic optical elements.

As described in the introduction, volume holography is a highly promising technology for optical data storage. However, current rewritable materials still present certain disadvantages, for example the writing speed of *holographic volume gratings*. Material concepts especially for improving this property are challenging. In this work, we will combine the superior long-term stability of polymer systems with the higher photo-physical sensitivity of molecular glasses for the first time, thus creating a holographic material which has the advantages of both material classes. In order to tailor a suitable blending material with optimized physical and photo-physical properties, a variety of different azobenzene-containing molecular glasses have to be synthesized and screened with respect to their holographic properties. The most suitable material will be selected and employed in blending experiments. Furthermore, we will verify if this concept is also applicable for photoaddressable block copolymer systems in order to demonstrate that photoresponsive molecular glasses are promising candidates for enhancing the holographic recording sensitivity of rewritable materials for volume holography.

In addition, azobenzene-containing low molecular weight materials are an interesting material class for inscription of holographic volume gratings for themselves. Unfortunately the long-term stability of such compounds is often inferior compared to polymers. By incorporation of bisazobenzene chromophores, we intend to introduce a more shape-anisotropic moiety to foster liquid-crystalline behaviour. Therewith a stable photo-orientation can be achieved, which would make these compounds interesting candidates for inscription of holographic volume gratings with long-term stability.

SYNOPSIS

This thesis addresses the topic of tailored azobenzene-containing molecular glasses as functional materials for holographic applications. In a series of five individual publications, this cumulative thesis describes the materials and methods for achieving this goal. In this chapter, first and foremost, a general overview of my work is presented, followed by a short summary of key results of each publication. The different aspects of this work are elaborated in more detail in their respective publications, specified in the chapters 4.2 to 4.6.

The azobenzene-functionalized molecular glasses discussed in this work are based on several different core compounds functionalized with three or four azobenzene side groups. These azobenzene moieties feature distinct substituents which opened the way to study their influence on the physical and photo-physical properties of the whole material. The chromophores are linked to the cores by esterification reactions as the formation of ester linkages provides an easy access to a large variety of compounds. In turn, this modular design principle allows us to fine-tune the required material characteristics. These include e.g. the glassforming ability, light absorption properties and the photo-physical sensitivity in holographic experiments. Consequently, the azobenzene-containing molecular glasses discussed here can be easily tailored by changing the building blocks in order to fulfill specific purposes in holographic experiments (see Figure 15).

The presented publications can be subdivided into three different topics, which are arranged in a sequence reflecting their affiliation to a specific holographic application.

In the first two chapters, materials for the inscription of *surface relief nanostructures* are presented. By employing a voluminous core and dipolar substituents at the azobenzene moiety, materials with high glass transitions and high optical susceptibility could be synthesized, which make them ideal candidates for SRG formation.

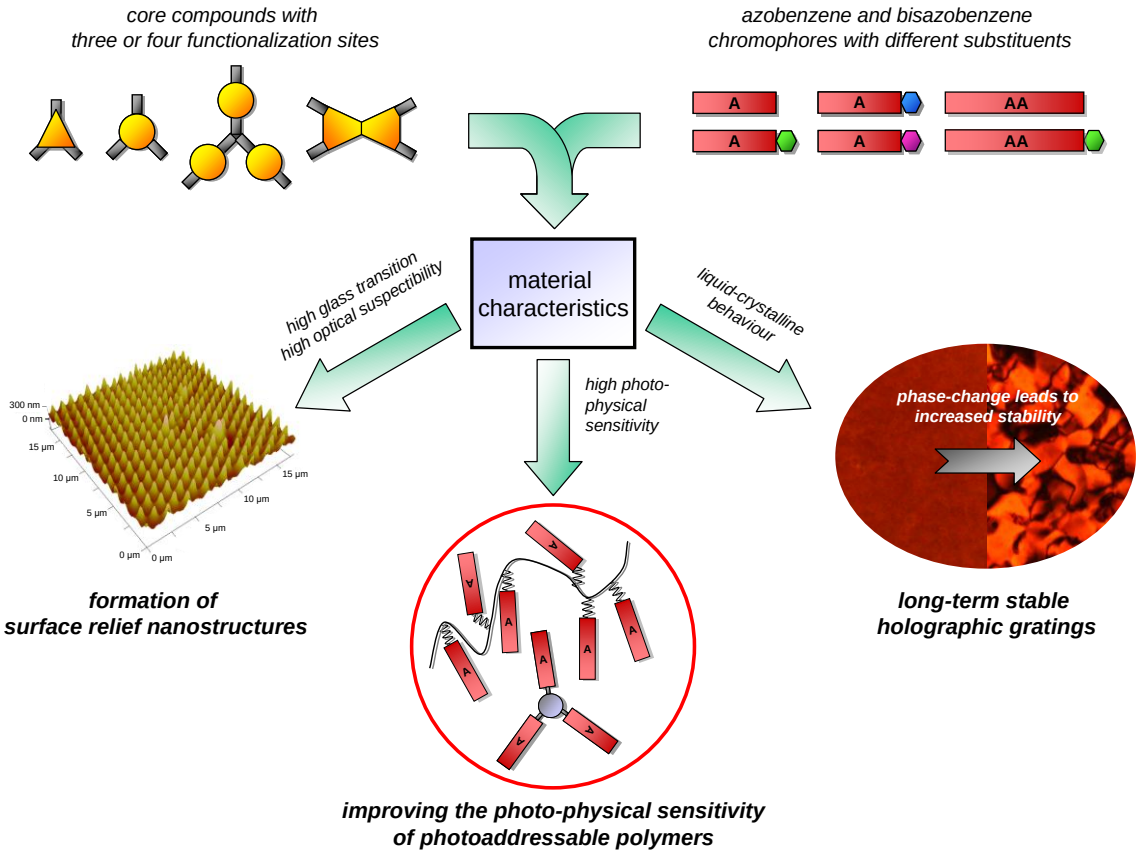

Figure 15: Modular design principle for tailoring azobenzene-functionalized molecular glasses as functional materials for holographic experiments.

The next two chapters are dedicated to azobenzene-containing molecular glasses which are investigated as *components in blends* to improve the holographic recording sensitivity of photoaddressable polymers. For this purpose, a variety of molecular glasses was synthesized and screened with respect to their photo-physical properties. The material with the best combination of structural variations was employed for blending to obtain an improved material which combines the superior long-term stability of polymer systems with the higher photo-physical sensitivity of molecular glasses.

In the last chapter low molecular-weight materials in which *long-term stable holographic gratings* can be inscribed are presented. Ordinarily azobenzene-functionalized low molecular-weight compounds do not exhibit stable photo-orientation. However by incorporation of bisazobenzene moieties, a liquid-crystalline phase could be introduced. Thus, the long-term stability in holographic experiments is enhanced and post-development of the refractive index modulation is achieved.

Synthesis and structure-property relations of a series of photochromic molecular glasses for controlled and efficient formation of surface relief nanostructures

The first chapter of this thesis is dedicated to the synthesis and characterization of a new series of photochromic molecular glasses based on a triphenylamine core and different azobenzene moieties. By changing the substitution at the azobenzene moiety, the formation of a stable amorphous phase is promoted and the absorption properties of the molecular glasses can be fine-tuned. Structure-property relations are established with respect to an efficient formation of surface relief nanostructures. We demonstrated that the maximum achievable SRG height increases with the optical susceptibility at the wavelength of the writing laser and decreases with larger chromophore size (Figure 16).

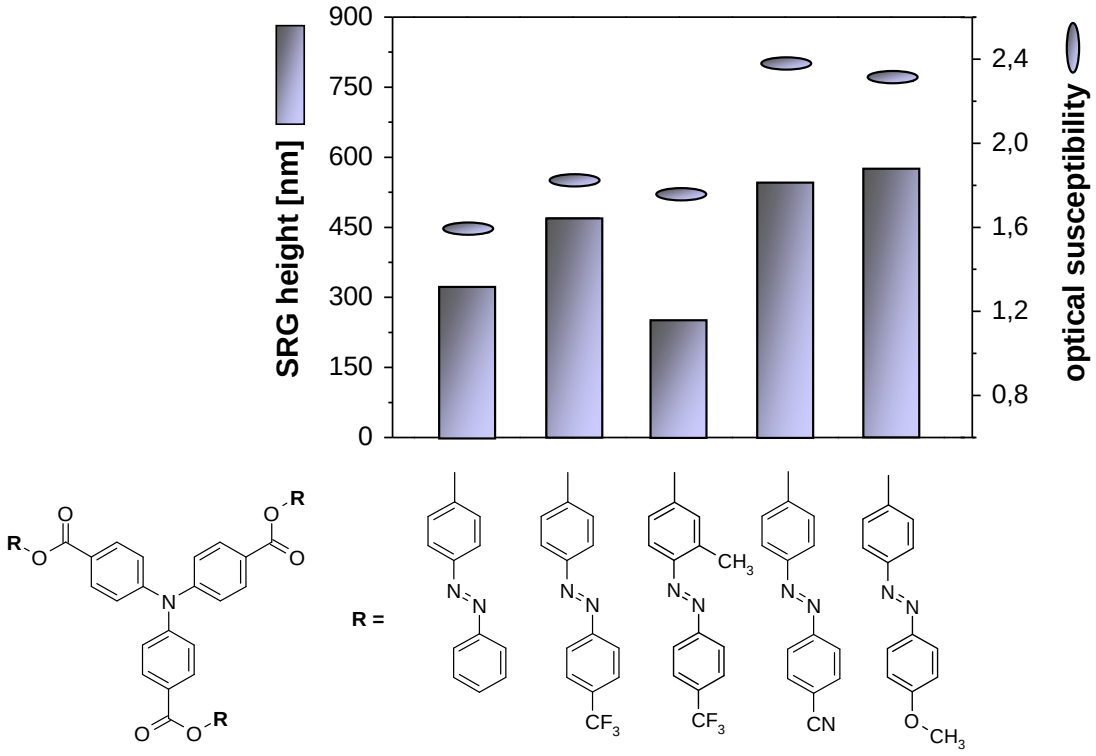

Figure 16: Maximum SRG height (bars) as measured at room temperature with polarization configuration ±45° and optical susceptibility (ellipses) of the sample films.

By employing temperature-dependent holographic measurements we were able to monitor SRG build-up and stability at elevated temperatures as well as determine the glass transition temperature of the material.

Furthermore, the holographically generated SRGs of molecular glass films are stable enough to be transferred easily and with high accuracy to the surface of thermoplastic polymers such as polycarbonate via common replica/imprinting procedures (see Figure 17).

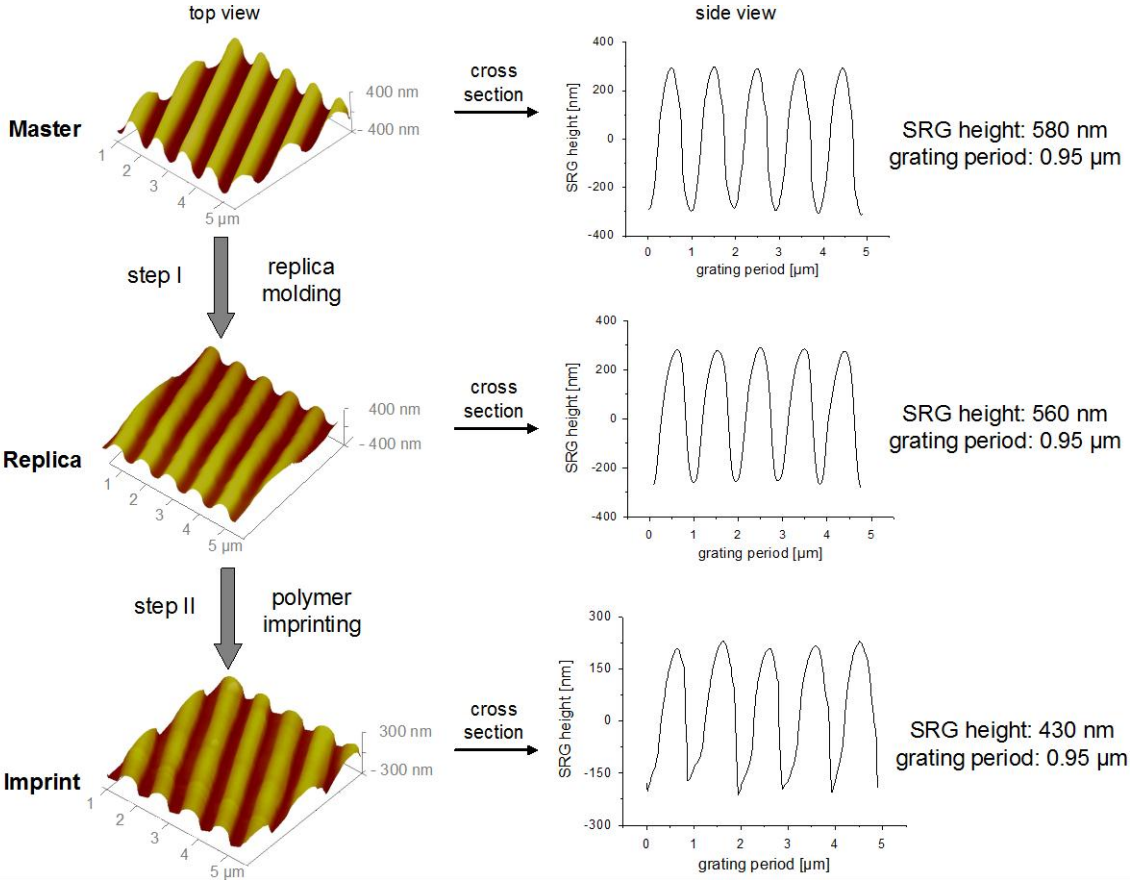

Figure 17: Example of transferring a SRG to a polymer surface. AFM characterization: 3D surface plots (left) and the corresponding cross sections (right) for the original SRG structures (top), the replica (middle), and the imprint on polycarbonate (bottom) are shown.

Polarization dependence of the formation of surface relief gratings in azobenzene-containing molecular glasses

In this part of the thesis a comprehensive study on the formation of surface relief gratings is presented. As seen in Figure 18, there are two main processes which contribute the growth of the diffraction efficiency: the volume grating, which is due to chromophore reorientation dominating in the first few seconds, and the SRG, which mostly contributes to the observed diffraction efficiency at later times. From the measured diffraction efficiencies, the corresponding modulation heights can be directly calculated. The achieved maximum SRG heights could be independently confirmed by atomic force microscopy.

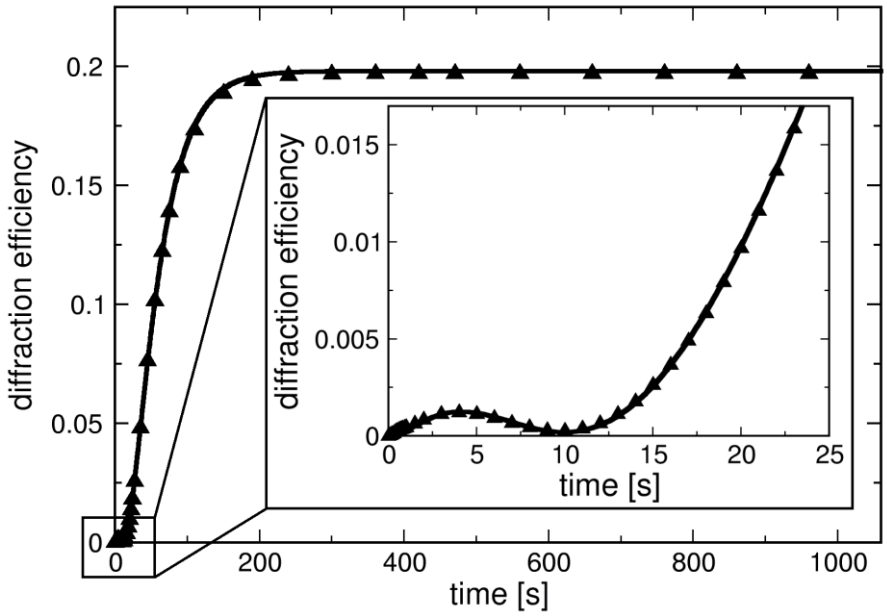

Figure 18: Typical temporal evolution of the diffraction efficiency η *(t)* during hologram inscription on a thin film of the azobenzene-containing molecular glass. Writing was performed with the laser polarization configuration ±45º. The black triangles correspond to measured data, whereas the curve represents the fit. In the first few seconds, the diffraction efficiency due to reorientation of the chromophores in the bulk is visible (see inset); later on the influence of the SRG dominates.

By systematically applying seven different polarization configurations of the laser beams, we found that these experimental conditions have a major influence on the rate of formation and the achievable amplitude of SRGs (shown in Figure 19). Our results are in good agreement with the gradient force model and we suggest that the grating heights generated with different writing polarizations can be ascribed to the varying strengths of the gradient force.

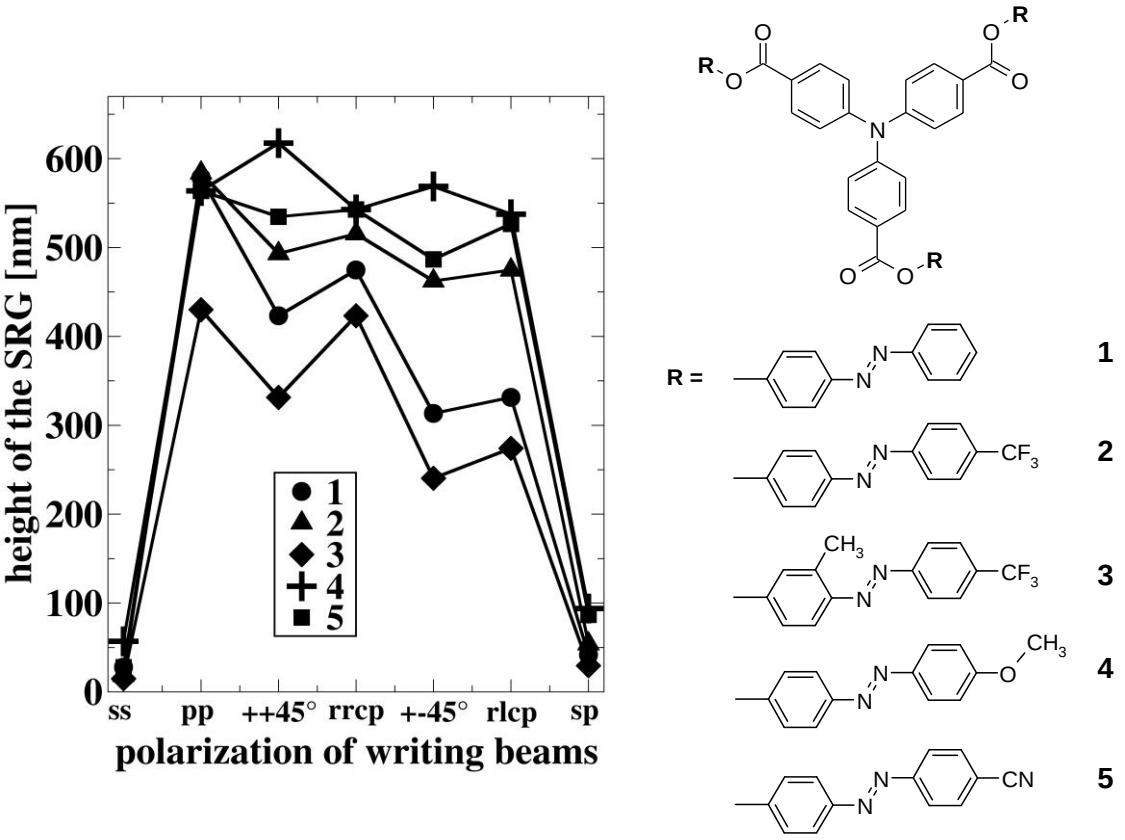

Figure 19: Maximum height of the SRGs of all five materials with the different polarization settings. The lines are a guide to the eye.

Holographic investigations of azobenzene-containing low molecular weight compounds in pure materials and binary blends with polystyrene

This chapter of my thesis deals with the formation of holographic phase gratings in molecular glasses containing azobenzene moieties. A variety of molecular glasses was synthesized (Figure 20) and screened with respect to their photo-physical properties. Various end groups at the azobenzene chromophore and different core compounds were employed to obtain high thermal stability and good glass-forming properties as well as high sensitivity.

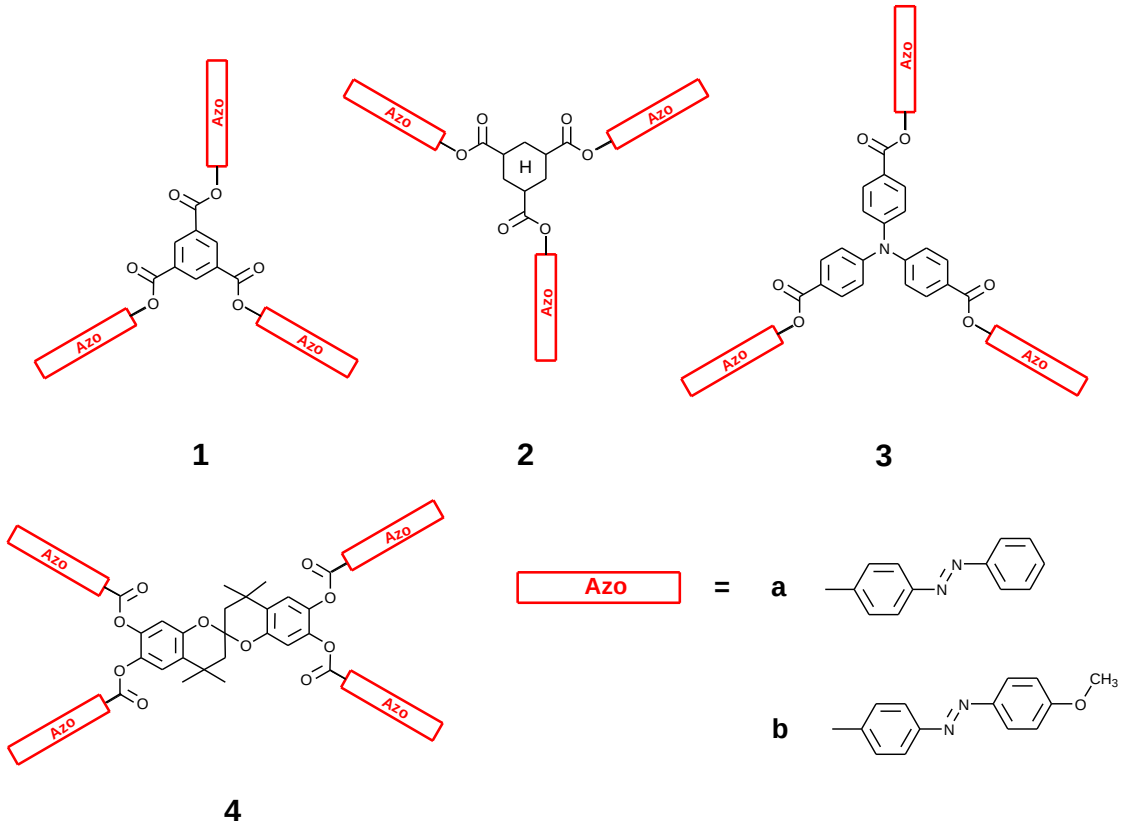

Figure 20: Schematic illustration of the photo-addressable azobenzene-containing molecular glasses.

The best combination of structural variations (compound **2b**) was investigated at elevated temperatures where the inscription times of the holographic volume gratings could be further improved (see Figure 21). Hence, this photochromic compounds appear to be attractive candidates towards rewritable holographic recording media with improved writing speed.

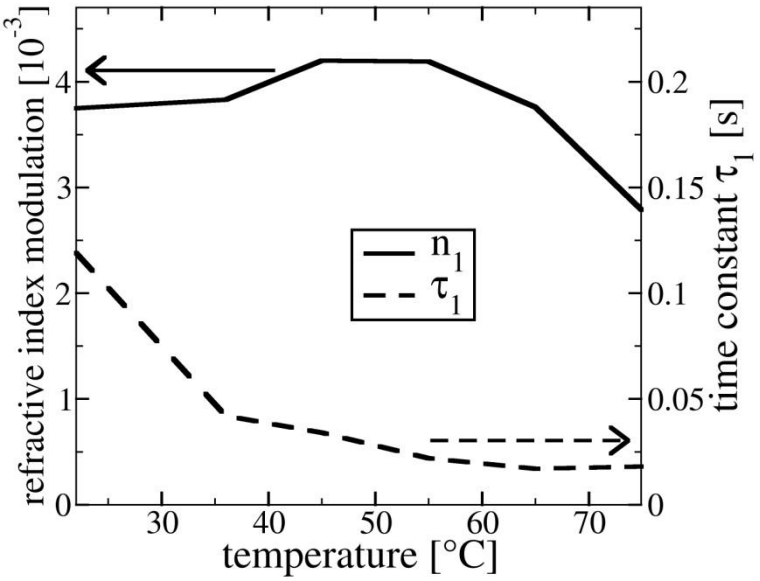

Figure 21: Temperature dependence of time constant τ_1 describing the hologram growth during inscription (broken line; right-hand scale) and maximum refractive-index modulation $n_{1\ max}$ (solid line; left-hand scale). Holographic gratings were inscribed at 22 °C 36 °C, 45 °C, 55 °C, 65 °C, and 75 °C.

Improving the holographic recording sensitivity of photoaddressable azobenzene-containing polymers with photochromic molecular glasses

After screening the photo-physical properties of the azobenzene-containing molecular glasses (previous chapter), the best suited compound is utilized as blending material to improve the holographic recording sensitivity of different photoaddressable polymers (see Figure 22).

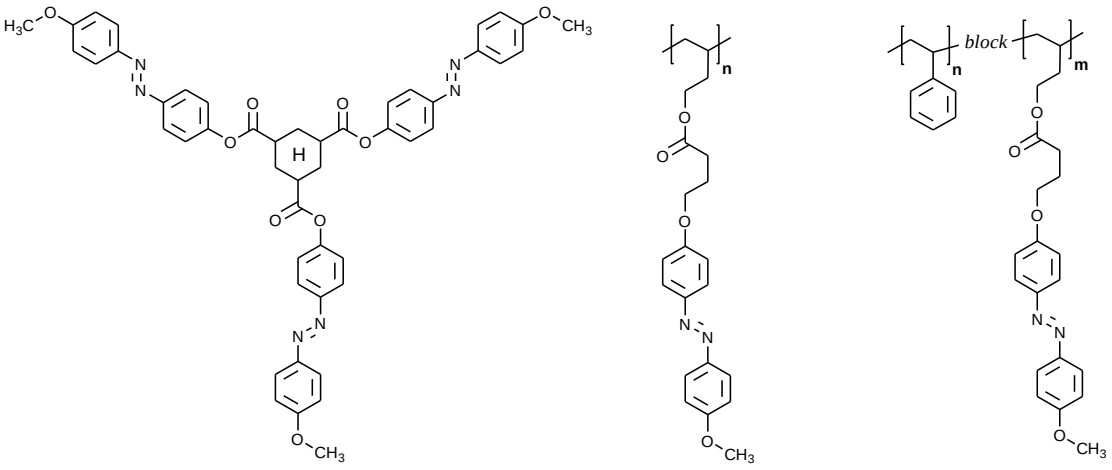

1 **2** **3**

Figure 22: Chemical structures of the utilized photoaddressable azobenzene-containing materials; molecular glass **1**, homopolymer **2** and blockcopolymer **3**.

By blending this photoresponsive molecular glass (compound **1**) into a photoaddressable homopolymer (**2**) we prove that the high stability of a polymer system can be combined with the faster response of a molecular glass to form a photoaddressable material which clearly exhibits a higher sensitivity and, in addition, has the superior long-term stability of polymers (shown in Figure 23).

By verifying that this concept is also suitable for a blockcopolymer system (**3**) we demonstrate that photoresponsive molecular glasses are a promising candidate for improving stable rewritable materials for volume holography. Already a blend comprising as less as 10wt% allowed us to significantly decrease the holographic time of the whole system (see Figure 24).

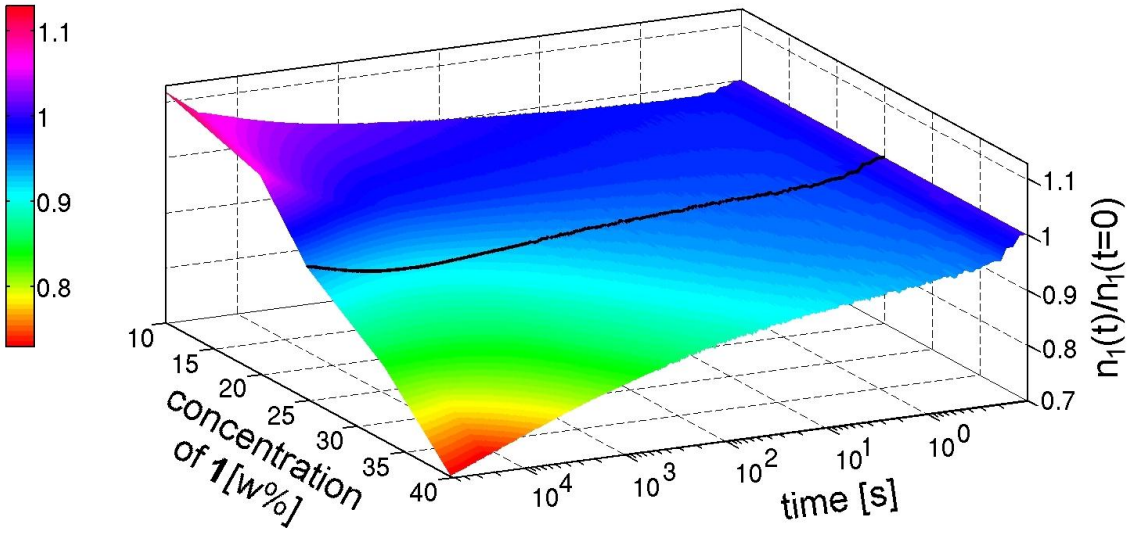

Figure 23: Temporal evolution of the normalized refractive-index modulation of blends of the molecular glass **1** with a photoaddressable homopolymer **2** as a function of the content of **1**. The refractive index modulation is normalized to a value of one at the time zero when the writing laser is turned off. The black line indicates the blend with 25 wt% of molecular glass, which still exhibits a positive slope of n_1 after 12 h.

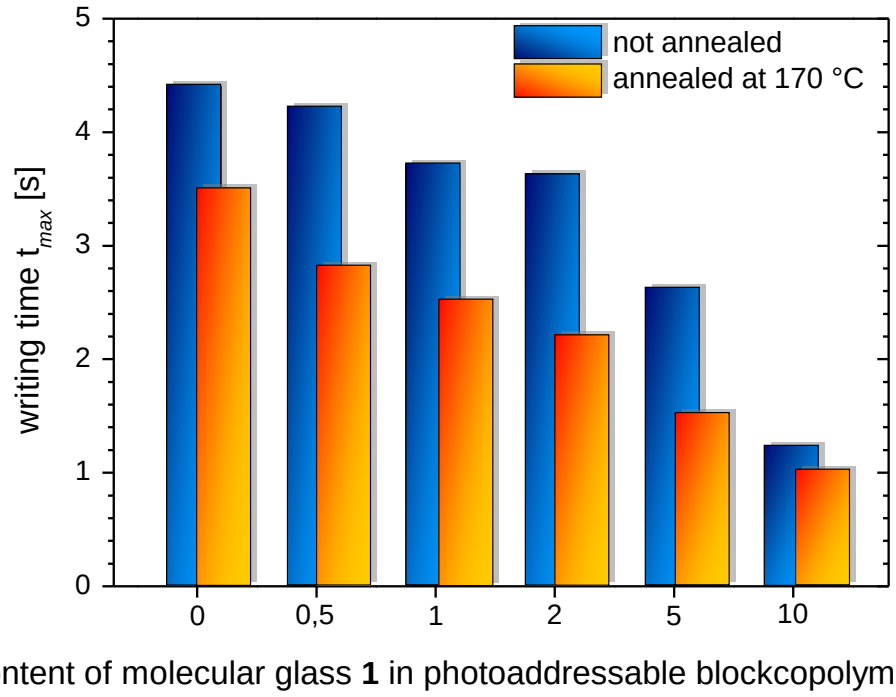

Figure 24: Holographic properties of blends of the molecular glass **1** with a photoaddressable block copolymer **3**. Writing time to 90 % of the maximum of the refractive-index modulation is plotted as a function of the content of **1**. The dark columns correspond to not annealed samples, the light columns to samples annealed at 170 °C.

Stable holographic volume gratings with novel photochromic bisazobenzene-based low molecular weight compounds

In the last chapter the synthesis and characterization of novel photochromic bisazobenzene-functionalized low molecular-weight compounds based on a triphenylamine core are presented (Figure 25). Additionally, these materials were screened with respect to their photo-physical response in holographic experiments. By employing bisazobenzene chromophores it is possible to enhance the maximum refractive index modulation compared to similar molecular glasses with ordinary azobenzene moieties. With the introduction of a methoxy substituent at the chromophores we were able to introduce a liquid-crystalline phase in the compound.

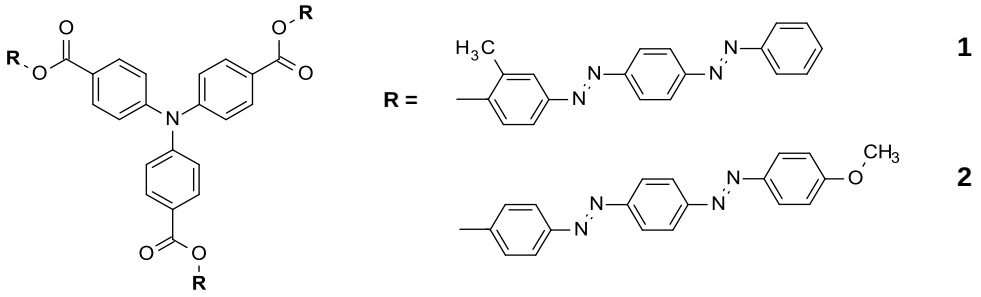

Figure 25: Molecular structures of bisazobenzene-functionalized low molecular-weight compounds.

For the first time, a long-term stable photoorientation in bisazobenzene-functionalized low molecular-weight materials could be verified (as shown in Figure 26). This behaviour is attributed to the present, latent liquid-crystalline phase in the amorphous state. The possibility of inscribing long-term stable volume gratings in systems which are solely based on small molecular materials make these compounds an interesting candidate for holographic data storage.

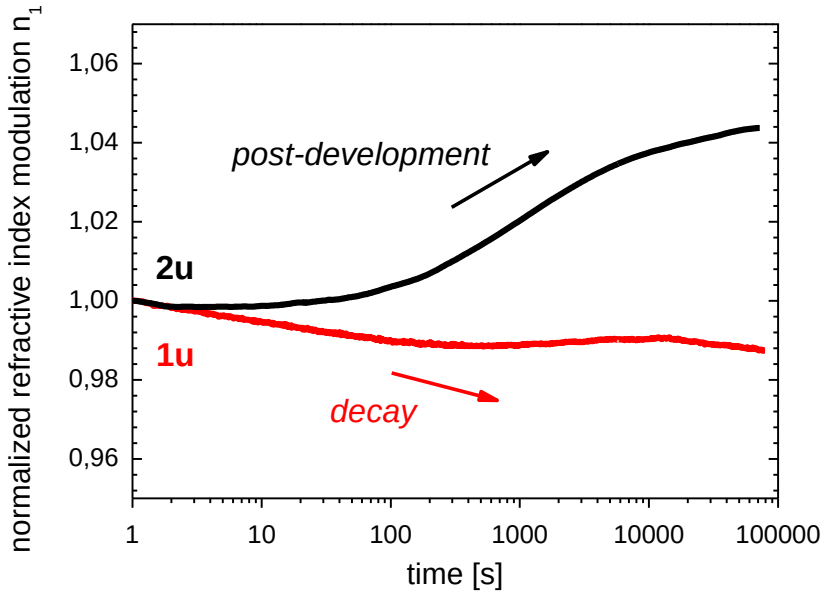

Figure 26: Temporal evolution of the normalized refractive index modulation (norm. to t = 1 s) of volume phase gratings inscribed in blends of **1** and **2** with 10 wt% of ULTEM©. The writing laser was turned off at t = 0. The general trend of evolution of the refractive index modulation is depicted by the arrows. Note the logarithmic time scale.

PUBLICATIONS & MANUSCRIPTS

4.1 Individual contributions to joint publications

The work presented in this thesis was carried out under the supervision of Prof. Dr. Hans-Werner Schmidt at the chair of Macromolecular Chemistry I, and in close cooperation with Prof. Dr. Lothar Kador and Dipl. Phys. Hubert Audorff in the "Bayreuth Institute of Macromolecular Research". In the following, individual contributions to the publications of this thesis are presented.

Chapter 4.2

SYNTHESIS AND STRUCTURE-PROPERTY RELATIONS OF A SERIES OF PHOTOCHROMIC MOLECULAR GLASSES FOR CONTROLLED AND EFFICIENT FORMATION OF SURFACE RELIEF NANOSTRUCTURES

published in *Advanced Functional Materials* **2009**, *19*(16), 2630-2638
by *Roland Walker, Hubert Audorff, Lothar Kador,* and *Hans-Werner Schmidt*

The synthesis as well as the characterization of all materials was carried out by myself. Additionally, I did the work concerning the replica and imprinting techniques. Hubert Audorff did the holographic experiments. I wrote the manuscript which was finalized with the help of all coauthors. Hans-Werner Schmidt and Lothar Kador were involved in discussions.

Chapter 4.3

POLARIZATION DEPENDENCE OF THE FORMATION OF SURFACE RELIEF GRATINGS IN AZOBENZENE-CONTAINING MOLECULAR GLASSES

published in *Journal of Physical Chemistry B* **2009**, *113*, 3379-3384
by *Hubert Audorff, Roland Walker, Lothar Kador,* and *Hans-Werner Schmidt*

I did the synthesis of the utilized compounds as well as the sample preparation. The holographic experiments were carried out by Hubert Audorff. He also wrote the manuscript. Lothar Kador and Hans-Werner Schmidt were involved in discussions and corrections of the manuscript.

Chapter 4.4

HOLOGRAPHIC INVESTIGATIONS OF AZOBENZENE-CONTAINING LOW MOLECULAR WEIGHT COMPOUNDS IN PURE MATERIALS AND BINARY BLENDS WITH POLYSTYRENE
submitted to *Chemistry – A European Journal*
by *Hubert Audorff, Roland Walker, Lothar Kador,* and *Hans-Werner Schmidt*

The synthetic work and the characterization of all materials were performed by myself. I did the sample preparation for the holographic experiments, which were subsequently carried out by Hubert Audorff. He wrote the first draft which afterwards was finalized by myself, Lothar Kador and Hans-Werner Schmidt.

Chapter 4.5

IMPROVING THE HOLOGRAPHIC RECORDING SENSITIVITY OF PHOTOADDRESSABLE AZOBENZENE-CONTAINING POLYMERS WITH PHOTOCHROMIC MOLECULAR GLASSES
intended for publication in *Advanced Materials*
by *Roland Walker, Hubert Audorff, Lothar Kador,* and *Hans-Werner Schmidt*

The synthesis and characterization of the molecular glass, the sample preparation as well as the annealing experiments were carried out by myself. Hubert Audorff did the holographic experiments. Afterwards I wrote the first draft of the manuscript. It was completed with the help of Hans-Werner Schmidt and Lothar Kador.

Chapter 4.6

STABLE HOLOGRAPHIC VOLUME GRATINGS WITH NOVEL PHOTOCHROMIC BISAZOBENZENE-BASED LOW MOLECULAR WEIGHT COMPOUNDS
intended for publication in *Chemistry of Materials*
by *Roland Walker, Hubert Audorff, Lothar Kador,* and *Hans-Werner Schmidt*

This paper originated from my additional synthetic work and the complete characterization of the novel materials. The necessary holographic experiments were done by Hubert Audorff. The first draft was written by myself and finalized with the help of Hans-Werner Schmidt and Lothar Kador.

4.2 Synthesis and Structure-Property Relations of a Series of Photochromic Molecular Glasses for Controlled and Efficient Formation of Surface Relief Nanostructures

By *Roland Walker*, *Hubert Audorff*, *Lothar Kador* and *Hans-Werner Schmidt**

[*] Prof. H.-W. Schmidt, R. Walker
University of Bayreuth, Macromolecular Chemistry I and
"Bayreuth Institute of Macromolecular Research"
D-95440 Bayreuth (Germany)
E-mail: hans-werner.schmidt@uni-bayreuth.de

Prof. L. Kador, H. Audorff
University of Bayreuth, "Bayreuth Institute of Macromolecular Research"
D-95440 Bayreuth (Germany)
E-mail: lothar.kador@uni-bayreuth.de

This paper is published in
Advanced Functional Materials 2009*, 19(16), 2630-2638*

Keywords: molecular glasses, photochromic glasses, azobenzene, surface relief nanostructures, photoinduced mass transport

Abstract

This paper reports on the synthesis and properties of a new series of photochromic molecular glasses and their structure-property relations with respect to a controlled and efficient formation of surface relief nanostructures. The aim of the paper is to establish a correlation between molecular structure, optical susceptibility and the achievable surface relief heights. The molecular glasses consist of a triphenylamine core and three azobenzene side groups attached via an ester linkage. Structural variations are performed with respect to the substitution at the azobenzene moiety in order to promote a formation of a stable amorphous phase and to tune absorption properties and molecular dynamics. Surface relief gratings (SRGs) and complex surface patterns can easily be inscribed via holographic techniques. The modulation heights are determined with an equation adopted from the theory for thin gratings, and the values are confirmed with AFM measurements. Temperature-dependent holographic measurements allow us to monitor SRG build-up and decay and the stability at elevated temperatures, as well as determination of the glass transition temperature. SRG modulation heights of above 600 nm are achieved. These are the highest values reported for molecular glasses to date. The surface patterns of the molecular glasses are stable enough to be copied in a replica molding process. It is demonstrated that the replica can be used to transfer the surface pattern onto a common thermoplastic polymer.

Introduction

Molecular glasses represent an emerging material class of great relevance for electronic, optical, and electrooptic applications. Such materials are used in a wide range of devices, e.g., in photoconductor drums, organic light emitting diodes, organic solar cells, etc.[1] In contrast to functional polymers[2] used in these applications, molecular glasses have the advantage of a well-defined molecular structure, no molecular weight distribution and no undefined endgroups. They can be highly purified with established methods of organic chemistry such as absorption chromatography or recrystallization.

Another subject of current interest are photochromic materials based on azobenzene moieties. Here, possible applications are, e.g., in the field of optical information storage and security devices.[3] Upon light absorption, the azobenzene moiety undergoes multiple reversible *trans-cis-trans* photo-isomerization cycles. In the bulk these motions finally cause a reorientation of the chromophores perpendicular to the polarization plane of the incident light. In addition to the photoinduced reorientation, a macroscopic mass transport which leads to the formation of surface relief gratings (SRGs) can be induced by illumination with two interfering laser beams.[4-6] Hereby it is possible to fine-tune modulation heights and grating period as well as to create more complex surface relief patterns by sequentially inscribing several superimposed gratings. The phenomenon of SRG formation has been mainly investigated in polymers carrying azobenzene moieties as side groups.[7-10] The group of Stumpe et al. optically generated microstructures in polymers based on ionic interactions between azobenzene units and polyelectrolytes.[11] This concept was also extended to sol-gel based materials with ionic interactions.[12] Furthermore SRG formation was demonstrated in photochromic molecular glasses with modulation heights ranging between 150 and 490 nm.[13] Kim *et al*. showed that the photoinduced growth of SRGs can be more efficient in thin films of a molecular glass as compared to polymers, since the mass transport is not hindered by entanglements of the polymer chains.[14,15] Up to date SRG formation is mainly performed at room temperature, and the achieved heights are often correlated to the glass transition temperature of the molecular glass. Above T_g the surface patterns are destroyed and the initial smooth sample surface is restored.[14,16] Possible applications of SRGs are, for example, liquid-crystal anchoring, waveguide couplers, polarization discriminators,[17] or antireflection coatings for the visible region.[18,19] In addition, SRGs might be used as optical devices [20] such as channel waveguides.[21] Wang et al.[22] demonstrated recently that surface relief structures, which had been formed on azobenzene side chain polymers, can be copied to elastomeric replicas by employing crosslinkable poly(dimethyl)siloxane (PDMS) derivatives, one of the most commonly employed material classes for replica molding.[23-25]

In this study we present the synthesis of a novel series of photochromic molecular glasses and demonstrate the inscription of SRGs by holographic methods and their transfer to polymer surfaces. The goal of the paper is to reveal structure-property relationships for the controlled formation of SRGs and the maximal achievable SRG heights. Temperature-dependent measurements were carried out to gain more insight into the SRG build-up and decay. By replica molding with PDMS and subsequent imprinting we were able to transfer the surface structures from the azobenzene-containing molecular glasses to a common polymer.

Results and discussion

Synthesis, thermal, and optical properties of the photochromic molecular glasses

A new set of photochromic molecular glasses was synthesized to study the formation of surface relief gratings. The materials described in this work are based on a triphenylamine core and three azobenzene side groups (see **figure 1**). The core is built by a slightly modified version of the Ullmann coupling as done by Walter,[26] merging 4-aminobenzoic acid methyl ester with 2 equivalents of 4-iodo benzoic acid methyl ester. After cleavage of the ester groups, the carboxylic acid units are converted into the corresponding carboxylic acid chlorides. The side groups are linked to the core by an aryl-aryl esterification in good yields (approx. 55% after purification; purity was confirmed by size exclusion chromatography suitable oligomeric compounds (oligo-SEC), NMR and elemental analysis). The hydroxyl-functionalized azobenzene moieties are accessible by a common azo coupling reaction as described in basic literature. Tailoring the azobenzene moieties with several distinct substituents and introducing them into the molecular glass opened the way to study their effects on the physical and photo-physical properties of the whole molecule. The formation of the ester linkages between the triphenylamine core and the sidegroups is an easy access to a large variety of compounds in order to tailor the required material properties. Few reports have been published with respect to different substituents which influence the photoresponsive properties of the azobenzene moiety.

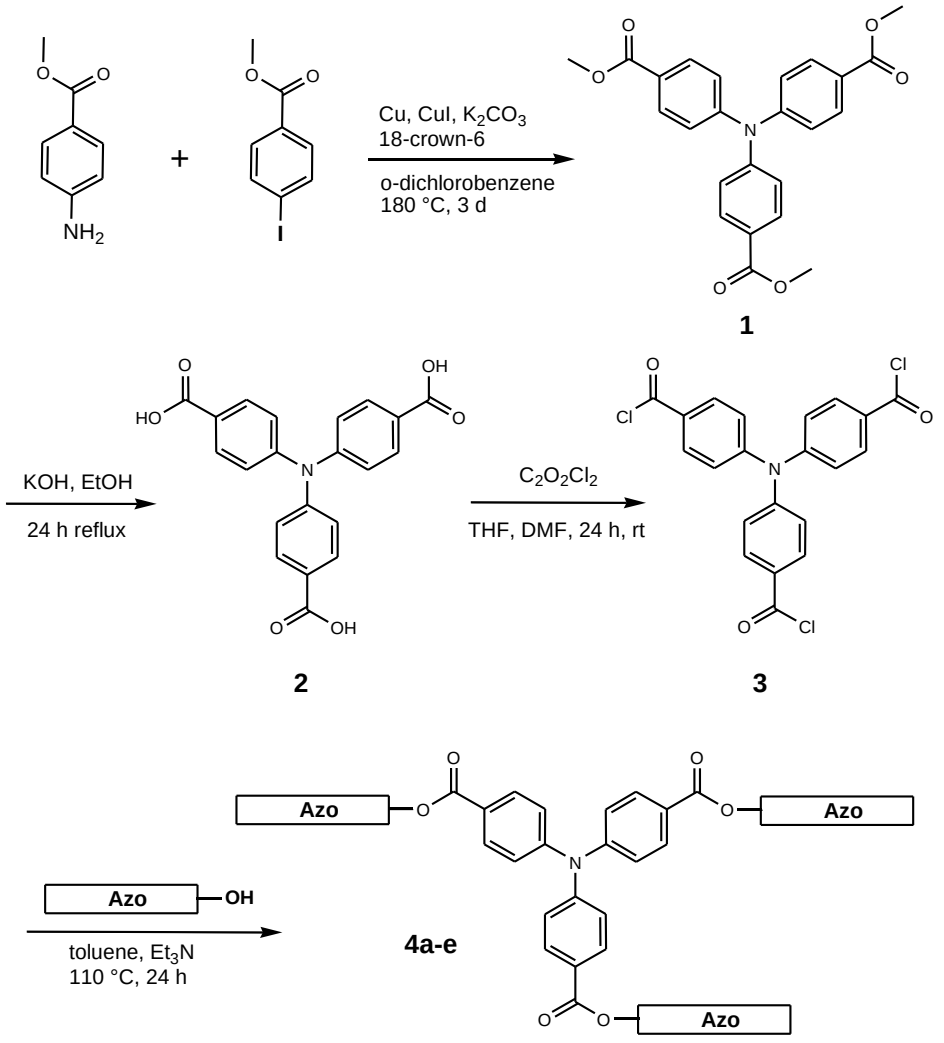

No.	Azo	No.	Azo
4a	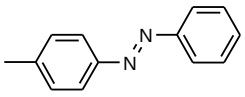	4d	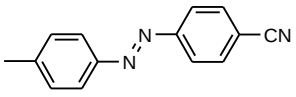
4b	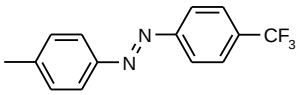	4e	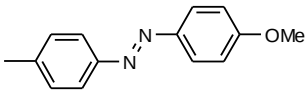
4c	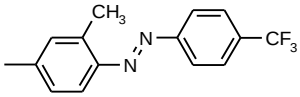		

Figure 1. Synthetic route to the photochromic azobenzene-containing molecular glasses **4a-e**.

The position of T_g as well as the glass-forming ability and recrystallization behaviour are important parameters of molecular glasses, since homogeneous, scatter-free thin films with optically isotropic properties are required for holographic experiments. The thermal and morphological properties of compounds **4a-e** are investigated with differential scanning calorimetry (DSC), optical polarized light microscopy (polmic), X-ray diffraction, and thermogravimetric analysis (TGA). The thermal properties are summarized in **table 1**. All compounds exhibit a decomposition temperature above 300 °C allowing thermal treatment in a wide temperature range. Furthermore, all materials form a stable amorphous phase with glass transition temperatures in the range of 88-122 °C. The T_g values extend over a temperature range of more than 30 °C, although the molecules exhibit only slight modifications at the azobenzene moiety. High glass transitions are of particular importance for our study, since SRGs are only stable below T_g. For some compounds the first heating curves show a polymorphic melting behaviour with rather low melting enthalpies. Such behaviour can often be found in molecular glasses. Except for **4b**, the heating curves revealed no recrystallization followed by a melting, as it is shown in **figure 2** (A) for compounds **4a** and **4d**. Even with a moderate cooling rate of 10 K/min, no crystallization occurs during cooling, supporting that the compounds have a strong tendency to form a stable amorphous phase. In case of **4b**, an amorphous phase can be achieved by quenching the melt.

In general, molecular structures which inhibit tight packing, e.g., rigid or bridged moieties, tend to increase T_g. On the contrary, conformational and constitutional isomers or asymmetric molecules increase the glass-forming ability but lower T_g. This can be seen by comparing compounds **4b** and **4c**, where the additional lateral methyl groups enhance glass formation, although T_g drops by 6 °C. Increasingly stronger intermolecular interactions, such as dipole-dipole interactions, favour the crystallization tendency, but they raise also the glass transition temperature. This can be seen from **4a** and **4d**, whose structures differ only by the polar cyano end group but which have T_g values 30 degrees apart. Compound **4d** shows no significant tendency to crystallize. The existence of an amorphous phase at room temperature is additionally confirmed by X-ray diffraction. Only a halo at ~10° can be seen. (see **figure 2**, B). Thin

films of the molecular glasses feature a high stability of the amorphous phase over months, stored at room temperature and below the glass transition temperature.

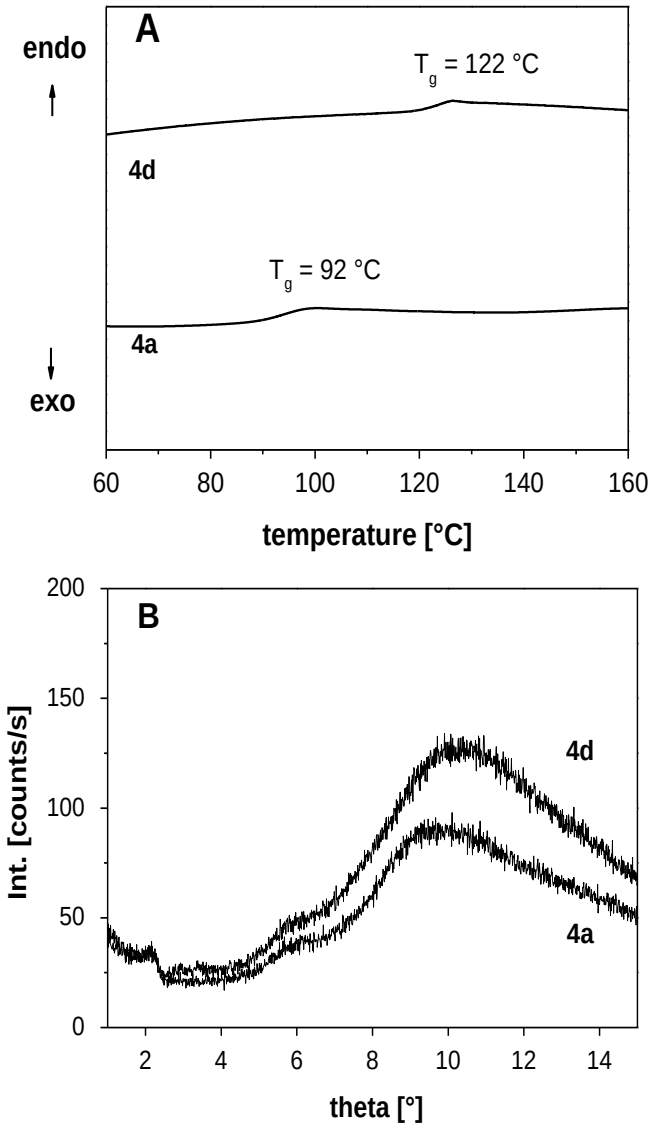

Figure 2. Thermal and morphological behavior of compounds **4a** and **4d**. A) DSC scans (second heating, heating rate 10 K/min), B) X-ray diffractograms of the glassy bulk material sealed in a capillary and measured at room temperature.

The optical properties of the molecular glasses **4a**-**4e** in thin films and solutions are characterized by UV-Vis spectroscopy. In **figure 3** the absorption spectra of compounds **4a** and **4d** are shown as examples. The spectra in solution and thin films do not differ significantly with respect to the wavelengths

of the absorption maxima, however the film spectra are slightly broadened. Furthermore, there is hardly any difference between the spectra of freshly prepared solutions and those stored in the dark. Therefore it can be concluded that in both cases the thermodynamical more stable *trans* state is investigated.

Table 1. Thermal [a] and optical [b] properties of the molecular glasses **4a-e**.

	4a	**4b**	**4c**	**4d**	**4e**
T_m [°C] *first heating*	160, 175	137, 145	157	n.d.	127
T_{cryst} [°C] *first cooling*	n.d.	139, 115	n.d.	n.d.	n.d.
T_g [°C] *second heating*	92	99	93	122	89
$T_{recryst}$ [°C] *second heat.*	n.d.	121	n.d.	n.d.	n.d.
T_m [°C] *second heating*	n.d.	137, 145	n.d.	n.d.	n.d.
λ_{max} (π-π*) [nm]	359	360	365	365	366
λ_{max} (n-π*) [nm]	438	439	445	444	434
OD/µm at 488 nm [c]	0.188	0.218	0.226	0.275	0.265

[a] obtained from DSC: heating and cooling rate: 10 K/min under N_2, [b] 10^{-5} molar solution in $CHCl_3$, [c] measured in thin films (thickness 0.70-0.95 µm)

In contrast to most other photochromic molecular glasses described in the literature, which possess a conjugated π-electron-system including the azobenzene moiety, the ester linkage in the here presented molecular glasses substantially reduces conjugation over the entire molecule. This allows us to investigate the optical properties of the azobenzene moieties alone, since the electronic system of the core is largely decoupled. In the absorption spectra (**figure 3**) two peaks can be distinguished which arise from the azobenzene moiety, an intense π-π* transition at approx. 360 nm and a much weaker n-π*

transition at approx. 440 nm. The absorption of the triphenylamine core is visible as a shoulder at about 310 nm. In contrast to the π-π* transition, the corresponding n-π* transition cannot be easily correlated with the molecular structure (see table 1). The extinction coefficient of both transitions increases as compared to **4a**, when substituents are introduced. It is well-known that introducing a polar group at the azobenzene moiety leads to an increase of the absorption coefficient.[27,28] Thus, the transition dipole moments can easily be influenced by slight modifications of the molecular structure. As indicated in the insert of **figure 3**, the holographic gratings are inscribed at a wavelength of 488 nm where both possible isomerizations, *cis* to *trans* and *trans* to *cis*, are induced. Hence, the extinction coefficient at the writing wavelength has a strong influence on the SRG formation.

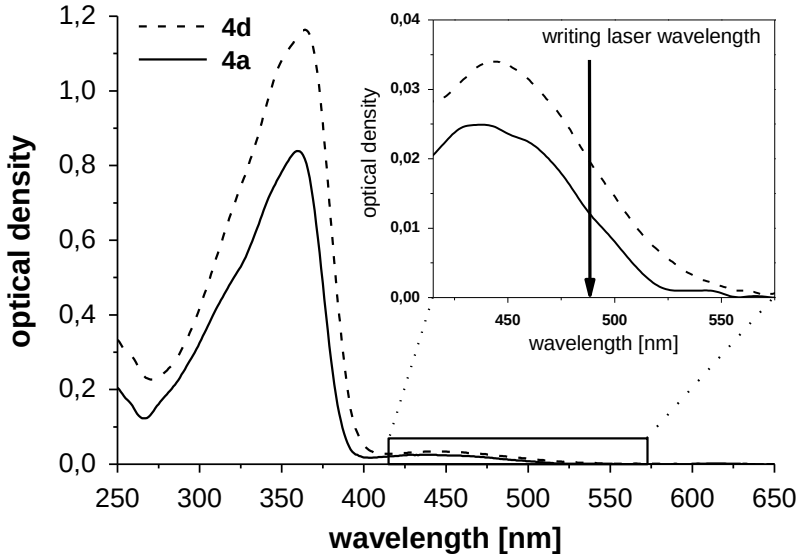

Figure 3. UV/Vis spectra of **4a** and **4d** in solution (10^{-5} M in $CHCl_3$). The insert shows the n-π* transition on a smaller scale; the writing laser wavelength of the holographic experiments is indicated by an arrow.

SRG formation at room temperature

Holographic experiments were performed on homogeneous thin films. Amorphous films of all materials can be obtained by spin-coating, which yields a thickness between 700 and 950 nm and good optical quality. Gratings were inscribed with two laser beams of 488 nm wavelength under an angle of ±14°, corresponding to a grating period of one µm (for details see experimental section). The polarization configuration of the laser beams is an important issue, since it strongly influences the SRG height. In this work we have mostly chosen the polarizations ±45° with respect to the plane of incidence. A detailed study of the influence of the polarization settings has been published elsewhere.[29] The configuration ±45° generates mainly a polarization grating with a small admixture of an intensity grating. Since polarization gratings are connected with a homogeneous light intensity, a light-induced plastification is expected to occur throughout the sample film. This softening of the material can accelerate macroscopic material transport below T_g.

The diffraction efficiency (DE) of a holographic grating, which is defined as the ratio of the first-order diffracted light intensity and the irradiated intensity, is monitored during the writing process with a reading laser whose wavelength is well outside of the absorption band of the chromophores and which, therefore, does not affect the writing process. Since after some seconds of irradiation the SRG always gives rise to a much higher DE than the orientation grating of the chromophores in the bulk,[29] we can calculate the height *d* of the SRG directly from the measured DE. To this end the theory of Magnusson and Gaylord,[30] which is usually applied to thin volume gratings, is modified to account for SRGs. The relation between diffraction efficiency η and SRG height *d* (valley to peak) then reads

$$\eta = J_1^{\,2}\left(\frac{2\pi\, d\, \Delta n}{\lambda_{read}\cos\theta}\right) \qquad (1)$$

with the Bessel function J_1, λ_{read} being the vacuum wavelength of the reading laser and Δn the amplitude of the refractive index modulation at the regions of sample film and air. Typical values of the maximum achievable DE are around

30%. The maximum heights were independently measured by atomic-force microscopy (AFM). The SRG heights calculated from equation 1 differed by no more than 12% from those determined by AFM. A typical AFM image is shown in figure 4. The SRG, which in this case was inscribed with the ++45° polarization configuration, exhibits a sinusoidal shape and a modulation height of 610 nm. Additionally so-called “egg-crate” like structures are shown, which could be formed, if two holographic gratings are orthogonally superimposed yielding a height (peak to valley) of approx. 300 nm and a spacing (peak to peak) of 1 µm. With a few exceptions, which we attribute to some surface inhomogeneity of the original smooth film, such surface structuring could be uniform and homogeneously obtained over many microns. These or similar superimposed structures could be of interest for potential application as mentioned in the introduction of this work.

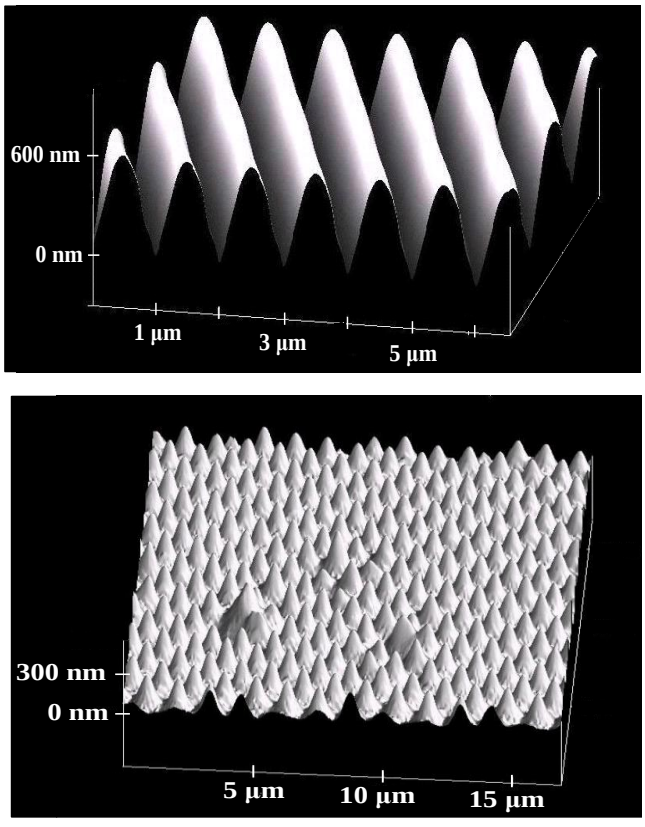

Figure 4. AFM image of a sinusoidal SRG inscribed in compound **4e** (top). AFM image of a SRG-pattern which was formed by two inscription processes between which the sample was rotated by 90° (bottom).

The maximum achievable SRG heights of the compounds **4a** to **4e** in ±45° configuration are in the range between 250 nm and 580 nm (see **figure 5**). This big difference of more than a factor of two is surprising, since the molecules feature only slight modifications. The different SRG heights can then be interpreted in the framework of the gradient force model of Kumar. Here the gradient force, which is assumed to be the driving force of SRG formation, is related to the optical susceptibility.[31] The refractive index n and the absorption constant k were measured with an ellipsometer and from these values the susceptibility was calculated.[29] With respect to optical susceptibility there are two exceptions, **4c** and, less pronounced, **4e**. Whereas **4c** always features very low SRGs and long writing times, **4e** develops comparatively high SRGs with fast build-up. In the case of **4c** one may attribute this result to the lateral methyl group, which seems to impede the SRG formation. In general, however, we can conclude that an increasing optical susceptibility at the writing wavelength favours SRG formation. Other polarization configurations yield the same trend, although not always as pronounced as with the ±45° scheme.[29]

A clear correlation with the maximum SRG height in respect to the glass transition could not be established. For example the glass transition temperatures of compounds **4a**, **4b**, **4c** differ by only 7 °C (**4a**: 92 °C; **4b**: 99 °C; **4c**: 93 °C) but the achievable SRGs differ substantially. Comparing compounds **4d** and **4e**, with a similar achievable SRG heights, the glass transition temperatures differ by more than 30 °C (**4d**: 122 °C; **4e**: 89 °C). On the other hand, they do play a role when the experiments are performed at elevated temperatures, as will be demonstrated in the following.

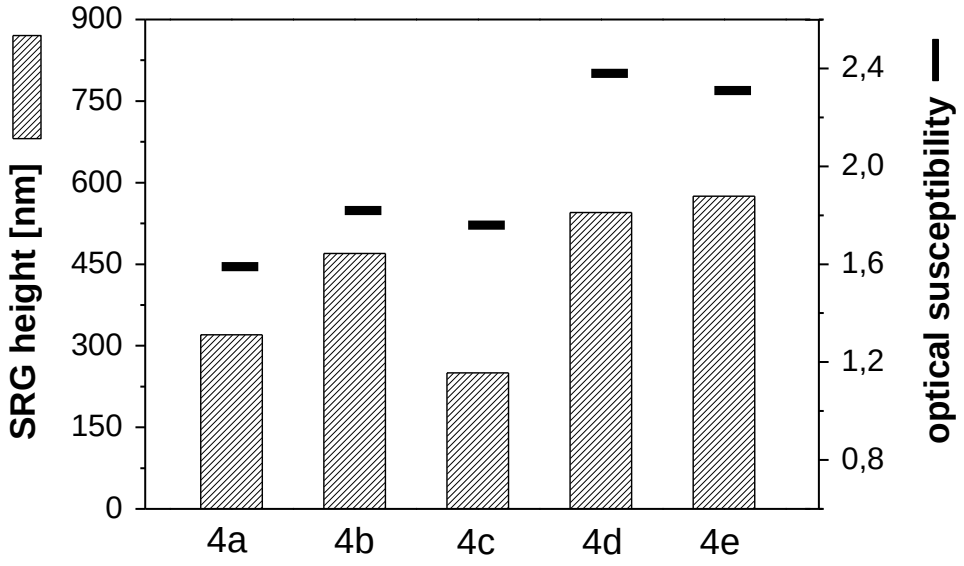

Figure 5. Maximum SRG height (bars) as measured at room temperature with polarization configuration ±45° and optical susceptibility (dots) of the sample films.

Temperature-dependent growth and decay of SRGs

SRGs on films of molecular glasses are expected to be stable at room temperature, if their glass transition temperatures are several ten degrees higher. Few experiments have been performed to investigate the stability of SRGs at elevated temperatures. One exception is the study by Kim et al. in which the DE of SRGs on a molecular glass was monitored during the application of a constant heating rate. The authors found that the DE drastically drops when T_g is reached.[14]

In this section we present the temperature-dependent growth and decay behaviour of SRGs on our molecular glasses. Especially the stability of the SRGs is of interest for applications in the field of replica molding, since the prepolymer for the replica must be cured at elevated temperatures. In contrast to the dynamical method of Kim et al. we investigated the formation and decay of SRGs at constant temperature.

First we tested the reversibility of SRG formation. A grating was inscribed up to its maximum DE at room temperature, then the sample was annealed above the glass transition temperature and kept at this temperature until the diffraction efficiency had dropped completely. After cooling to room temperature, a new grating was inscribed at the same spot. This procedure was

repeated several times. We found no significant changes with respect to the writing time or maximum SRG height between the different cycles. Therefore we can assume that the molecular glasses do not undergo recrystallization as a result of the annealing step or undergo light-induced photobleaching.

In **figure 6** the growth of the SRG height is shown for compound **4b** in the temperature range between 22°C and 110°C; writing was performed with two p-polarized beams. The heights were again calculated from the measured DE according to equation 1. Some general features can be seen. The SRG with highest modulation was inscribed at the lowest temperature. The sensitivity, which is proportional to the initial slope of the DE vs. time, is almost constant in the temperature range from 333 K to 373 K, so the SRG growth is not significantly enhanced by the increasing molecular mobility. Below 333 K, however, the initial growth rate is continuously decreasing. As expected, the maximum SRG amplitude drops strongly in the vicinity T_g, but even above T_g a DE arising from an SRG can still be detected.

The temperature dependence of the maximum achievable SRG height is plotted in part B of **figure 6**. The crossover from constant amplitudes at low temperatures to the strong decrease indicates the structural relaxation of the material which we have described in a similar way for photoaddressable polymers.[32] The crossover temperature of 338 K is significantly lower (by 35 degrees) than the glass transition temperature as measured by DSC (372 K). One of the reasons for this difference is the light-induced increase of the local temperature by the writing laser which is discussed later.

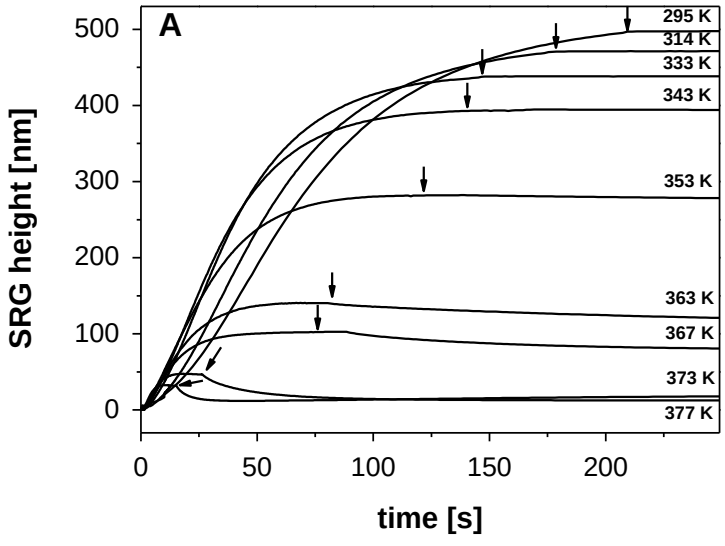

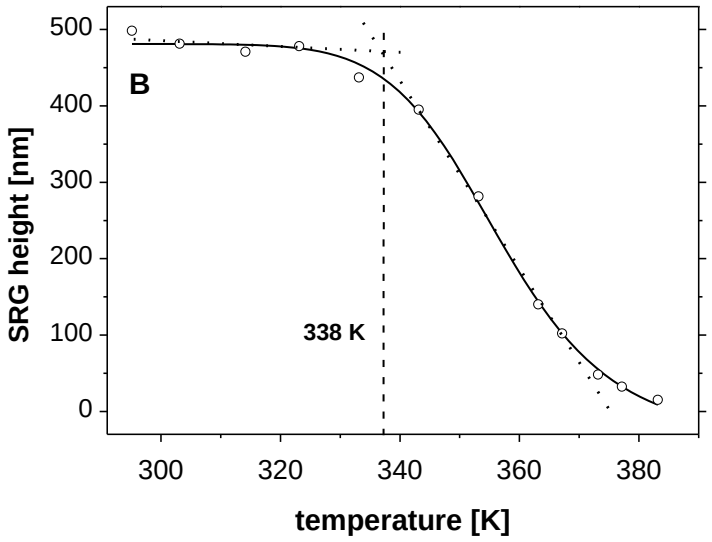

Figure 6. A) SRG build-up and initial decay at different temperatures for thin films of **4b**. The arrows indicate the times when the writing laser was turned off. B) Temperature-dependent variation of the maximum SRG heights for **4b** (circles). The solid line is a guide to the eye; the dotted lines represent the behaviour at low temperatures and in the region of the strong decrease. Their intersection (dashed line) indicates the onset of softening of the material.

For the temporal decay of the holograms, neither a bi-exponential nor a stretched exponential function yields a satisfactory fit to the experimental data. Hence, we believe that the heat deposited by the writing laser has an additional influence. Light absorption by the chromophores can cause the local temperature of the illuminated spot to increase so that a temperature gradient with its environment results. After turning the laser off, the temperature starts to equilibrate. The light-induced heating has its biggest effects at temperatures near T_g, and the time to reach thermal equilibrium increases at lower temperatures. Below 343 K the SRGs are stable which indicates that the local increase of temperature is longer sufficient to reduce the SRG height.

The light-induced heating effect is taken into account by the following decay function, which yields very good fits to the data

$$d(t) = d_{\max} \cdot \exp\left(\frac{-t}{t_2 - t_1 \cdot \exp(-t/t_3)} \right) \qquad (2)$$

d_{max} is the maximum grating height immediately after turning the writing laser off, and $(t_2\text{-}t_1)$ and t_2 are its decay times at the initial (locally increased)

temperature and the equilibrium temperature, respectively. t_3 is the thermal relaxation time. By comparing the time constants (t_2-t_1) and t_2 at the external (equilibrium) temperatures, we can estimate the light-induced increase of the local temperature to be approximately 15 K. This is in good agreement with the literature.[33,34]

The decay of the SRGs after the end of writing indicates the T_g of the material. In **figure 7** we plotted the temporal decay of the relative height during 1000 s (part A) and the residual height at the end of this period as a function of temperature (part B). Since thermal equilibrium had not yet been reached after 1000 s in all cases, the temperatures were calculated from the temperature dependence of the time constants t_1, t_2, and t_3 as discussed above. The transition from solid-like behaviour with constant SRG heights at low temperatures to rapid decay at high temperatures is well visible. The intersection indicates a glass point of 365 K, which is close to the T_g measured by DSC (372 K).

In contrast, the crossover temperature of the maximum achievable SRG height is lower by more than 25 degrees (see fig. 6B). We attribute this difference in part to the laser-induced local heating effects. Also the plastification of the material due to the *trans-cis-trans* isomerization cycles of the chromophores may have some influence. The combination of both effects is probably responsible for the fact that already at temperatures well below T_g (303 -323 K) different heights of the SRGs are achieved, although their stability is temperature-independent in this regime (compare **figure 6A and 7**).

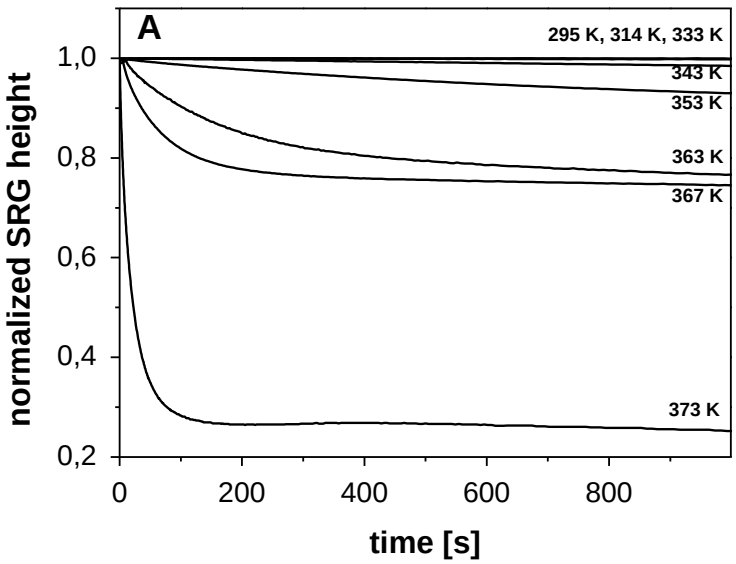

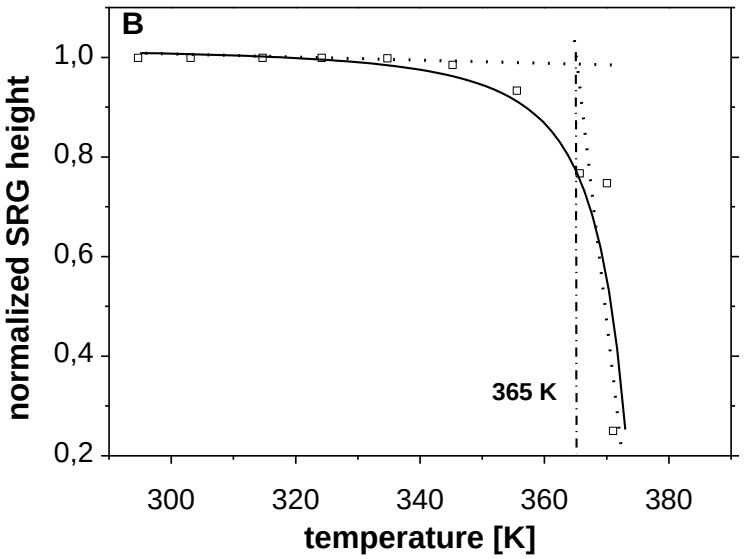

Figure 7. A) Temporal decay of the SRG height after the end of the writing process at different temperatures for thin films of **4b**. B) Temperature-dependent residual SRG height after 1000s for **4b** (squares). The solid line is a guide to the eye, the dotted lines represent the constant height at low temperatures and the rapid decay at high temperatures, respectively. Their intersection (dash-dotted line) indicates the glass transition temperature.

Replica molding of SRGs and imprinting on polymer surfaces

An important potential application of adjustable surface relief gratings and surface relief patterns on films of molecular glasses consists in transferring the structure to another polymer surface, where it can be used, e.g., for holographic optical elements (HOEs) such as security devices. The capability to emboss the surface structures directly to other polymers is determined by the required embossing temperature and limited by the glass transition temperature of the molecular glass. However commonly applied replica molding can be used to circumvent this problem. In our case compound **4d** was used, because its glass transition temperature is high enough to withstand temperatures of 60 °C for several hours so that exact replicas can be made. A grating was written on the material's surface and the liquid commercially available PDMS prepolymer (Sylgard 184, DOW Chemical) was cast over the molecular glass master. The cured PDMS replica was removed from the master without destroying the original grating. The PDMS replica was used to prepare the grating at 180 °C under slight pressure in the polycarbonate melt and by subsequent cooling preserving the grating into the polymer solid state. All surface structures of each

step (master, replica, and imprint) were characterized by atomic force microscopy (**figure 8**). In all three cases they show the same spacing of 0.95 µm. Their amplitudes decrease slightly from 580 nm (master) and 560 nm (replica) to 430 nm (imprint).

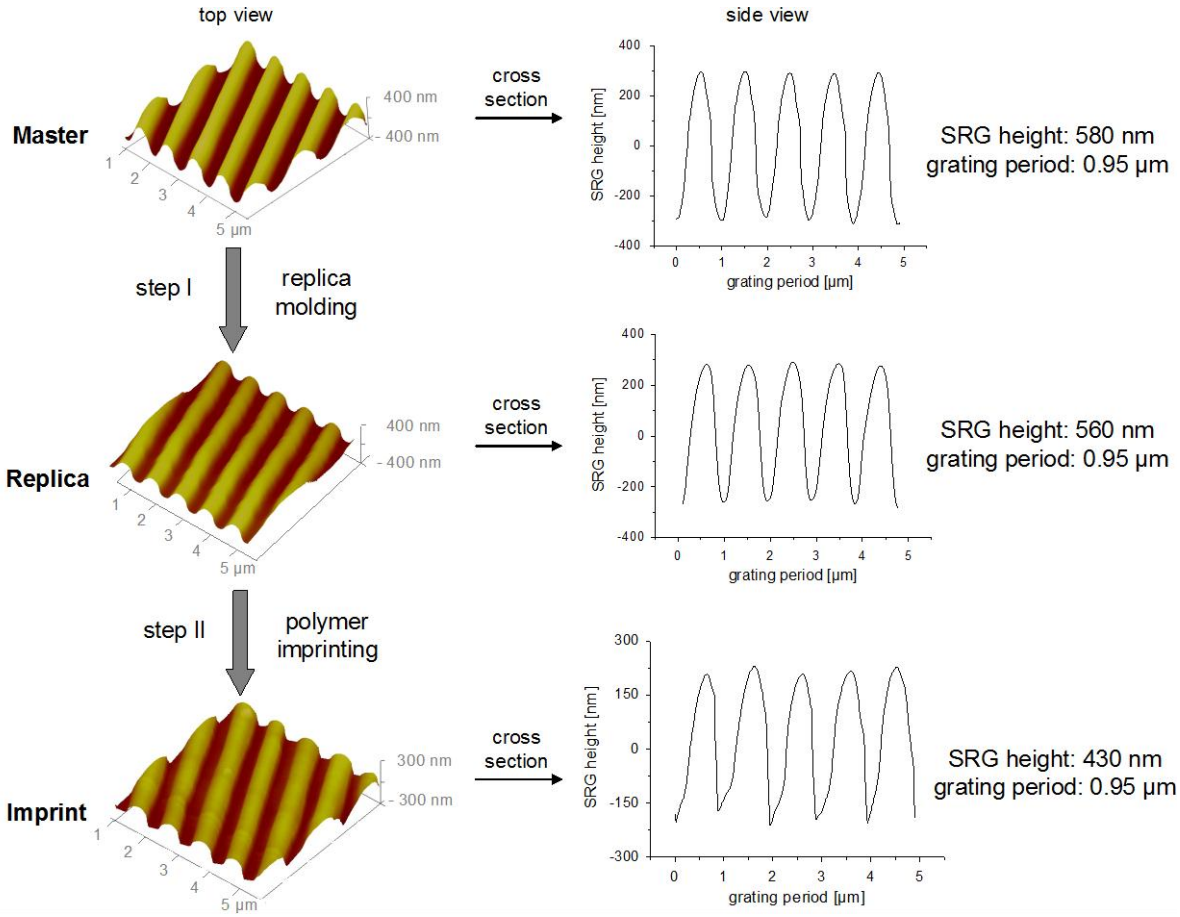

Figure 8. Example of transferring a SRG to a polymer surface. AFM characterization: 3D surface plots (left) and the corresponding cross sections (right) for the original SRG structures (top), the replica (middle), and the imprint on polycarbonate (bottom) are shown.

Conclusions

A series of well tuneable photochromic molecular glasses based on a triphenylamine core and different azobenzene moieties has been successfully applied to form holographic surface relief nanostructures. The maximum achievable SRG height is not clearly correlated with the glass transition temperature of the molecular glass, but increases with the optical susceptibility at the wavelength of the writing laser. The SRGs exhibit a high quality

sinusoidal cross section with modulation heights above 600 nm which are to our knowledge the so far highest values for molecular glasses. The holographically generated SRGs of molecular glass films are stable enough to be transferred easily and with high accuracy to the surface of thermoplastic polymers such as polycarbonate via common replica/imprinting procedures.

Experimental

Materials and Methods

All starting materials were commercially available and were used without further purification. Dry toluene was refluxed over potassium for one day. All synthesized compounds were identified by ^{1}H-NMR spectroscopy with a BRUKER AC250 spectrometer (250 MHz). To confirm purity, SEC measurements were employed utilizing a WATERS model 515 HPLC-pump with a UV-detector at 254 nm (WATERS model 486) and a Differential RI-detector (WATERS model 410). The column set-up consists of a guard column (PSS: SDV-gel; length 5 cm, diameter 0.8 cm, particle size 5 µm, pores size 100 Å) and two separation columns (PL: PL-gel; length 60 cm, diameter 0,8 cm, particle size 5µm, pores size 100 Å). Stabilized THF at a constant flow rate of 0.5 ml/min was used as eluent. Molecular weights were given with respect to an additional internal standard (o-dichlorbenzene) and to narrowly distributed PS standards. Characterization of the thermal properties by DSC measurements with a PERKIN-ELMER DSC7 (standard heating rate: 10K/min) utilizing 10 mg of the compounds in 40 µl pans. Verification of the data obtained from the DSC was done in an optical microscope with crossed polarizers (NIKON DIAPHOT 300) on a heating table (METTLER FP82 with METTLER FP 80 control unit). Mass spectra were recorded with a FINNIGAN mass spectrometer (MAT 800, MAT 112 S, Varian, EI-ionisation (70eV), direct inlet). UV/Vis absorption spectra of the compounds were recorded from 250 nm – 650 nm with HITACHI U-3000 spectral photometer. X-ray diffractograms were measured with a HUBER GUNIER-DIFFRAKTOMETER 6000 with a HUBER QUARZ-MONOCHROMATOR 611 and a Cu-anode ($CuK_{\alpha 1}$-radiation, λ = 1.54051 Å; SEIFERT x-ray generator), HUBER SMC 9000 stepping motor controller, HUBER HTC 9634 temperature controller. Elemental analysis was carried out

with an EURO EA 3000 analyzer (HEKATECH), yet, compound **4b** and **4c** could not be measured due to the fluor content.

Film preparation

Samples for the holographic experiments were prepared by spin-coating a filtered 9 wt.-% THF solution at 1000 rpm for 60s onto a commercially available glass substrate. The films were annealed at 70 °C for 4 hours to remove residual solvent. The film thickness of the samples varied from 700 nm to 950 nm; it was measured with a Dektak (Veeco 3300ST auto remote control stage profiler). All samples showed good optical properties and absence of light scattering.

Holographic Setup

A typical holographic set-up was used for the experiments. The gratings were inscribed with the blue-green line (488 nm) of an Argon-ion-laser. A beam splitter generates two coherent beams which are superimposed in the plane of the sample. Their diameter was about 2 mm; the intensity of each beam was adjusted to 1 W/cm². The state of polarization of each writing beam was adjusted separately by $\lambda/2$ or $\lambda/4$ plates. The angles of incidence with respect to the surface normal are ±14°, resulting in a grating period of 1 μm. A laser diode at 685 nm, which is outside the absorption band of the azobenzene moiety, was used for monitoring the diffraction efficiency *in situ* without affecting the writing process. The power of the transmitted and the diffracted beam was measured with two photodiodes, whose signals yield the diffraction efficiency. For improving the signal-to-noise ratio, the laser diode was modulated at 10 kHz and lock-in detection was used. The temperature-dependent measurements were performed with a similar holographic set-up, yet, the sample was placed in a temperature-controlled box. The temperature can be adjusted between 5 °C and 120 °C with an accuracy of 1 °C.

Replica molding

Replica molding was accomplished by casting the liquid prepolymer in cast molds of polystyrene which contained the samples with inscribed SRG

structures. The prepolymer was prepared by mixing the elastomer base and the curing agent in a 10 : 1 wt% ratio. Afterwards the prepolymer was cured at 60 °C for 4 h, cooled to room temperature, and the replicas were separated from the samples.

Polymer imprinting

For polymer imprinting the SRG replica and a polycarbonate sheet (thickness one mm) were placed on top of each other and inserted between two 125 µm Kapton® films. These layers were sandwiched between two steel plates. The whole setup was placed in a P.O. Weber PW10 laboratory press, and the polymer was heated to 180 °C and pressed with a force of 5 kN for two minutes.

Atomic force microscopy

Atomic force microscopy was performed in tapping mode with a commercial AFM, model dimension, 3100, Veeco Instruments Inc., equipped with a Nanoscope IV Controller and Closed Loop XY Dimension Head.

Synthesis of molecular glasses

4,4',4''-Tris[p-carbomethoxy]phenylamine **1**: 4-Iodobenzoic acid methyl ester (22.3 g, 85 mmol) is placed in a flame-dried Schlenck flask and suspended in 35 ml o-dichlorbenzene under argon atmosphere. Crown ether 18K6 (2.70 g, 10.2 mmol), K_2CO_3 (25.0 g, 181 mmol), copper (13.0 g, 205 mmol) and 4-aminobenzoic acid methyl ester (5.15 g, 34.1 mmol) are added. The reaction solution is stirred under reflux for 3 days. Subsequently o-dichlorbenzene is distilled off, the remaining solid is dissolved in THF and filtered over a frit with silica gel. The crude product is purified by flash column chromatography with cyclohexane : ethyl acetate = 5 : 1 as eluent. The resulting yellowish solid is recrystallized in EtOH yielding 6.35 g (57 %) of the title compound as white crystals. ^{1}H-NMR (250°MHz, DMSO, δ): 3.83 (s, 9H, CH_3) 7.15 (d, *J* = 3°Hz, 6H, Ar-H), 7.92 (d, *J* = 3°Hz, 6H, Ar-H)

4,4',4''-Tris[p-carboxy]phenylamine **2**: The 4,4',4''-tris[p-carbomethoxy]phenyl-amine **1** (4.80 g, 11.4 mmol) is suspended under stirring in a solution of ethanol : water = 2 : 1. Four equivalents of KOH per ester group (7.70 g, 137.4

mmol) are also dissolved and the reaction solution is stirred under reflux for 24 h. After evaporation of most of the EtOH, the solution is acidified with semi-concentrated hydrochloric acid and five times washed with diethyl ether. The combined organic phases are dried with Na_2SO_4. Subsequently the solution is filtered, the solvent is distilled off and the remaining solid is dried at high vacuum yielding 4.15 g (96 %) of the title compound as white solid. ^{1}H-NMR (250°MHz, DMSO, δ): 7.14 (d, *J* = 3°Hz, 6H, Ar-H), 7.90 (d, *J* = 3°Hz, 6H, Ar-H), 12.80 (s, 3H, COOH)

4,4',4''-Tris[p-carboxylchloride]phenylamine **3**: One equivalent of 4,4',4''-Tris-[p-carboxy]-phenylamine **2** (1.00 g, 2.7 mmol) is placed in a flame-dried Schlenck flask under argon atmosphere. By addition of a minimum of four equivalents of oxalyl chloride per carboxylic acid group (2.7 ml, 32 mmol) and 0.1 ml DMF a suspension is formed which has to be stirred under reflux for 24 h. The acid chloride is dried at high vacuum with the use of an additional cooling trap and the remaining solid is placed under argon atmosphere. The yield is 1.15 g (quant.) of the title compound as yellowish solid. ^{1}H-NMR (250°MHz, THF, δ): 7.32 (d, *J* = 3°Hz, 6H, Ar-H), 8.10 (d, *J* = 3°Hz, 6H, Ar-H)

General preparation method (GPM 1): Ester coupling of tris acid chlorides
In a flame-dried Schlenck flask the corresponding trisfunctionalized acid chlorides (1 equiv.) are dissolved in 150 ml toluene under argon atmosphere. A threefold molar excess of anhydrous triethylamine per acid chloride group and 3.3 equivalents of the corresponding azobenzene compound are added. The dark red solution is stirred for 24 h under reflux at 110 °C. The solution is filtered, washed with additional toluene and thereafter the solvent is distilled off. The crude product is solved in THF and precipitated in EtOH. The precipitate is filtered with a frit and dried at high vacuum. Remaining impurities are removed by a second precipitation in EtOH.

4,4',4''-Tris[p-carbo(4-phenylazo)phenoxy]phenylamine **4a**:
4,4',4''-Tris[p-carboxylchloride]-phenylamine (**3**) (0.55 g, 1.3 mmol) is coupled with 4-(Phenylazo)phenol (**a**) (0.83 g, 4.2 mmol) according to GPM 1 yielding

0.76 g (56 %) of the title compound as orange powder. ^{1}H-NMR (250°MHz, $CDCl_3$, δ): 7.28 (d, *J* = 3°Hz, 6H, Ar-H), 7.38 (d, *J* = 3°Hz, 6H, Ar-H), 7.48-7.56 (m, 9H, Ar-H), 7.91 (dd, *J* = 3°Hz, *J* = 1°Hz, 6H, Ar-H), 8.01 (d, *J* = 3°Hz, 6H, Ar-H), 8.18(d, *J* = 3°Hz, 6H, Ar-H), EIMS (*m/z* (%)): 917 (2) [M^+], 720 (32) [M^+ - $C_{12}H_9N_2O$], 198 (74) [$C_{12}H_{10}N_2O$], 121 (44) [$C_7H_5O_2^+$], 93 (100) [$C_6H_5O^+$], 77 (81) [$C_6H_5^+$], elem. anal. calcd for $C_{57}H_{39}N_7O_6$: C 74.58, H 4.28, N 10.68; found: C 75.15, H 4.67, N 10.54.

4,4',4''-Tris[p-carbo(4-(4-trifluormethyl)phenylazo)phenoxy]phenylamine **4b**:
4,4',4''-Tris-[p-carboxylchloride]phenylamine (**3**) (0.60 g, 1.4 mmol) is coupled with 4-((4-(Trifluoromethyl)phenylazo)phenol (**b**) (1.22 g, 4.6 mmol) according to GPM 1 yielding 0.86 g (55 %) of the title compound as orange powder. ^{1}H-NMR (250°MHz, $CDCl_3$, δ): 7.28 (d, *J* = 3°Hz, 6H, Ar-H), 7.40 (d, *J* = 3°Hz, 6H, Ar-H), 7.78 (d, *J* = 3°Hz, 6H, Ar-H), 8.00-8.08 (m, 12H, Ar-H), 8.18(d, *J* = 3°Hz, 6H, Ar-H), EIMS (*m/z* (%)): 1121 (1) [M^+], 856 (100) [M^+ - $C_{13}H_8N_2OF_3$], 266 (30) [$C_{13}H_9N_2OF_3$], 145 (46) [$C_7H_4F_3^+$], 93 (59) [$C_6H_5O^+$],

4,4',4''-Tris[p-carbo(3-methyl-4-(4-trifluormethyl)phenylazo)phenoxy]phenyl-amine **4c**: 4,4',4''-Tris[p-carboxylchloride]-phenylamine (**3**) (0.60 g, 1.4 mmol) is coupled with (3-Methyl-4-(4-trifluormethyl)phenylazo)phenol (**c**) (1.29 g, 4.6 mmol) according to GPM 1 yielding 0.86 g (53 %) of the title compound as orange powder. ^{1}H-NMR (250°MHz, $CDCl_3$, δ): 2.80 (s, 9H, CH_3), 7.14 (dd, *J* = 3°Hz, *J* = 1°Hz, 3H, Ar-H), 7.24-7.31 (m, 9H, Ar-H), 7.77-7.82 (m, 9H, Ar-H),7.99 (d, *J* = 3°Hz, 6H, Ar-H), 8.18(d, *J* = 3°Hz, 6H, Ar-H), EIMS (*m/z* (%)): 1162 (1) [M^+], 884 (11) [M^+ - $C_{14}H_9N_2OF_3^+$], 280 (61) [$C_{14}H_{10}N_2OF_3$], 145 (54) [$C_7H_4F_3^+$], 107 (100) [$C_6H_5NO^+$], 77 (76) [$C_6H_5^+$],

4,4',4''-Tris[p-carbo(4-(4-cyano)phenylazo)phenoxy]phenylamine **4d**:
4,4',4''-Tris-[p-carboxylchloride]-phenylamine (**3**) (1.00 g, 2.3 mmol) is coupled with (4-(4-Cyano)phenylazo)phenol (**d**) (1.70 g, 7.6 mmol) according to GPM 1b yielding 1.37 g (60 %) of the title compound as orange powder. ^{1}H-NMR (250°MHz, $CDCl_3$, δ): 7.28 (d, *J* = 3°Hz, 6H, Ar-H), 7.41 (d, *J* = 3°Hz, 6H, Ar-H), 7.81 (d, *J* = 3°Hz, 6H, Ar-H), 7.98-8.08 (m, 12H, Ar-H), 8.19 (d, *J* = 3°Hz, 6H,

Ar-H), EIMS (*m/z* (%)): 993 (1) [M^+], 223 (43) [$C_{13}H_9N_3O$], 121 (38) [$C_6H_5N_2O^+$], 93 (100) [$C_6H_5O^+$], elem. anal. calcd for $C_{60}H_{36}N_{10}O_6$: C 72.57, H 3.65, N 14.11; found: C 72.62, H 3.82, N 13.73.

4,4',4''-Tris[p-carbo(4-(4-methoxy)phenylazo)phenoxy]phenylamine **4e**: 4,4',4''-Tris-[p-carboxylchloride]-phenylamine (**3**) (0.60 g, 1.4 mmol) is coupled with (4-(4-Methoxy)phenylazo)phenol (**e**) (1.05 g, 4.6 mmol) according to GPM 1 yielding 0.83 g (59 %) of the title compound as orange powder. ^{1}H-NMR (250°MHz, $CDCl_3$, δ): 3.90 (s, 9H, CH_3), 7.01 (d, *J* = 3°Hz, 6H, Ar-H), 7.28 (d, *J* = 3°Hz, 6H, Ar-H), 7.36 (d, *J* = 3°Hz, 6H, Ar-H), 7.92 (d, *J* = 3°Hz, 6H, Ar-H), 7.96 (d, *J* = 3°Hz, 6H, Ar-H), 8.18 (d, *J* = 3°Hz, 6H, Ar-H), EIMS (*m/z* (%)): 1007 (2) [M^+], 780 (34) [M^+ - $C_{13}H_{11}N_2O_2^+$], 228 (84) [$C_{13}H_{12}N_2O_2$], 107 (100) [$C_6H_5NO^+$], 93 (73) [$C_6H_5O^+$], 77 (53) [$C_6H_5^+$], elem. anal. calcd for $C_{60}H_{45}N_7O_9$: C 71.49, H 4.50, N 9.73; found: C 71.31, H 4.64, N 9.54.

Literature

[1] see, for example:
a) Y. Shirota, *J. Mater. Chem.* **2005**, *15*(1), 75-93
b) P. Strohriegl, J. V. Grazulevicius, *Adv. Mater.* **2002**, *14*(20), 1439-1452
c) M. Thelakkat, C. Schmitz, C. Hohle, P. Strohriegl, H.-W. Schmidt, U. Hofmann, S. Schloter, D. Haarer, *Phys. Chem. Chem. Phys.* **1999**, *1*(8), 1693-1698
d) F. Steuber, J. Staudigel, M. Stössel, J. Simmerer, A. Winnacker, H. Spreitzer, F. Weissörtel, J. Salbeck, *Adv. Mater.* **2000**, *12*, 130-133

[2] see, for example:
a) R. H. Friend, R. W. Gymer, A. B. Holmes, J. H. Burroughes, R. N. Marks, C. Taliani, D. D. C. Bradley, D. A. Dos Santos, J. L. Bredas, M. Logdlund, W. R. Salaneck, *Nature* **1999**, *397*(6715), 121-128
b) S. Guenes, H. Neugebauer, N. S. Sariciftci, *Chem. Rev.* **2007**, *107*(4), 1324-1338
c) M. T. Bernius, M. Inbasekaran, J. O'Brien, W. Wu, *Adv. Mater.* **2000**, *12*(23), 1737-1750

[3] see, for example:
a) M. Haeckel, L. Kador, D. Kropp, H.-W. Schmidt, *Adv. Mater.* **2007**, *19*(2), 227-231
b) M. Haeckel, L. Kador, D. Kropp, C. Frenz, H.-W. Schmidt, *Adv. Funct. Mater.* **2005**, *15*(10), 1722-1727
c) R. Hagen, T. Bieringer, *Adv. Mater.* **2001**, *13*(23), 1805-1810
d) K. G. Yager, C. J. Barrett, *J. Photochem. Photobiol., A* **2006**, *182*(3), 250-261

e) S. Schloter, U. Hofmann, P. Strohriegl, H. W. Schmidt, D. Haarer, *J. Opt. Soc. Am. B* 1998, 15(9), 2473-2475

[4] A. Natansohn, P. Rochon, *Chem. Rev.* **2002**, *102*(11), 4139-4175

[5] P. Rochon, E. Batalla, A. Natansohn, *Appl. Phys. Lett.* **1995**, *66*(2), 136-8

[6] D. Y. Kim, S. K. Tripathy, L. Li, J. Kumar, *Appl. Phys. Lett.* **1995**, *66*(10), 1166-1168

[7] L. L. Carvalho, T. F. C. Borges, M. R. Cardoso, C. R. Mendonca, D. T. Balogh, *Eur. Polym. J.* **2006**, *42*(10), 2589-2595

[8] B. M. Schulz, M. R. Huber, T. Bieringer, G. Krausch, S. J. Zilker, *Synth. Met.* **2001**, *124*(1), 155-157

[9] K. G. Yager, O. M. Tanchak, C. Godbout, H. Fritzsche, C. J. Barrett, *Macromolecules* **2006**, *39*(26), 9311-9319

[10] C. Frenz, A. Fuchs, H.-W. Schmidt, U. Theissen, D. Haarer, *Macromol. Chem. Phys.* **2004**, *205*(9), 1246-1258

[11] O. Kulikovska, L. M. Goldenberg, J. Stumpe, *Chem. Mater.* **2007**, *19*(13), 3343-3348

[12] O. Kulikovska, L. M. Goldenberg, L. Kulikovsky, J. Stumpe, *Chem. Mater.* **2008**, *20*(10), 3528-3534

[13] see, for example:
a) H. Nakano, T. Tanino, T. Takahashi, H. Ando, Y. Shirota, *J. Mater. Chem.* **2008**, *18*(2), 242-246
b) E. Ishow, B. Lebon, Y. He, X. Wang, L. Bouteiller, L. Galmiche, K. Nakatani, *Chem. Mater.* **2006**, *18*(5), 1261-1267
c) A. Perschke, T. Fuhrmann, *Adv. Mater.* **2002**, *14*(11), 841-843
d) A. Stracke, J. H. Wendorff, D. Goldmann, D. Janietz, B. Stiller, *Adv. Mater.* **2000**, *12*(4), 282-285
e) C. Chun, M.-J. Kim, D. Vak, D. Y. Kim, *J. Mater. Chem.* **2003**, *13*(12), 2904-2909
f) H. Ando, T. Takahashi, H. Nakano, Y. Shirota, *Chem. Lett.* **2003**, *32*(8), 710-711

[14] M.-J. Kim, E.-M. Seo, D. Vak, D.-Y. Kim, *Chem. Mater.* **2003**, *15*(21), 4021-4027

[15] E.-M. Seo, M. J. Kim, Y.-D. Shin, J.-S. Lee, D.-Y. Kim, *Mol. Cryst. Liq. Cryst.* **2001**, *370*, 143-146

[16] C. Chun, J. Ghim, M.-J. Kim, D. Y. Kim, *J. Polym. Sci., Part A: Polym. Chem.* **2005**, *43*(16), 3525-3532

[17] N. K. Viswanathan, D. Y. Kim, S. Bian, J. Williams, W. Liu, L. Li, L. Samuelson, J. Kumar, S. K. Tripathy, *J. Mater. Chem.* **1999**, *9*, 1941-1955

[18] J. A. Delaire, K. Nakatani, *Chem. Rev.* **2000**, *100*(5), 1817-1845

[19] P. Rochon, A. Natansohn, C. L. Callender, L. Robitaille, *Applied Physics Letters* **1997**, *71*(8), 1008-1010

[20] J. Kato, I. Yamaguchi, H. Tanaka, *Opt. Lett.* **1996**, *21*(11), 767-769

[21] O. Watanabe, M. Tsuchimori, A. Okada, H. Ito, *Appl. Phys. Lett.* **1997**, *71*(6), 750-752

[22] B. Liu, M. Wang, Y. He, X. Wang, *Langmuir* **2006**, *22*(17), 7405-10

[23] J. L. Wilbur, A. Kumar, E. Kim, G. M. Whitesides, *Adv. Mater.* **1994**, *6*(7/8), 600-4

[24] S. R. Quake, A. Scherer, *Science* **2000**, *290*(5496), 1536-1540

[25] J. Park, P. T. Hammond, *Adv. Mater.* **2004**, *16*(6), 520-525

[26] R. I. Walter, *J. Am. Chem. Soc.* **1955**, *77*, 5999-6002

[27] P. P. Birnbaum, J. H. Linford, D. W. G. Style, *Trans. Faraday Soc.* **1953**, *49*, 735-44

[28] A. Burawoy, *J. Chem. Soc.* **1937**, 1865-1869

[29] H. Audorff, L. Kador, R. Walker, H.-W. Schmidt, *J. Phys. Chem. B* **2009**, *113*, 3379-3384

[30] R. Magnusson, T. K. Gaylord, *J. Opt. Soc. Am.* **1978**, *68*, 806-809

[31] J. Kumar, L. Li, X. L. Jiang, D. Y. Kim, T. S. Lee, S. Tripathy, *Appl. Phys. Lett.* **1998**, *72*(17), 2096-2098

[32] K. Kreger, C. Loeffler, R. Walker, N. Wirth, D. Bingemann, H. Audorff, E. A. Roessler, L. Kador, H.-W. Schmidt, *Macromol. Chem. Phys.* **2007**, *208*(14), 1530-1541

[33] K. G. Yager, C. J. Barrett, J. Chem. Phys. 2004, 120(2), 1089-1096

[34] S. Bauer-Gogonea, S. Bauer, W. Wirges, R. Gerhard-Multhaupt, J. Appl. Phys. 1994, 76(5), 2627-35

Acknowledgements

Financial support by the German Science Foundation (DFG) within the framework of the Collaborative Research Centre (SFB 481) is gratefully acknowledged. The authors thank Dr. Klaus Kreger for many helpful discussions and Christina Löffler for her assistance in the preparation of the molecular glasses.

4.3 Polarization Dependence of the Formation of Surface Relief Gratings in Azobenzene-Containing Molecular Glasses

By *Hubert Audorff, Roland Walker, Lothar Kador* and *Hans-Werner Schmidt**

[*] Prof. H.-W. Schmidt, R. Walker
University of Bayreuth, Macromolecular Chemistry I and
"Bayreuth Institute of Macromolecular Research"
D-95440 Bayreuth (Germany)
E-mail: hans-werner.schmidt@uni-bayreuth.de

Prof. L. Kador, H. Audorff
University of Bayreuth, "Bayreuth Institute of Macromolecular Research"
D-95440 Bayreuth (Germany)
E-mail: lothar.kador@uni-bayreuth.de

This paper is published in
J. Phys. Chem. B 2009, *113*, 3379-3384

Keywords: holographic grating, photoresponsive, low-molecular-weight glasses, gradient force

Abstract

This paper presents a comprehensive study of the formation of surface relief gratings in a series of photoresponsive molecular glasses. Holographic experiments were performed on films of the azobenzene-containing molecular glasses. Seven relevant polarization configurations of the writing beams were systematically applied, and simultaneously the diffraction efficiency was monitored during the process of inscription. The temporal evolution of the diffraction efficiency can be precisely simulated with a model which takes both the surface relief and the phase grating in the volume into account. From the measured diffraction efficiencies, the modulation heights can be directly calculated and they were independently confirmed by atomic force microscopy. We found that all experimental results can be explained with the gradient force model, and we suggest that the grating heights generated with different writing polarizations can be ascribed to the varying strengths of the gradient force. For materials with different substituents at the azobenzene chromophore, the optical susceptibility at the writing laser wavelength and, therefore, the gradient force varies. By applying the most efficient polarization configuration in combination with the best material, we were able to reach modulation heights of up to 600 nm, which is a factor of two higher than modulations usually reported for azobenzene-containing polymers.

Introduction

Molecular glasses are a subject of intense current studies, mainly with respect to their electronic and optoelectronic properties. Molecular glasses form a stable amorphous phase and possess a glass transition temperature (T_G) above room temperature. In contrast to amorphous polymers, they exhibit more uniform physical properties and are therefore ideal candidates for comparative investigations.[1-3]

Another subject of current interest are photochromic compounds with azobenzene groups. Important technical applications of these materials are envisaged in the field of optical information storage.[4-7] The azobenzene chromophore undergoes multiple reversible *trans-cis-trans* photo-isomerization

cycles upon light absorption, which finally reorient the chromophores perpendicular to the polarization direction of the incident light so that excitation is no longer possible.[8-9] This effect is called angular hole burning.

In addition to the photoinduced reorientation, a second phenomenon, the formation of surface relief gratings (SRGs)[10-12] during holographic experiments, takes place. It is related to a mass transport in azobenzene-containing films induced by the irradiation of two interfering laser beams at temperatures much lower than T_G. The phenomenon of SRG formation was mainly investigated in polymer systems carrying azobenzene units as side groups.[13-16] Recently, in photoresponsive molecular glasses, the formation of stable SRGs was also successfully demonstrated.[17-19] Since the photo-induced formation of SRGs is not impeded by polymer chain entanglements, it is more efficient on molecular glass films than on polymer films of similar composition.[19,20]

In the past decades, much experimental and theoretical work has been performed to clarify the mechanism of SRG formation. It is widely accepted that the SRG build-up requires a free surface of the material and depends on the polarization of the writing laser beams. A number of models have been proposed to describe the SRG formation process.[21-26] However, none of them is able to explain all experimental details. In particular, most of the models do not explicitly take the polarization state of the laser beams into account. The only exception is a model proposed by Kumar et al.[27] which relates the formation of SRGs to a gradient force. This force and, hence, the height of a SRG depend on the laser polarization and the susceptibility of the material. The susceptibility of the azobenzene chromophores can simply be changed by introducing different substituents. A detailed comparison of the influence of different light polarizations and different substituents of the azobenzene moiety on the efficiency of SRG formation, however, has not been reported to date. Such a study will improve our general understanding of the response of azobenzene-functionalized materials to light irradiation and is, therefore, of high practical importance. The process of SRG formation is detrimental to data storage in volume gratings, because the SRGs are thin gratings and, therefore, possess no angular selectivity. Hence, the application of azobenzene-containing materials to holographic data storage is only possible, if the

formation of SRGs can be suppressed.[28-30] The SRGs must be better understood in order to be able to inhibit their formation more effectively.

In the present paper, the tunable formation of surface relief gratings of heights up to more than 600 nm on molecular glasses containing azobenzene moieties will be demonstrated. Holographic experiments were performed with seven polarization configurations of the writing beams and with five different materials. The SRG build-up was monitored during the inscription process and confirmed by atomic force microscopy (AFM). It is demonstrated that the results are in agreement with the predictions of the gradient force model.

Experimental methods

Materials

The photoresponsive molecular glasses are based on a triphenylamine core carrying three azobenzene moieties as side groups. Various electron donating and electron withdrawing substituents are attached to the chromophores for tailoring the optical and thermodynamic properties. All compounds form stable amorphous phases with glass transition temperatures in the range 88 to 121°C. The chemical structure of the molecular glasses is shown in Figure 1.

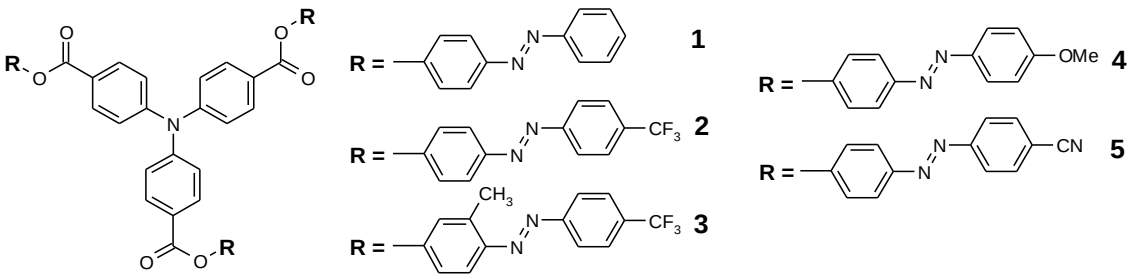

Figure 1. Chemical structure of the azobenzene-based molecular glasses **1**-**5**.

Sample preparation

Samples for the holographic experiments were prepared by spin-coating an 8 wt.-% solution of the compounds in THF onto glass substrates at 1000 rpm for 60 s. The films were annealed at 70 °C for 4 h to remove residual solvent. Their thickness was measured with a Dektak profilometer (Veeco 3300ST) and was found to be homogeneous ranging between 700 and 950 nm. All samples exhibit good optical properties with very low light scattering. The optical densities per µm at 488nm are between 0.19 and 0.28.

Holographic set-up

The holographic set-up which was used for the experiments is shown in Figure 2. The gratings are inscribed with the blue-green line (488 nm) of an argon ion laser at room temperature. A beam splitter generates two coherent laser beams which are superimposed in the plane of the sample. Their diameter is about 2 mm; the intensity of each beam is adjusted to 1 W/cm² yielding a total intensity of 2 W/cm^2. The angle of incidence to the surface normal in air is ±14°, resulting in a grating period of 1 μm. A laser diode in s-polarization at 685 nm, which is outside the absorption band of the azobenzene chromophores, is used for monitoring the diffraction efficiency *in situ* without affecting the writing process. The power of the transmitted and the diffracted beam is measured with two photodiodes, allowing the determination of the diffraction efficiency. For improving the signal-to-noise ratio, the laser diode is modulated at 10 kHz and lock-in detection is used.

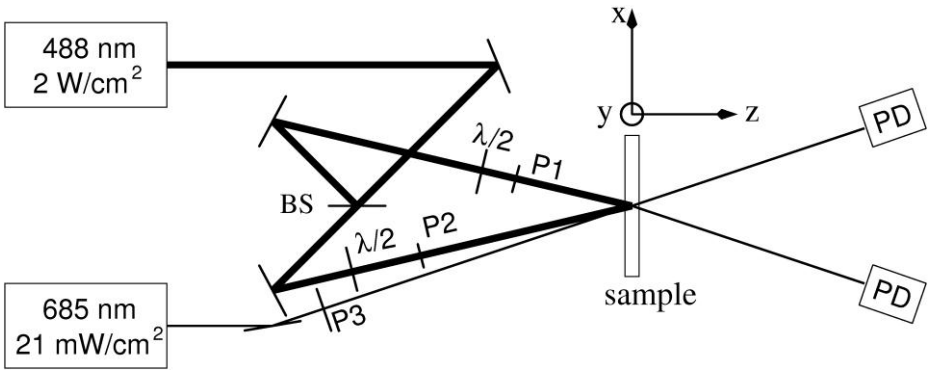

Figure 2. Scheme of the holographic set-up. *λ*/2 plates or *λ*/4 plates are used to obtain different polarization states. PD: photodiode, P: polarizer, BS: beam splitter. The coordinate system defines the directions which are referred to in the text.

The different polarizations of the writing beams were separately adjusted for each beam with *λ*/2 or *λ*/4 plates. The polarizations are denoted as s, p, 45°, rcp and lcp. In the case of p and s polarization, the electric-field vector oscillates in the plane of incidence and perpendicular to it, respectively. A 45° polarization corresponds to an angle of 45° with respect to this plane. Furthermore, clockwise (right-circularly polarized: rcp) and counter-clockwise circularly polarized light (left-circularly polarized: lcp) was used. These polarizations can be combined to achieve different polarization configurations, which are summarized in Figure 3. They generate either intensity or polarization gratings or a combination of both types. For example, if an s-polarized and a p-polarized wave interfere, the resulting so-called sp-configuration generates a pure polarization grating with spatially constant intensity but varying polarization direction. A pure intensity grating is obtained with the combination ss. ±45° and “right and left circularly polarized” (rlcp) are mainly polarization gratings with a small amount of intensity variation, whereas pp, ++45°, and “right and right circularly polarized” (rrcp) are mainly intensity gratings with a slight variation of the polarization direction.

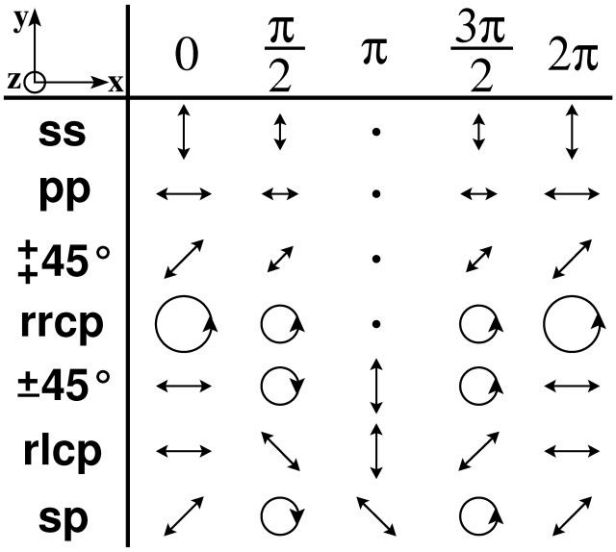

Figure 3. Total electric field vector distribution at the sample surface for seven different polarization configurations at five phase differences between the writing beams. In the upper left corner, the coordinate system of the electric field vector, which corresponds to the coordinate system in Figure 2, is shown.

AFM measurements

Atomic force microscopy was performed in tapping mode with a Veeco model dimension 3100 AFM equipped with a Nanoscope IV Controller and Closed Loop XY Dimension Head.

Results and discussion

Temporal evolution of the SRG formation

During illumination of the sample films with two superimposed laser beams, optical gratings are created which, in general, consist of a refractive-index modulation in the bulk and a surface relief grating (SRG). The diffraction efficiency (DE) is defined as the ratio of the first-order diffracted light intensity and the irradiated intensity. Figure 4 shows a typical example of the time-dependent diffraction efficiency during inscription. The inset indicates that mainly two processes contribute to the light diffraction. In the beginning, the DE of the volume grating grows faster than that of the SRG. Here, the volume grating reaches its maximum after about 5 s, whereas the maximum of the SRG is reached only after some minutes, depending on the polarization configuration

of the writing beams and the material. After 60 s of inscription, the DE of the SRG in our set-up is always larger by at least one order of magnitude, so the influence of the volume hologram can then be neglected. Typical values of the maximum DEs of volume gratings in our experiments are around 0.1%, whereas the DEs of SRGs reach 30%, i.e., more than two orders of magnitude higher.

In simulations of the temporal evolution of the diffraction efficiency, both of the above processes must be taken into account. The time-dependent diffraction efficiencies of combinations of a volume and a surface relief grating have been described by Reinke and co-workers.[31] Later-on the theory was expanded by Sobolewska and Miniewicz.[32] We applied the formula of the latter group, as given in Eq. 1, to simulate the measured diffractions efficiencies:

$$\eta(t) = J_1^2 \left\{ 2\pi \left[(n_1(t)\, d_o)^2 + (\Delta d(t)\, \Delta n)^2 + 2\, n_1(t)\; d_o\; \Delta d(t)\; \Delta n \cos(\Delta\varphi) \right]^{\frac{1}{2}} \left[\lambda \cos(\theta) \right]^{-1} \right\} \quad (1)$$

$n_1(t) = n_{1,\max}\left[1 - \exp\left(\frac{-t}{\tau_1}\right)\right]$ describes the increase of the refractive-index modulation of the volume grating up to its maximum value $n_{1,\,max}$,

$\Delta d(t) = \Delta d_{\max}\left[1 - \exp\left(\frac{-t}{\tau_2}\right)\right]$ the growth of the SRG height up to its maximum Δd_{max}. τ_1 and τ_2 are the corresponding time constants. Δn is the amplitude of the refractive index change between sample and air, and d_0 the thickness of the film. λ is the vacuum wavelength of the reading laser, $\Delta\varphi$ is phase difference between volume and surface relief grating which is assumed to grow to a maximum value $\Delta\varphi_{max}$ with time.

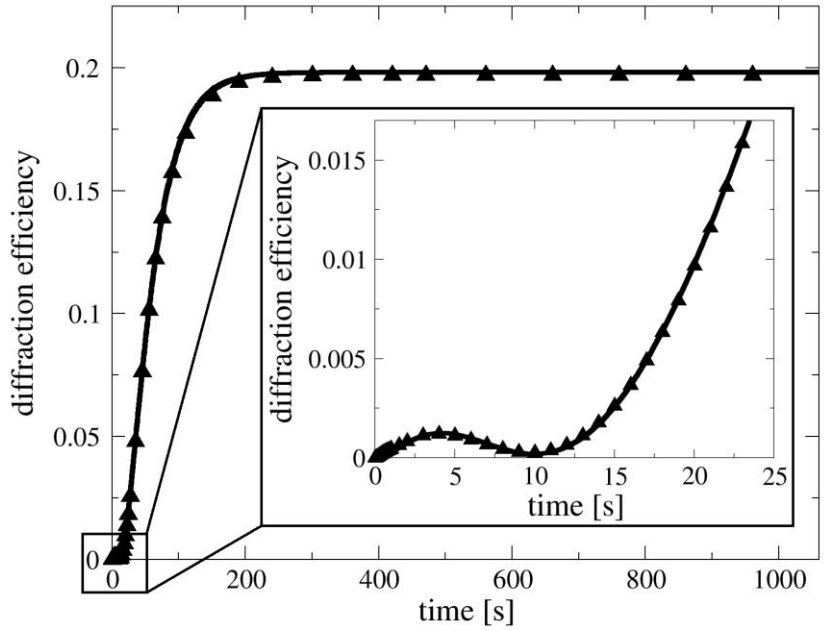

Figure 4. Temporal evolution of the diffraction efficiency $\eta(t)$ during hologram inscription (black triangles) as measured on a film of compound **2**. Writing was performed with the configuration ±45°. The black curve represents the fit of Eq. 1 with the parameters τ_1 = 6 s and τ_2 = 39 s. In the first seconds of the writing process, the diffraction efficiency due to reorientation of the azobenzene chromophores in the bulk is visible (see inset). Later-on the influence of the SRG dominates.

Figure 4 shows the temporal growth of the measured total diffraction efficiency $\eta(t)$. The fit according to Eq. 1 matches the experimental curve very well. From the calculations, a phase difference $\Delta\varphi_{max}$ = 180° between the volume grating and the SRG can be obtained for the polarization settings pp, ±45°, ++45°, rlcp, and rrcp. This phase difference is reached very quickly, as has been reported several times.[31,33] The diffraction efficiency of the SRG compensates the initial orientational diffraction efficiency and then becomes the dominating contribution. For pp, ±45°, and rlcp, which exhibit a fast SRG build-up, the diffraction efficiency goes to zero as shown in the inset of Figure 4, for the other two polarizations it reaches a minimum. For ss and sp, no phase difference could be determined.

Eq. 1 can be used to calculate the modulation height of the SRG, $\Delta d(t)$, from the measured diffraction efficiency $\eta(t)$. In the case of high SRGs, however, the DE of the SRG becomes larger than that of the volume grating by more than

two orders of magnitude. Therefore we neglect the latter at long writing times and use a simpler equation, which can be also derived on the basis of a theory for thin gratings of Magnusson and Gaylord.[30,34] The relation between diffraction efficiency η and modulation height d of the SRG (valley to peak) then reads

$$\eta = J_1^{\,2}\left(\frac{2\,\pi\,\Delta d(t)\,\Delta n}{\lambda\,\cos\theta}\right). \qquad (2)$$

With Eq. 2 we can easily calculate the height of the SRG from the measured diffraction efficiency *in situ*. For high SRGs, Eqs. 1 and 2 obviously yield the same result.

In order to verify the calculated modulation height, the long-term stable surface relief gratings were independently measured with atomic force microscopy (AFM). Figure 5 shows the AFM image of a SRG on a thin film of the molecular glass **4**. Its shape is sinusoidal with a modulation depth of 610 nm and a spacing of 1 μm. This amplitude is significantly higher than those reported in the literature for any photochromic molecular glass.[12,35]

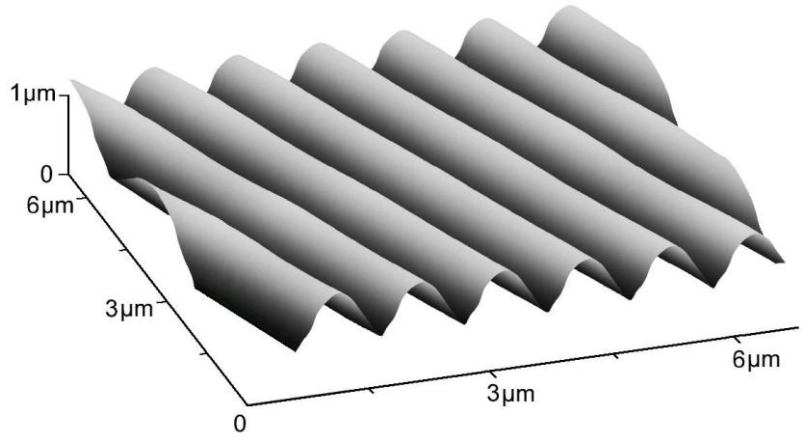

Figure 5. AFM image of a SRG on a thin film of compound **4**. The modulation height of the SRG is 610 nm, its grating spacing 1 µm. It was generated with the polarization configuration ±45°.

Theory of Kumar

Different theories exist which try to explain the formation of surface relief gratings. Although each model describes part of the observed effects correctly, no theory is able to reproduce all experimental results. Hvilsted *et al*. applied a mean-field model[36] to the formation of SRGs[22]. Rochon and co-workers[21,37] developed a model in which this effect is ascribed to a pressure gradient between illuminated and non-illuminated areas. The theory of Yager *et al*.[26] explains the SRG build-up by a competition between photoexpansion and photocontraction. Henneberg and co-workers[24] introduced a viscoelastic-flow model. According to the model proposed by Lefin *et al*.[25], the azobenzene chromophore moves like an inchworm owing to the isomerization between the stretched *trans* and the bent *cis* state, so a translational movement resulting in material transport can occur.

The theory of Kumar *et al*.[27,38] explains the formation of the SRG by the presence of a time-averaged gradient force *f*,

$$\vec{f} = \left\langle \left(\vec{P}\nabla\right)\vec{E} \right\rangle = \left\langle \left(\left(\varepsilon_0 \chi \vec{E}\right)\nabla\right)\vec{E} \right\rangle, \tag{3}$$

where $\vec{P}$ is the optically induced polarization and χ the electric susceptibility of the material at the optical frequency of the laser. This is the only theory which can account for different polarizations of the laser beams.

In the following we refer to the coordinate system shown in Figure 2. The *x* axis defines the direction of the grating vector, the *y* axis is perpendicular to the plane of incidence, and the *z* axis is perpendicular to the surface of the sample. The only direction in which macroscopic material transport can occur is along the *x* axis, parallel to the grating vector. Hence, Eq. 3 can be simplified to[38,39]

$$f_x = \varepsilon_o \left[\chi'_{ix} E_x \frac{\partial}{\partial x} E_x \right], \tag{4}$$

where the subscript i stands for the spatial coordinates *x*, *y*, *z*. The real part of the optical susceptibility $\chi'_{ix} = \chi'_{ix,ini} \pm \Delta\chi'_{ix}$ is the sum of the initial material

susceptibility $\chi'_{ix,ini}$ prior to recording and its spatially varying component after irradiation $\Delta\chi'_{ix}$.

The electric-field vector in the *x*-*y* plane is shown in Figure 3 for different polarizations of the writing beams at several values of the phase difference between them.

When comparing different polarization settings, only the terms coming from the electric field influence f_x. We assume the influence of the electric field to be constant, when different materials at a given polarization setting are compared, so only χ' changes f_x in this case. The optical susceptibility of the material can also be written as:

$$\chi = (n - ik)^2 - 1 = n^2 - k^2 - 1 - i\,2nk \quad \rightarrow \quad \chi' = n^2 - k^2 - 1. \tag{5}$$

The absorption coefficient *k* and the refractive index *n* depend on the material and can be changed by the substituents of the azobenzene.

Intensity holograms cause the minima of the refractive-index modulation of the volume grating to be located in the illuminated regions, the maxima in the dark areas. For a phase shift of 180° between SRG and volume grating as discussed above, the maxima of the SRGs must then be in the illuminated areas. Therefore the direction of the material transport of the SRGs is supposed to be from dark to bright regions, which is also predicted by Eq. 4 for positive values of the susceptibility, as is the case for our materials.

Influence of the polarization of the writing beams

Holographic measurements were performed with different polarization settings of the writing beams, as discussed above. The differences of the resulting SRG heights can be explained by the different strengths of the gradient force f_x. The term $E_X\left(\frac{\partial}{\partial x}E_x\right)$, which is proportional to f_x, is calculated for each polarization configuration. $E_X\left(\frac{\partial}{\partial x}E_x\right)$ can be written as the product of a periodic function of *x*, which is the same in all seven settings, and an amplitude |*A*| which depends

on the polarization. The normalized values of |*A*| are summarized in Table 1. In the ss and sp configuration, either E_x or its derivative is zero, so f_x is zero and no significant SRG is observed. The settings ±45°, ++45°, rlcp, and rrcp have all the same normalized value |*A*| = 0.5 and, hence, they generate comparable maximum heights of the SRG as listed in Table 1 and graphically displayed Figure 6.

Table 1. Comparison of selected characteristics of the SRGs for different states of polarization of the writing beams

polarization configuration	**ss**	**pp**[a)]	**++45°**	**rrcp**	**±45°**	**rlcp**	**sp**
$\lvert A\rvert \propto f_x$	0	1	0.5	0.5	0.5	0.5	0
normalized average maximum height of SRG [b)]	0.05	1	0.83	0.92	0.77	0.77	0.12
normalized average height of SRG after 60 s [b)]	0.09	1	0.38	0.41	0.96	0.93	0.07
maximum growth rate of **4** [nm/s]	0.9	17.7	10.6	9.5	21.2	20.7	1.3
time to reach maximum growth rate of **4** [s]	67	29	49	49	16	16	70

[a)] For all normalized quantities, the value of pp has been arbitrarily set to 1.

[b)] Heights are given as an average of all materials with respect to the corresponding polarization configuration.

The biggest value |*A*| = 1 is obtained with two p-polarized laser beams. Consequently, this configuration yields the highest SRGs of all polarizations. One can assume that the maximum SRG height is reached when f_x is balanced by the surface energy. If the surface energy varies with the height in a nonlinear

fashion, the height obtained with “pp” is not twice as large as the height of, e.g., rlcp.

In Table 1, the amplitudes of the SRGs after 60 s of illumination are listed. The settings ±45° and rlcp result in much higher SRGs than ++45° and rrcp, which all have the same value of f_x. According to Kumar, an important factor for the build-up of the SRGs is the plastification of the material caused by repeated *trans-cis-trans* isomerization cycles. A softening of the material accelerates macroscopic material transport below T_G. In the case of polarization gratings, such a plastification can take place throughout the material, because the light intensity in the sample is homogeneous. Intensity holograms, on the contrary, show no plastification in the dark regions and, therefore, their SRGs build up more slowly. On the other hand, intensity holograms on the average reach a slightly higher maximum height of the SRGs. A possible reason might be that the light intensity in the illuminated areas is higher so that nonlinear effects (e.g., a nonlinear dependence of the plastification on the light intensity) give rise to higher values of f_x and, hence, to larger surface modulations.

The intensity grating pp creates a SRG height comparable to that of the polarization gratings after 1 minute of irradiation, but it has twice the value of f_x as compared to the latter, which is in agreement with the slower SRG build-up by intensity gratings. The maximum SRG growth rate of each material, i.e., the slope of the holographic growth curve, which is proportional to the sensitivity, is much higher in the case of the polarization gratings as compared to the intensity gratings and, therefore, the final SRG amplitude is reached after a shorter period of time.

To summarize, we can state that polarization gratings show a faster SRG build-up because of the homogeneous plastification in the material; intensity gratings form the SRGs more slowly due to the reduced area of plastification, but their SRGs reach slightly larger heights, possibly caused by nonlinear effects. The results of high SRGs obtained with the polarization settings ++45° and rrcp have not been reported before, perhaps due to the required long writing times which necessitate a very good stability of the holographic set-up.

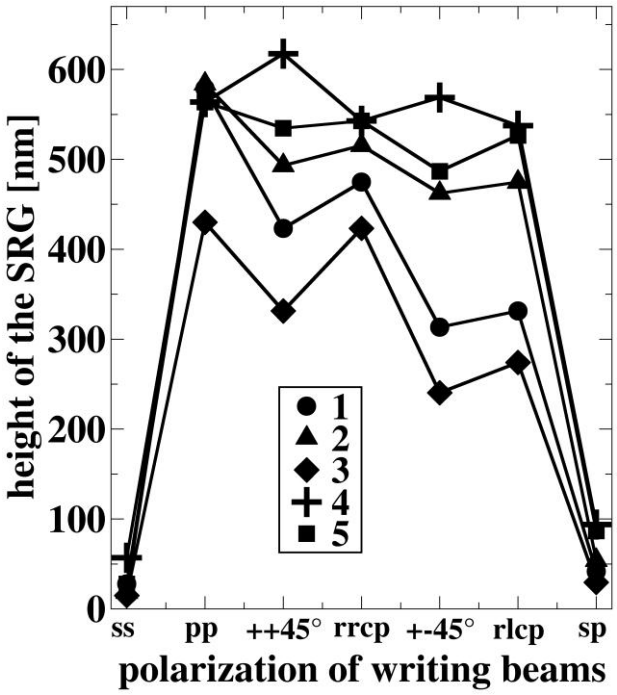

Figure 6. Maximum height of the SRGs of all five materials as calculated from the DE according to Eq. 2 with the different polarization settings. The lines are a guide to the eye.

Influence of the substituents at the azobenzene unit

For the comparison of the five molecular glasses we focus on three important parameters: the absorption coefficient, the susceptibility and the volume of the chromophore. The T_G of the investigated materials has no measurable influence on the formation of the SRGs. The T_G values of all samples differ by only 30 °C and are much higher than room temperature, where the experiments were performed; the lowest T_G is 89 °C. The optical densities per µm at 488 nm, which are proportional to the absorption constants, can be measured by absorption spectroscopy and are listed in Table 2. Larger absorption leads, due to the increased rate of *trans-cis-trans* isomerization cycles, to a stronger plastification of the material and, therefore, to an increased height of the SRGs. The wavelength of 488 nm of the writing laser is in the long-wavelength wing of the nπ* absorption band. Since *k* and *n* are related via the Kramers-Kronig relations, an increase of the optical density (i.e., the absorption constant), either by a shift of the absorption maximum to longer wavelengths or by an increase of the height of the absorption band, in this case leads to an increase of the

refractive index. Both constants can be measured by ellipsometry. Since *n* is 2 orders of magnitude larger than *k* and usually decreases more slowly with increasing distance from the absorption maximum, the refractive index yields the main contribution to the susceptibility. Therefore, the effect of plastification by the higher absorption constant is enhanced by an increase of the susceptibility, resulting in higher SRGs. The relative susceptibilities of the five materials, which determine the driving force f_x for material transport, are listed in Table 2; they are correlated to the maximum SRG heights.

Table 2. Parameters of SRG formation of the five molecular glasses

molecular glass	**1**	**2**	**3**	**4** [a)]	**5**
normalized OD/µm at 488nm	0.71	0.82	0.85	1	1.04
normalized χ at 488 nm	0.69	0.79	0.76	1	1.03
normalized average maximum height of SRG [b)]	0.73	0.84	0.58	1	0.89
normalized average height of SRG after 60 s [b)]	0.48	0.48	0.21	1	0.66
average writing time [s] [b)]	201	272	356	87	121
(normalized average writing time)$^{-1}$ [1/s] [b)]	0.43	0.32	0.18	1	0.72
maximum growth rate with pp [nm/s]	7.9	7.2	4.2	17	11
time to reach maximum growth rate with pp [s]	40	47	64	27	40

a) For all normalized quantities, the value of **4** has been arbitrarily set to 1.

b) Heights and writing times for each material are an average of the polarization configurations.

The volume or “bulkiness” of the chromophores basically has the opposite effect: With increasing size, the isomerization rate is expected to slow down, since the molecule requires a larger free volume in its environment. Also the macroscopic material transport is decelerated, because bigger molecules are transported more slowly than smaller chromophores.

Compound **1** exhibits the lowest absorption constant and susceptibility and also the lowest resulting modulation height. With increasing values of these parameters the SRGs become higher. The SRGs on compound **3** show a slow growth rate and, in addition, they reach only a small modulation height. We attribute this to steric-hindrance effects caused by the lateral methyl group.

The influence of the substituents follows this trend already in the early stages of SRG formation. When comparing materials **1** - **3**, the latter has the lowest SRG height after a writing time of 60 s because of the methyl group, whereas **1** and **2** show the same height. **1** has a lower absorption coefficient than **2** but also a smaller volume, so the two effects compensate each other. **4** features very fast SRG formation. The inverse writing times up to the maximum SRG height show the same variation with absorption constant and susceptibility as the SRG height after 60 s. Also the growth rate for pp polarization behaves in a very similar way. Regarding the SRG formation rate, **4** is the material with the fastest build-up, followed by **5**, **1** (smallest volume), **2**, and **3** (methyl group). To our knowledge, this is the first detailed comparison of the influence of different substituents of low-molecular-weight glass formers based on azobenzene chromophores.

Conclusion

In this paper, we report on the formation of surface relief gratings with heights up to 600 nm in photochromic molecular glasses. The temporal evolution of the diffraction efficiency during the inscription of the SRGs can be simulated for the whole process and can be used to determine the grating height.

By applying seven polarization configurations which give rise to various combinations of intensity and polarization gratings, we found that these experimental conditions have a major influence on the rate of formation and the

achievable amplitude of SRGs. All our experimental results are in good agreement with the gradient force model proposed by Kumar et al.

In addition, the experiments revealed that also different substituents of the azobenzene chromophores influence the growth rate and the maximum height of the SRGs. We attribute this to the varying susceptibility of the chromophores at the writing wavelength.

Acknowledgement

This work was supported by the German Science Foundation in the framework of collaborative research center (Sonderforschungsbreich) 481 (projects B2 and Z2). We thank Dr. Klaus Kreger for helpful discussions.

References

(1) Shirota, Y. J. Mater. Chem. 2000, 10, 1.
(2) Shirota, Y. J. Mater. Chem. 2005, 15, 75.
(3) Strohriegl, P.; Grazulevicius, J. V. Adv. Mater. 2002, 14, 1439.
(4) Hesselink, L.; Orlov, S. S.; Bashaw, M. C. Proc. IEEE 2004, 92, 1231.
(5) Breiner, T.; Kreger, K.; Hagen, R.; Häckel, M.; Kador, L.; Mueller, A. H. E.; Kramer, E. J.; Schmidt, H.-W. Macromolecules 2007, 40, 2100.
(6) Haw, M. Nature 2003, 422, 556.
(7) Ashley, J.; Bernal, M. P.; Burr, G. W.; Coufal, H.; Guenther, H.; Hoffnagle, J. A.; Jefferson, C. M.; Marcus, B.; Macfarlane, R. M.; Shelby, R. M.; Sincerbox, G. T. IBM J. Res. Dev. 2000, 44, 341.
(8) Hagen, R.; Bieringer, T. Adv. Mater. 2001, 13, 1805.
(9) Yager, K. G.; Barrett, C. J. J. Photochem. Photobiol. A 2006, 182, 250.
(10) Natansohn, A.; Rochon, P. Chem. Rev. 2002, 102, 4139.
(11) Rochon, P.; Batalla, E.; Natansohn, A. Appl. Phys. Lett. 1995, 66, 136.
(12) Kim, D. Y.; Tripathy, S. K.; Li, L.; Kumar, J. Appl. Phys. Lett. 1995, 66, 1166.
(13) Carvalho, L. L.; Borges, T. F. C.; Cardoso, M. R.; Mendonca, C. R.; Balogh, D. T. Eur. Polym. J. 2006, 42, 2589.
(14) Schulz, B. M.; Huber, M. R.; Bieringer, T.; Krausch, G.; Zilker, S. J. Synth. Met. 2001, 124, 155.
(15) Yager, K. G.; Tanchak, O. M.; Godbout, C.; Fritzsche, H.; Barrett, C. J. Macromolecules 2006, 39, 9311.
(16) Helgert, M.; Wenke, L.; Hvilsted, S.; Ramanujam, P. S. Appl. Phys. B 2001, 72, 429.

(17) Chun, C.; Kim, M.-J.; Vak, D.; Kim, D. Y. J. Mater. Chem. 2003, 13, 2904.
(18) Kim, M.-J.; Seo, E.-M.; Vak, D.; Kim, D.-Y. Chem. Mater. 2003, 15, 4021.
(19) Ando, H.; Takahashi, T.; Nakano, H.; Shirota, Y. Chem. Lett. 2003, 32, 710.
(20) Seo, E.-M.; Kim, M. J.; Shin, Y.-D.; Lee, J.-S.; Kim, D.-Y. Mol. Cryst. Liquid Cryst. 2001, 370, 143.
(21) Barrett, C. J.; Rochon, P. L.; Natansohn, A. L. J. Chem. Phys. 1998, 109, 1505.
(22) Pedersen, T. G.; Johansen, P. M.; Holme, N. C. R.; Ramanujam, P. S.; Hvilsted, S. Phys. Rev. Lett. 1998, 80, 89.
(23) Yang, K.; Yang, S.; Kumar, J. Phys. Rev. B 2006, 73, 165204.
(24) Henneberg, O.; Geue, T.; Saphiannikova, M.; Pietsch, U.; Rochon, P.; Natansohn, A. Appl. Surf. Sci. 2001, 182, 272.
(25) Leffin, P.; Fiorini, C.; Nunzi, J.-M. Opt. Mater. 1998, 9, 323.
(26) Yager, K. G.; Barrett, C. J. Macromolecules 2006, 39, 9320.
(27) Kumar, J.; Li, L.; Jiang, X. L.; Kim, D. Y.; Lee, T. S.; Tripathy, S. Appl. Phys. Lett. 1998, 72, 2096.
(28) Frenz, C.; Fuchs, A.; Schmidt, H.-W.; Theissen, U.; Haarer, D. Macromol. Chem. Phys. 2004, 205, 1246.
(29) Häckel, M.; Kador, L.; Kropp, D.; Schmidt, H.-W. Adv. Mater. 2007, 19, 227.
(30) You, F.; Paik, M. Y.; Häckel, M.; Kador, L.; Kropp, D.; Schmidt, H.-W.; Ober, C. K. Adv. Funct. Mat. 2006, 16, 1577.
(31) Reinke, N.; Draude, A.; Fuhrmann, T.; Franke, H.; Lessard, R. A. Appl. Phys. B 2004, 78, 205.
(32) Sobolewska, A.; Miniewicz, A. J. Phys. Chem. B 2007, 111, 1536.
(33) Holme, N. C. R.; Nikolova, L.; Ramanujam, P. S.; Hvilsted, S. Appl. Phys. Lett. 1997, 70, 1518.
(34) Magnusson, R.; Gaylord, T. K. J. Opt. Soc. Am. 1978, 68, 806.
(35) Nakano, H.; Takahashi, T.; Tanino, T.; Shirota, Y. J. Photopolym. Sci. Tec. 2007, 20, 87.
(36) Pedersen, T. G.; Johansen, P. M. Phys. Rev. Lett. 1997, 79, 2470.
(37) Barrett, C. J.; Natansohn, A. L.; Rochon, P. L. J. Phys. Chem. 1996, 100, 8836.
(38) Viswanathan, N. K.; Kim, D. Y.; Bian, S.; Williams, J.; Liu, W.; Li, L.; Samuelson, L.; Kumar, J.; Tripathy, S. K. J. Mater. Chem. 1999, 9, 1941.
(39) Viswanathan, N. K.; Balasubramanian, S.; Li, L.; Tripathy, S. K.; Kumar, J. Jpn. J. Appl. Phys. 1999, 38, 5928.

4.4 Holographic Investigations of Azobenzene-Containing Low Molecular Weight Compounds in Pure Materials and Binary Blends with Polystyrene

By *Hubert Audorff, Roland Walker, Lothar Kador* and *Hans-Werner Schmidt**

[*] Prof. H.-W. Schmidt, R. Walker
University of Bayreuth, Macromolecular Chemistry I and
"Bayreuth Institute of Macromolecular Research"
D-95440 Bayreuth (Germany)
E-mail: hans-werner.schmidt@uni-bayreuth.de

Prof. L. Kador, H. Audorff
University of Bayreuth, "Bayreuth Institute of Macromolecular Research"
D-95440 Bayreuth (Germany)
E-mail: lothar.kador@uni-bayreuth.de

This paper is submitted to
Chemistry – A European Journal

Keywords: azobenzene, photoactive low molecular weight compunds, binary blends, holography

Abstract

This paper reports on the synthesis and the thermal and optical properties of photochromic low-molecular-weight compounds, especially with respect to the formation of holographic volume gratings in the pure materials and in binary blends with polystyrene. Its aim is to provide a basic understanding of the holographic response with regard to the molecular structure and, thus, to show a way for obtaining suitable rewritable materials with high sensitivity for holographic data storage. The photoactive low-molecular-weight compounds consist of a central core with three or four azobenzene-based arms attached via esterification. Four different cores were investigated which influence the glass transition temperature and the glass-forming properties. Additional structural variations were introduced by the polar terminal substituent at the azobenzene chromophore to fine-tune the optical properties and the holographic response. Films of the neat compounds were investigated in holographic experiments, especially with regard to the material sensitivity. In binary blends of the low-molecular-weight compounds with polystyrene, the influence of a polymer matrix on the behavior in holographic experiments was studied. The most promising material combination was also investigated at elevated temperatures, where the holographic recording sensitivity is even higher.

Introduction

Low-molecular-weight materials, especially molecular glasses, are a new class of materials which are the subject of intense current studies, mainly with respect to their electronic, optical, and optoelectronic properties. Like polymers, they are characterized by their glass transition temperature (T_g) and form a stable amorphous phase.[1-3] In contrast to functional polymers,[4-6] low-molecular-weight materials possess a well-defined molecular structure, no molecular-weight distribution, and no undefined or undesired end groups, which results in more uniform physical properties. Therefore, low-molecular glasses are ideal candidates for comparative investigations.

Another subject of current interest are photochromic compounds carrying azobenzene groups. Upon illumination with polarized light, the azobenzene moiety undergoes multiple reversible *trans-cis-trans* isomerization cycles, which finally reorient the long axis of the *trans* form, since it is parallel to the transition dipole moment, into the plane perpendicular to the polarization axis of the incident light. Electronic excitation is then no longer possible ("orientational hole burning"). [7] The resulting effects such as pronounced birefringence and the formation of a refractive-index modulation in the bulk of the sample upon holographic illumination were mainly investigated in polymer systems, in which the azobenzene chromophores are usually covalently linked as side groups.[8-13] Azobenzene chromophores were also introduced into small molecular species yielding photochromic molecular glasses.[1,3] The focus of holographic studies of these azobenzene-containing amorphous molecular materials has mainly been on the formation of surface relief gratings (SRGs).[14-19] By choosing appropriate polarization configurations of the holographic writing beams, however, SRG formation can be suppressed and the inscription of pure phase gratings in the bulk is possible..[3,16,20] An important difference as compared to their polymeric counterparts is that low-molecular materials are expected to exhibit faster photo-physical response because of the absence of polymer chain entanglements.[20,21] So far, only few reports on holographic volume gratings in amorphous low-molecular azobenzene compounds have been published,[22, 23] although they are suitable for many potential applications such as, *e.g*., optical switches, security devices and materials for holographic data storage.

In the present paper, holographic experiments on photochromic low-molecular-weight materials are reported. Thin films of the pure materials and of blends with polystyrene were investigated. Holographic volume gratings in materials with different azobenzene chromophores and various cores were inscribed and studied in view of the holographic sensitivity. The temporal behavior of the formation and decay of the refractive-index gratings at ambient conditions and elevated temperatures is discussed.

Experimental

Material and methods

All starting materials were commercially available and were used without further purification. Dry toluene and dry tetrahydrofurane (THF) were refluxed over potassium. All synthesized compounds were identified by 1H-NMR spectroscopy with a BRUKER AC250 spectrometer (250 MHz). To confirm purity, SEC measurements were employed utilizing a WATERS model 515 HPLC-pump with a UV-detector at 254 nm (WATERS model 486) and a Differential RI-detector (WATERS model 410). The column set-up consists of a guard column (PSS: SDV-gel; length 5 cm, diameter 0.8 cm, particle size 5 µm, pores size 100 Å) and two separation columns (PL: PL-gel; length 60 cm, diameter 0.8 cm, particle size 5 µm, pores size 100 Å). Stabilized THF at a constant flow rate of 0.5 ml/min was used as eluent. Characterization of the thermal properties was done by DSC measurements with a PERKIN-ELMER DSC7 (standard heating rate: 10 K/min) using approx. 10 mg of the compounds in 40 µl pans. Verification of the data obtained from the DSC was performed in an optical microscope with crossed polarizers (NIKON DIAPHOT 300) on a heating table (METTLER FP82 with METTLER FP 80 control unit). UV/Vis absorption spectra of the compounds were recorded in the range from 250 nm to 650 nm with HITACHI U-3000 spectral photometer. Elemental analysis was carried out with an EURO EA 3000 analyzer (HEKATECH).

General preparation method (GPM 1): Ester coupling of tris carboxylic acids

The corresponding tris carboxylic acids were placed in a flame-dried Schlenck flask and 10 ml of thionylchloride were added. The suspension was stirred for 24 h under reflux at 70 °C. During this time the carboxylic acids were slowly dissolving. Thereafter the thionylchloride was distilled off and the crude product was used without further purification. The obtained carboxylic acid chlorides (1 equiv.) were dissolved in 150 ml toluene under argon atmosphere. A threefold molar excess of anhydrous triethylamine per acid chloride group and 1.1 equivalents of the corresponding azobenzene compound for each acid chloride group were added. The dark red solution was stirred for 24 h under

reflux at 110 °C. The solution was filtered, washed with additional toluene, and thereafter the solvent was distilled off. The crude product was dissolved in THF and precipitated in EtOH. The precipitate was filtered with a frit and dried in high vacuum. Remaining impurities were removed by a second precipitation in EtOH.

General preparation method (GPM 2): Ester coupling of tetraols

In a flame-dried Schlenck flask the corresponding tetraols (1 equiv.) were dissolved in 150 ml THF under argon atmosphere. A threefold molar excess of anhydrous pyridine per hydroxyl group and 1.1 equivalents of the corresponding azobenzene acid chloride compound per hydroxyl group were added. The dark red solution was stirred for 24 h under reflux at 70 °C. The solution was filtered, washed with additional THF, and thereafter the solvent was distilled off. The crude product was dissolved in THF and precipitated in EtOH. The precipitate was filtered with a frit and dried in high vacuum. Remaining impurities were removed by a second precipitation in EtOH.

Synthesis of low molecular weight materials

Benzene-based 1,3,5-Trisester **1a**: 1,3,5-Tri(carboxylic acid chloride)benzene (**1**) (0.50 g, 1.9 mmol) is coupled with 4-(Phenylazo)phenol (1.23 g, 6.2 mmol) according to GPM 1 yielding 0.57 g (40 %) of the title compound as orange powder. ^{1}H-NMR (250°MHz, $CDCl_3$, δ): 7.45-7.48 (m, 15H, Ar-H), 7.94 (dd, *J* = 3°Hz, *J* = 1°Hz, 6H, Ar-H), 8.06 (d, *J* = 3°Hz, 6H, Ar-H), 9.31 (s, 3H, Ar-H), elem. anal. calcd for $C_{45}H_{30}N_6O_6$: C 71.99, H 4.03, N 11.19; found: C 71.15, H 4.37, N 11.31.

Benzene-based 1,3,5-Trisester **1b**: 1,3,5-Tri(carboxylic acid chloride)benzene (**1**) (0.50 g, 1.9 mmol) is coupled with 4-((4-Methoxy)phenylazo)phenol (1.42 g, 6.2 mmol) according to GPM 1 yielding 0.84 g (53 %) of the title compound as orange powder. ^{1}H-NMR (250°MHz, $CDCl_3$, δ): 3.91 (s, 9H, CH_3), 7.02 (d, *J* = 3°Hz, 6H, Ar-H), 7.43 (d, *J* = 3°Hz, 6H, Ar-H), 7.94 (d, *J* = 3°Hz, 6H, Ar-H), 8.01 (d, *J* = 3°Hz, 6H, Ar-H), elem. anal. calcd for $C_{48}H_{36}N_6O_9$: C 68.58, H 4.32, N 9.99; found: C 68.77, H 4.45, N 9.67.

Cyclohexane-based 1,3,5-Trisester **2a**: 1,3,5-Cyclohexanetricarbonyl chloride (**2**) (0.75 g, 2.8 mmol) is coupled with 4-(Phenylazo)phenol (1.81 g, 9.1 mmol) according to GPM 1 yielding 1.14 g (55 %) of the title compound as orange powder. ^{1}H-NMR (250°MHz, $CDCl_3$, δ): 1.84-1.99 (m, 3H, CH), 2.67-2.76 (m, 3H, CH), 2.79-2.89 (m, 3H, CH), 7.21 (d, *J* = 3°Hz, 6H, Ar-H), 7.45-7.48 (m, 9H, Ar-H), 7.87 (dd, *J* = 3°Hz, *J* = 1°Hz, 6H, Ar-H), 7.94 (d, *J* = 3°Hz, 6H, Ar-H), elem. anal. calcd for $C_{45}H_{36}N_6O_6$: C 71.42, H 4.79, N 11.10; found: C 69.71, H 5.00, N 11.16.

Cyclohexane-based 1,3,5-Trisester **2b**: 1,3,5-Cyclohexanetricarbonyl chloride (**2**) (0.60 g, 2.2 mmol) is coupled with 4-((4-Methoxy)phenylazo)phenol (1.66 g, 7.3 mmol) according to GPM 1 yielding 1.10 g (59 %) of the title compound as orange powder. ^{1}H-NMR (250°MHz, $CDCl_3$, δ): 1.95-2.00 (m, 3H, CH), 2.73-2.78 (m, 3H, CH), 2.85-2.92 (m, 3H, CH), 3.92 (s, 9H, CH_3), 7.04 (d, *J* = 3°Hz, 6H, Ar-H), 7.29 (d, *J* = 3°Hz, 6H, Ar-H), 7.92-7.98 (m, 12H, Ar-H), elem. anal. calcd for $C_{48}H_{43}N_6O_9$: C 67.99, H 5.11, N 9.91; found: C 67.95, H 5.11, N 9.78.

Triphenylamine-based 4,4´,4´´-Trisester **3a**: The synthesis and characterization have already been reported elsewhere.[21]

Triphenylamine-based 4,4´,4´´-Trisester **3b**: The synthesis and properties have already been reported elsewhere.[21]

Spirobischroman-based 6,6´,7,7´-Tetraester **4a**: 6,6',7,7'-Tetrahydroxy-4,4,4',4'-tetramethyl-2,2-spirobischroman (**4**) (0.90 g, 2.4 mmol) is coupled with 4-(Phenylazo)benzoyl chloride (2.60 g, 10.6 mmol) according to GPM 2 yielding 0.79 g (27 %) of the title compound as orange powder. ^{1}H-NMR (250°MHz, $CDCl_3$, δ): 1.45 (s, 6H, CH_3), 1.68 (s, 6H, CH_3), 2.15 (q, *J* = 6°Hz, 4H, CH_2), 6.87 (s, 2H, Ar-H), 7.37 (s, 2H, Ar-H), 7.48-7.50 (m, 12H, Ar-H), 7.85-7.92 (m, 16H, Ar-H), 8.18-8.24 (m, 8H, Ar-H), elem. anal. calcd for $C_{73}H_{56}N_8O_{10}$: C 72.75, H 4.68, N 9.30; found: C 72.99, H 4.69, N 9.29.

Spirobischroman-based 6,6´,7,7´-Tetraester **4b**: 6,6',7,7'-Tetrahydroxy-4,4,4',4'-tetramethyl-2,2-spiro-bischroman (**4**) (0.23 g, 0.6mmol) is coupled with 4-((4-Methoxy)-phenylazo)benzoyl chloride (0.75 g, 2.7 mmol) according to GPM 2 yielding 0.40 g (49 %) of the title compound as orange powder. ^{1}H-NMR (250°MHz, $CDCl_3$, δ): 1.46 (s, 6H, CH_3), 1.69 (s, 6H, CH_3), 2.17 (q, *J* = 6°Hz, 4H, CH_2), 3.93 (s, 12H, CH_3), 6.88 (s, 2H, Ar-H), 7.01 (d, *J* = 3°Hz, 6H, Ar-H),

7.38 (s, 2H, Ar-H), 7.86 (d, *J* = 3°Hz, 6H, Ar-H), 7.92 (d, *J* = 3°Hz, 6H, Ar-H), 8.20 (d, *J* = 3°Hz, 6H, Ar-H), elem. anal. calcd for $C_{77}H_{64}N_8O_{14}$: C 69.78, H 4.87, N 8.45; found: C 69.48, H 5.04, N 7.97.

Sample preparation

Thin films of the pure materials were prepared by spin-coating a filtered solution of 6 wt% of the compound in THF at 1000 rpm for 60 s on a commercially available glass substrate. To produce samples of the materials blended with polystyrene, a filtered solution of 3 wt% low molecular weight compound and 3 wt% PS (BASF 165 H) in THF was spin coated at 1000 rpm for 60 s. The film thickness was measured with a Dektak profilometer (Veeco 3300ST). All samples showed good optical quality and absence of light scattering.

Set-up for holographic experiments

The holographic experiments were performed with a setup as described in literature.[24] The gratings were inscribed with the 488 nm line of an Ar^+ ion laser. A beam splitter generated two coherent s-polarized beams which were superimposed in the plane of the sample. The beam diameter was about 1.4 mm and the intensity of each beam was adjusted to 1 W/cm^2. The angles of incidence with respect to the surface normal are ±14°, resulting in a grating period of 1 µm. An *s*-polarized diode laser beam at 685 nm was used for monitoring the diffraction efficiency (DE) *in situ* without affecting the writing process. The power of the transmitted and the diffracted beam were measured with two photodiodes. From the diffraction efficiency, the refractive-index modulation was calculated according to Kogelnik's theory.[25] The temperature-dependent measurements were performed in a similar way with the sample placed in a temperature-controlled box of anodized aluminum. Its temperature could be adjusted between 20 and 120 °C with an accuracy of 1 °C.

Results and discussion

Thermal and optical properties of azobenzene-containing low molecular weight-compounds

The materials described in this work are based on a central core unit functionalized with azobenzene chromophores. Four different core compounds were chosen to cover a broad spectrum of glass transition temperatures. The azobenzene side arms were linked to the cores via esterification which provides easy access to a large variety of compounds. Furthermore, azobenzene moieties with different substituents can be readily introduced to study their effects on the optical and photo-physical properties. The influence of substitution at the azobenzene moiety on the photo-responsive properties of the whole molecule has only been studied in few reports so far. [3,26,27]

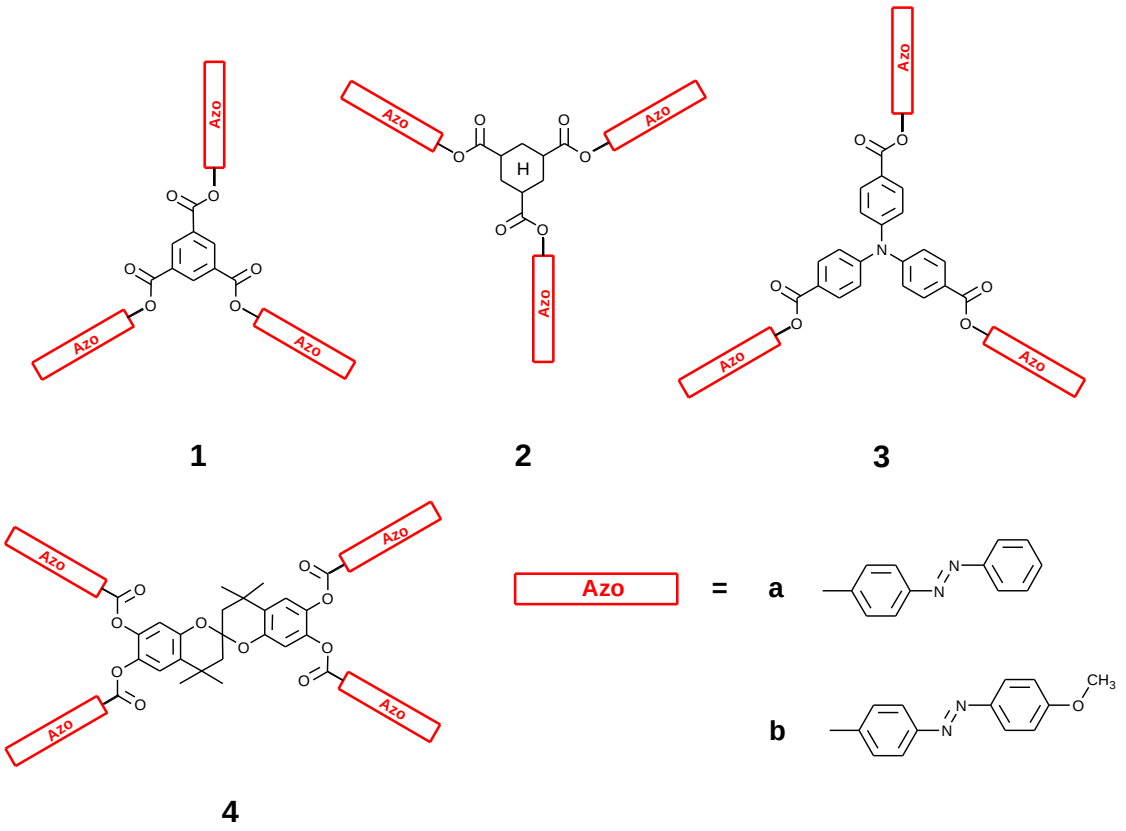

Figure 1. Schematic illustration of the photo-addressable azobenzene-containing low molecular weight compounds.

The thermal behavior of all neat compounds was investigated with common methods such as DSC and TGA. In addition, the solid-state properties of all compounds were confirmed by polarizing microscopy. A summary of the thermal and optical properties is given in table 1.

The materials discussed in this work have glass transition temperatures in the range 54 – 113 °C. The changes of the glass transition temperature due to the methoxy substituents at the azobenzene moiety are minor; the Tg values of all compounds with chromophore **b** differ by no more than 4 °C from the compounds with chromophore **a**. Compound **3a** shows a polymorphic melting behavior which can often be found in low molecular weight compounds.[4, 28] With exception of **1a** and **2a** the compounds vitrify upon cooling without crystallization; therefore, six of the eight materials can be regarded as molecular glasses.

The optical properties of all compounds were investigated by UV-Vis spectroscopy in solution. Most photo-responsive low molecular weight compounds described in the literature possess a widely conjugated π-electron system which comprises the azobenzene chromophore. I In contrast, the conjugation in the molecular glass formers presented here is largely interrupted by the ester linkage. Two absorption maxima can be distinguished in the absorption spectra. The maximum at shorter wavelengths is assigned to an intense π-π* transition and the second one to a weak n-π* transition (see table 1). The exact wavelength of both transitions can, on the one hand, be influenced by the core compound. For the materials **3a** and **3b**, the maximum of the π-π* transition is strongly red-shifted, since the absorption of the triphenylamine core is overlapping with that of the azobenzene chromophore. On the other hand, the transition maxima can shift because of the location of the carbonyl unit in relation to the chromophore or its substituent. For all compounds with chromophore **b**, the methoxy substituent leads to a red shift of the π-π* absorption maxima and a blue shift of the n-π* maxima.

Table 1. Data of the thermal and optical properties of the synthesized azobenzene-containing low-molecular-weight compounds. T_m, melting temperature; T_c, crystallization temperature; T_g, glass transition temperature; $\lambda(\pi\text{-}\pi^*_{max})$, wavelength of maximum of the π-π* transition; $\lambda(n\text{-}\pi^*_{max})$, wavelength of maximum of the n-π* transition; OD/µm, optical density per micrometer thickness; n.d., not distinguished.

	first heating [a]		second heating [a]					
Com-pound	T_m [°C]	T_c [°C]	T_g [°C]	T_c [°C]	T_m [°C]	$\lambda(\pi\text{-}\pi^*_{max})$ [nm] [c]	$\lambda(n\text{-}\pi^*_{max})$ [nm] [c]	OD / µm [d]
1a	247	211	74 [b]	102	247	324	438	0.10
1b	253	206	70	104	251	352	432	0.37
2a	185	125	54 [b]	97	163	324	438	0.08
2b	190	n.d.	58	98	185	351	433	0.09
3a	160, 175	n.d.	92	n.d.	n.d.	359	438	0.16
3b	127	n.d.	89	n.d.	n.d.	366	434	0.18
4a	257	n.d.	109	212	257	326	449	0.08
4b	n.d.	n.d.	113	n.d.	n.d.	358	442	0.19

[a] determined by DSC with heating and cooling rates of 10 K/min under N_2, [b] obtained after quenching of the sample, [c] measured in 10^{-5} molar solution in $CHCl_3$, [d] determined from thin films (for preparation see experimental)

Photo-physical properties of azobenzene-containing low molecular weight materials

A comprehensive investigation of the photo-physical response by holographic methods was conducted on thin films consisting of the pure photoactive compounds (see figure 1) and of blends with polystyrene. The applied ss-polarization of the writing beams is known to produce surface relief gratings (SRGs) very ineffectively.[20, 29] Furthermore, the irradiation times were far too short to form SRGs with a reasonable amplitude. Therefore, it was possible to investigate pure volume gratings. The growth of the refractive-index modulation can be well fitted with a stretched-exponential function, which is commonly used to describe the kinetics in disordered systems:[30, 31]

$$n_1(t) = n_{1\max}\left(1-\exp\left(-\left(\frac{t}{\tau_1}\right)^{0.9}\right)\right) \qquad \textbf{(1)}$$

Here $n_{1\ \max}$ is the maximum achievable refractive-index modulation and τ_1 the time constant of the build-up. The necessity of introducing a stretching exponent β < 1 indicates a size distribution of the voids of free volume around the chromophores. Since the exponent turned out to be the same for all fits, we can assume that the size distribution is roughly independent of the substituent and the core.The build-up of the refractive-index modulation results from the formation of a transient *cis-trans* population lattice and an orientation lattice of the thermally stable *trans* form of azobenzene.

The decay of the refractive-index modulation after turning the writing laser off shows a more complex behavior than the growth. It can be fitted with two stretched-exponential functions:

$$n_1(t) = n_{1\max}\left[A\exp\left(-\left(\frac{t}{1s}\right)^{0.25}\right)+(1-A)\exp\left(-\left(\frac{t}{\tau_2}\right)^{0.4}\right)\right] \qquad \textbf{(2)}$$

The fast relaxation component with amplitude *A* has a time constant of 1 second in all measurements and the slower one has amplitude 1-*A* and the variable time constant τ_2 which is longer than 1 second by several orders of magnitude. The fast process of the decay has a contribution of less than 28%. We interpret it as the thermal relaxation of the metastable *cis* isomers. In solution, where the back relaxation of the *cis* to the *trans* form is usually

determined, the *cis* state has much longer lifetimes in the order of minutes. According to Shirota, a solid environment where the *cis* isomers are trapped in constrained geometries, foster a faster relaxation.[3] Also interactions between adjacent molecules, which increase the thermal *cis*-*trans* relaxation rate, are possible.[32]

The slow relaxation process is assigned to a thermally induced reorientation of the *trans* azobenzene moieties. In most publications, the decay was only recorded during a few minutes and the refractive-index modulation was assumed to be constant for longer times. We recorded the decay for at least one day and found that the refractive-index modulation is not stable at longer times but decays to zero.

An important parameter for the characterization of holographic materials is the recording sensitivity *S*. It describes the slope of the square root of the holographic growth curve and can be calculated with the formula

$$S = \frac{\frac{\partial\sqrt{\eta}}{\partial t}}{I_0 d} \qquad \textbf{(3)}$$

whereby η is the diffraction efficiency, I_0 the laser intensity, and d the sample thickness.[33] The sensitivity depends mainly on the writing time and the corresponding refractive-index modulation. It is usually measured at the beginning of the writing process where it has its maximum value S_{max}.

For a systematic comparison of all eight materials, they were blended with 50 wt% of polystyrene to obtain films of sufficient optical quality, since **1a** and **2a** did not form scatter-free films in neat form. The growth and decay curves of the refractive-index modulation could be fitted with equations 1 and 2, respectively. As a typical example, these curves are shown in figure 2 for a blend of **2b**.

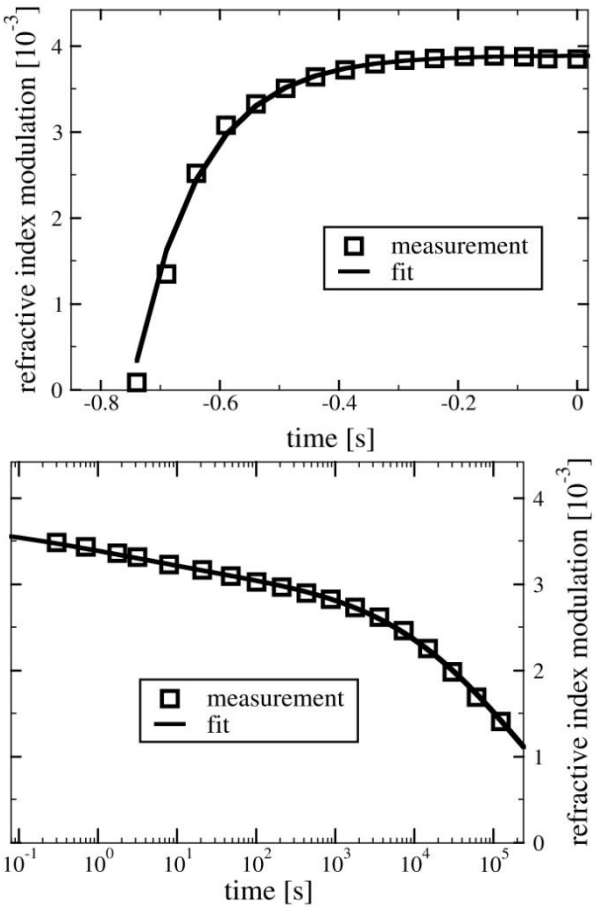

Figure 2. Build-up (left) and decay (right) of the refractive-index modulation of a volume phase grating inscribed in a film of **2b** blended with 50 wt% polystyrene. Symbols represent the experimental data, smooth curves the fits with Eq. 1 and 2, respectively. The hologram was inscribed at negative times and the writing laser was turned off at t = 0. Note the logarithmic time scale in part B.

The results of the fits are listed in table 2. The comparison of the blends with chromophore **a** shows that **2a** exhibits the highest sensitivity and the shortest time constant τ_1. It is known that a polar end group at the azobenzene moiety leads to an increased absorption of the molecule,[34,35] so the transition dipole moment can be influenced by slight modifications of the molecular structure. Different substituents at the azobenzene chromophore also influence the growth of phase gratings in the bulk.[36,37] All materials with chromophore **b** show a shorter build-up time τ_1 as well as a higher refractive-index modulation and sensitivity than the corresponding material with chromophore **a**.

Table 2. Summary of the experimental data for the different photo-addressable low molecular weight materials in blends consisting of 50 wt% polystyrene. T_g: glass transition temperature. The other symbols pertain to equations 1, 2, and 3.

	T_g [a] [°C]	$n_{1\,max}$	A	build-up τ_1 [s]	decay τ_2 [s]	S_{max} [cm/J]
1a	74	0.0046	0.17	0.29	$0.7 \cdot 10^6$	366
1b	70	0.0028	--	0.14	--	536
2a	54	0.0032	0.28	0.10	$0.2 \cdot 10^6$	647
2b	58	0.0038	0.08	0.09	$0.2 \cdot 10^6$	846
3a	92	0.0027	0.19	0.91	$5 \cdot 10^6$	66
3b	89	0.0056	0.10	0.32	$19 \cdot 10^6$	381
4a	109	0.0028	0.14	0.28	$6 \cdot 10^6$	225
4b	113	0.0025	0.13	0.11	$1.2 \cdot 10^6$	518

[a] measured for the pure material

The comparison of the decay times τ_2 of the unsubstituted materials reveals a correlation with T_g. Materials with methoxy substituent have longer decay time constants than their unsubstituted counterparts, which indicates stronger cooperative effects between the chromophores due to the larger dipole moment. Shirota[1] reported an increased *cis* population in materials without a substituent at the *para* position as compared to those with CH_3 substituent. The fit parameter *A*, which indicates the relative contribution of the *cis-trans* population lattice to the total refractive-index modulation, is also a measure of the overall cis-concentration. Unsubstituted samples indeed feature higher *A* values than those with methoxy substituent.

The maximum achievable sensitivity S_{max} was also measured for the neat compounds with methoxy substituent at the azobenzene chromophore, *i.e.* **1b**, **2b**, **3b** and **4b**. The materials with chromophore **b** were chosen, since the blends with polystyrene had already shown that they exhibit higher sensitivities than their counterparts with the unsubstituted chromophore **a**. Films of the neat compounds were studied in addition to the blends, since they are expected to possess higher sensitivities. Stable amorphous films were obtained by spin-coating from solution, and they remained amorphous, unless they were heated above their glass transition temperature. No crystallization was detected even after months when stored at room temperature. The growth and decay curves of the refractive-index modulation could be well fitted with equations 1 and 2, respectively. The results of the fits are listed in table 3. The refractive-index modulation and the sensitivity are twice as high as in the blends, which is expected, since the concentration of azobenzene has also increased by a factor of two. The time constants of the build-up were comparable for the diluted and the undiluted samples. Blending with polystyrene does not seem to affect the reorientation of the azobenzene chromophores. Hence, one can conclude that the photo-physical properties in the blends are almost the same as in the neat materials and the comparison between the blends is also valid for the latter.

The values of n_{1max} are smaller than in polymers bearing azobenzene side groups at a comparable concentration. The decoupling of the chromophore by a flexible spacer usually leads to an improved in-plane orientation and a higher refractive-index modulation. On the other hand, the lack of a spacer in the low-molecular-weight compounds, along with the missing polymer chain entanglements, results in very fast writing times. Azobenzene-containing block copolymers are a promising material class for rewritable holographic data storage, but their sensitivities are low.[39,40] The sensitivity of the neat molecular glass **2b** is larger than 1800 cm/J, which is higher by a factor of 5 than the values of block copolymers with a comparable optical density per µm thickness. The time constant of hologram inscription has been improved by a factor of 10.[41] Therefore, the low-molecular-weight compounds presented here are an interesting material class and may be used for blending with photo-addressable

polymers to improve the photo-physical response, especially the sensitivity, of the latter. Corresponding studies are under way.

Table 3. Summary of the experimental data for the different photo-addressable low molecular weight compounds with substituent **b** as measured in the neat materials. T_g: glass transition temperature. The other symbols pertain to equations 1, 2, and 3.

	T_g [°C]	$n_{1\,max}$	A	build-up τ_1 [s]	decay τ_2 [s]	S_{max} [cm/J]
1b	70	0.0112	0.19	0.24	$3 \cdot 10^4$	1102
2b	58	0.0078	0.10	0.10	$1 \cdot 10^6$	1843
3b	89	0.0103	0.10	0.27	$2 \cdot 10^6$	901
4b	113	0.0047	0.12	0.12	$4 \cdot 10^4$	925

Holographic experiments at elevated temperatures

Holographic measurements on compound **2b** diluted in polystyrene were also performed at elevated temperatures. The growth curves of the refractive-index modulation could be fitted with equation 1 again. The time constant τ_1 shortened with increasing temperature, as figure 3 shows. Already moderate heating to 50 °C resulted in a three times faster time constant of the build-up. This result can be ascribed to an increased mobility of the azobenzene chromophores. The maximum refractive-index modulation $n_{1\ max}$ remained constant up to 65 °C and then showed a steep drop due to the increasing thermal mobility of the azobenzene chromophores around T_g. The slow time constant of the decay, τ_2, followed an Arrhenius law with an activation energy of 32 kJ/mol (data not shown). This value is smaller than the activation energies obtained for azobenzene-containing block copolymers.[42]

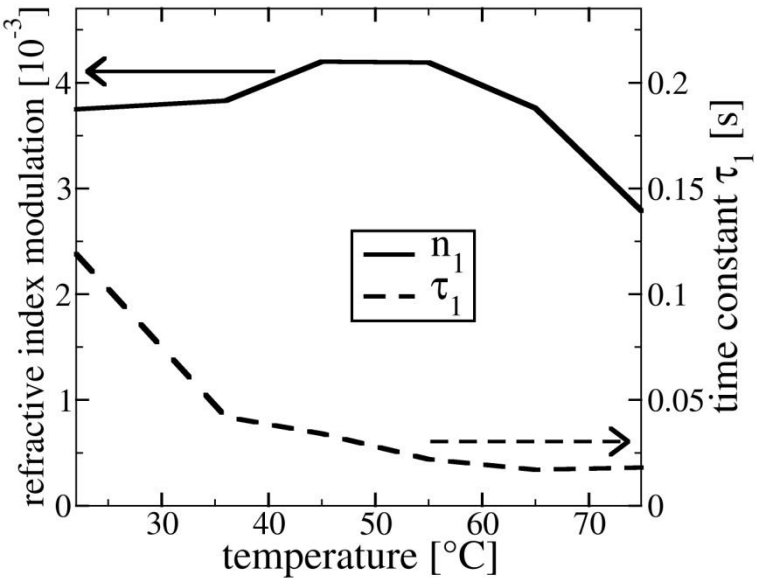

Figure 3. Temperature dependence of time constant τ_1 describing the hologram growth during inscription (broken line; right-hand scale) and maximum refractive-index modulation $n_{1\ max}$ (solid line; left-hand scale). Holographic gratings were inscribed at 22 °C 36 °C, 45 °C, 55 °C, 65 °C, and 75 °C.

Conclusion

We have presented the synthesis and characterization of a series of azobenzene-containing low-molecular-weight compounds which were mainly investigated with respect to holographic volume gratings. Most of our materials readily form amorphous phases. The comparison of thin films of the neat materials and blends with 50 wt% polystyrene showed that the photo-physical behavior was not significantly different. Most of the compounds exhibit remarkably high sensitivities exceeding those of comparable polymers by a factor of 5. Moderate heating improved the sensitivity even further. Hence, the photochromic low-molecular weight compounds appear to be attractive candidates for realizing rewritable holographic recording media with improved writing speed.

Acknowledgment

This work was financially supported by the German Science Foundation (DFG) in the collaborative research centre (Sonderforschungsbereich) 481 (projects B2 and Z2). The authors wish to thank Dr. Klaus Kreger for many helpful discussions.

Literature

1. Shirota, Y., *Organic materials for electronic and optoelectronic devices.* Journal of Materials Chemistry, 2000. **10**(1): p. 1-25.
2. Strohriegl, P. and J.V. Grazulevicius, *Charge-transporting molecular glasses.* Advanced Materials, 2002. **14**(20): p. 1439-1452.
3. Shirota, Y., *Photo- and electroactive amorphous molecular materials-molecular design, syntheses, reactions, properties, and applications.* Journal of Materials Chemistry, 2005. **15**(1): p. 75-93.
4. Friend, R.H., et al., *Electroluminescence in conjugated polymers.* Nature, 1999. **397**(6715): p. 121-128.
5. Groenendaal, L.B., et al., *Poly(3,4-ethylenedioxythiophene) and its derivatives: past, present, and future.* Advanced Materials, 2000. **12**(7): p. 481-494.
6. Gelinck, G.H., et al., *Flexible active-matrix displays and shift registers based on solution-processed organic transistors.* Nature Materials, 2004. **3**(2): p. 106-110.
7. Hagen, R. and T. Bieringer, *Photoaddressable polymers for optical data storage.* Advanced Materials, 2001. **13**(23): p. 1805-1810.
8. Ringsdorf, H. and H.-W. Schmidt, *Electro-optical effects of azo dye containing liquid crystalline copolymers.* Makromol. Chem., 1984. **185**: p. 1327-1334.
9. Eich, M., et al., *Nonlinear optical self diffraction in a mesogenic side chain polymer.* Makromolekulare Chemie, 1985. **186**(12): p. 2639-2647.
10. Hvilsted, S., et al., *Novel Side-Chain Liquid Crystalline Polyester Architecture for Reversible Optical Storage.* Macromolecules, 1995. **28**: p. 2172-2183.
11. Meng, X., A. Natansohn, and P. Rochon, *Azo polymers for reversible optical storage. 13. Photoorientation of rigid side groups containing two azo bonds.* Polymer, 1997. **38**(11): p. 2677-2682.
12. Cimrova, V., et al., *Optical Anisotropy in Films of Photoaddressable Polymers.* Macromolecules, 1999. **32**(25): p. 8496-8503.
13. Häckel, M., et al., *Holographic information storage in azobenzene-containing diblock copolymers.* Proceedings of SPIE-The International Society for Optical Engineering, 2005. **5939**: p. 08/1-10.
14. Kim, D.Y., et al., *Laser-induced holographic surface relief gratings on nonlinear optical polymer films.* Applied Physics Letters, 1995. **66**(10): p. 1166-1168.

15. Rochon, P., E. Batalla, and A. Natansohn, *Optically induced surface gratings on azo aromatic polymer films.* Applied Physics Letters, 1995. **66**(2): p. 136-138.
16. Chun, C., et al., *A novel azobenzene-based amorphous molecular material with a spiro linked bifluorene.* Journal of Materials Chemistry, 2003. **13**(12): p. 2904-2909.
17. Ando, H., et al., *Comparative studies of the formation of surface relief grating. Amorphous molecular material vs vinyl polymer.* Chemistry Letters, 2003. **32**(8): p. 710-711.
18. Audorff, H., et al., *Polarization Dependence of the Formation of Surface Relief Gratings in Azobenzene-containing Molecular Glasses.* Journal of Physical Chemistry B, 2009. **113**(11): p. 3379-3384.
19. Walker, R., et al., *Synthesis and structure-property relations of a series of photochromic molecular glasses for controlled and efficient formation of surface relief gratings.* Advanced Functional Materials, 2009. **19**(16): p. 2630-2638.
20. Kim, M.-J., et al., *Photodynamic Properties of Azobenzene Molecular Films with Triphenylamines.* Chemistry of Materials, 2003. **15**(21): p. 4021-4027.
21. Ando, H., et al., *Photoinduced surface relief grating formation using new polymers containing the same azobenzene chromophore as a photochoromic amorphous molecular material.* Materials Chemistry and Physics, 2009. **113**(1): p. 376–381.
22. Fuhrmann, T. and T. Tsutsui, *Synthesis and Properties of a Hole-Conducting, Photopatternable Molecular Glass.* Chemistry of Materials, 1999. **11**(8): p. 2226-2232.
23. Audorff, H., et al., *Holographic Gratings and Data Storage in Azobenzene-Containing Block Copolymers and Molecular Glasses*, Advances in Polymer Science Vol 228, 2010, Springer: Berlin Heidelberg. p. 57.
24. Audorff, H., et al., *Polarization dependence of the formation of surface relief gratings in azobenzene-containing molecular glasses.* Journal of Physical Chemistry B, 2009. **113**: p. 3379-3384.
25. Kogelnik, H., *Coupled Wave Theory for Thick Hologram Gratings.* Bell System Technical Journal, 1969. **48**: p. 2909-2947.
26. Ishow, E., et al., *Structural and Photoisomerization Cross Studies of Polar Photochromic Monomeric Glasses Forming Surface Relief Gratings.* Chemistry of Materials, 2006. **18**(5): p. 1261-1267.
27. Nakano, H., et al., *Synthesis and Photoinduced Surface Relief Grating Formation of a Novel Azobenzene-based Photochromic Amorphous Molecular Material.* Journal of Photopolymer Science and Technology, 2007. **20**(1): p. 87-89.
28. Ishikawa, W., et al., *Polymorphism of starbust molecules: methyl-substituted derivates of 1,3,5,-tris(diphenykamino)benzene.* Journal of Physics D: Applied Physics, 1993. **26**(8B): p. 94-99.
29. Nakano, H., et al., *Formation of a surface relief grating using a novel azobenzene-based photochromic amorphous molecular material.* Advanced Materials, 2002. **14**(16): p. 1157-1160.

30. Williams, G. and D.C. Watts, Transactions of the Faraday Society, 1969. **66**: p. 80-86.
31. Reinke, N., et al., *Electric field assisted holographic recording of surface relief gratings in an azo-glass.* Applied Physics B, 2004. **78**: p. 205-209.
32. Barrett, C., A. Natansohn, and P. Rochon, *Thermal Cis-Trans Isomerization Rates of Azobenzene Bound in Side Chain of Some Copolymers and Blends.* Macromolecules, 1994. **27**(17): p. 4781-4786.
33. Hesselink, L., S.S. Orlov, and M.C. Bashaw, *Holographic data storage systems.* Proceedings of the IEEE, 2004. **92**(8): p. 1231-1280.
34. Burawoy, A., *Light absorption of organic compounds. VIII. Azo compounds.* Journal of the Chemical Society, 1937: p. 1865-1869.
35. Birnbaum, P.P., J.H. Linford, and D.W.G. Style, *Absorption spectra of azobenzene and some derivatives.* Transactions of the Faraday Society, 1953. **49**: p. 735-44.
36. Ho, M.-S., et al., *Azo polymers for reversible optical storage. 8. The effect of polarity of the azobenzene groups.* Canadian Journal of Chemistry, 1995. **73**(11): p. 1773-8.
37. Pedersen, M., et al., *Influence of the substituent on azobenzene side-chain polyester optical storage materials.* Macromolecular Symposia, 1999. **137**: p. 115-127.
38. Kreger, K., et al., *Stable Holographic Gratings with Small-Molecular Trisazobenzene Derivatives.* Journal of the American Chemical Society, 2010. **132**(2): p. 509-516.
39. Häckel, M., et al., *Holographic gratings in diblock copolymers with azobenzene and mesogenic side groups in the photoaddressable dispersed phase.* Advanced Functional Materials, 2005. **15**(10): p. 1722-1727.
40. Häckel, M., et al., *Polymer Blends with Azobenzene-Containing Block Copolymers as Stable Rewritable Volume Holographic Media.* Advanced Materials, 2007. **19**(2): p. 227-231.
41. Haeckel, M., et al., *Holographic gratings in diblock copolymers with azobenzene and mesogenic side groups in the photoaddressable dispersed phase.* Advanced Functional Materials, 2005. **15**(10): p. 1722-1727.
42. Kreger, K., et al., *Dynamic behavior of the minority phase of photoaddressable block copolymers.* Macromolecular Chemistry and Physics, 2007. **208**(14): p. 1530-1541.
43. Pu, A., K. Curtis, and D. Psaltis, *Exposure schedule for multiplexing holograms in photopolymer films.* Optical Engineering, 1996. **35**: p. 2824-2829.
44. Sherif, H., et al., *Characterization of an acrylamide-based photopolymer for data storage utilizing holographic angular multiplexing.* Journal of Optics A: Pure and Applied Optics, 2005. **7**(5): p. 255-260.

4.5 Improving the Holographic Recording Sensitivity of Photoaddressable Azobenzene-Containing Polymers with Molecular Glasses

By *Roland Walker*, *Hubert Audorff*, *Lothar Kador* and *Hans-Werner Schmidt**

[*] Prof. H.-W. Schmidt, R. Walker
University of Bayreuth, Macromolecular Chemistry I and
"Bayreuth Institute of Macromolecular Research"
D-95440 Bayreuth (Germany)
E-mail: hans-werner.schmidt@uni-bayreuth.de

Prof. L. Kador, H. Audorff
University of Bayreuth, "Bayreuth Institute of Macromolecular Research"
D-95440 Bayreuth (Germany)
E-mail: lothar.kador@uni-bayreuth.de

This paper is intended for publication in
Advanced Materials

Keywords: azobenzene, molecular glasses, photoaddressable polymers, holographic recording sensitivity

In recent years, the amount of information to be stored has rapidly increased and high-capacity storage media are required to meet future demands. Volume holography is a promising technology in the field of optical data storage. In contrast to conventional optical storage media, the entire volume of the medium is used instead of a few thin layers only and capacities above 1 terabyte on a medium size of a compact disc are possible.[1] Developments in the field of holographic storage materials as well as advances in storage techniques and their applications have been reviewed by Ashley et al.[2] and Hesselink et al.[3] Write-once media are mainly based on photopolymer systems, which underlie a monomer diffusion mechanism and a final photo-crosslinking step.[3] In view of rewritable holographic media, largely photoaddressable materials were investigated.[4-13] Especially materials, based on azobenzene-containing polymers, are a promising material class and benefit from the unique photophysical behaviour. When irradiated with polarized light the azobenzenes undergoe - driven by repeated *trans*-*cis*-*trans* isomerization cycles - an in-plane orientation which result in a refractive index change. This effect is enhanced but most important stabilized by a cooperative effect between the shape-anisotropic side-groups.[14] In case of thick samples for angular multiplexing, ensuring a suitable optical density (in the range of 0.5 to 0.7) and maintaining the cooperative effect are basic requirements. Two concepts are literature known, which is the blending of a photoactive homopolymer with a similar but inactive polymer[15] and the utilization of block copolymers consisting of a photoactive minority segment and an inactive majority segment.[16] Recently we have demonstrated that in blends of such block copolymers with their inactive matrix polymer, rewritable and long-term stable holographic gratings can be inscribed.[17] An ongoing challenge for these systems is the improvement of the writing-time.

Since a few years several research groups investigate photoresponsive molecular glasses based on azobenzene-chromophores.[18-22] These photoactive amorphous molecular materials are mainly designed to understand and perform the formation process of surface relief gratings (SRGs). SRGs are detrimental for volume gratings since being thin gratings they feature no angle selectivity. Additionally it has also been demonstrated that birefringence can be

optically induced in thin films of these photo-responsive molecular glasses, whereby the formation is faster than in polymers.[23-26]

This communication reports on the improvement of the holographic recording sensitivity by blending photoaddressable polymers for the first time with an azobenzene-containing molecular glass. In order to address the influence of a photoactive molecular glass in a photoaddressable block copolymer with a inactive matrix, the photophysical behaviour of the molecular glass itself as well as blends with the corresponding active and inactive homopolymers have to be investigated first. With this blending approach, it is demonstrated that photoaddressable homopolymer systems can be combined with the faster response of a molecular glass while at the same time retaining their high long-term stability. Furthermore, a clear increase of the holographic recording sensitivity of the photoaddressable blockcopolymers is achieved. Hence, these materials are promising candidates for improving the holographic recording sensitivity of stable rewritable materials for volume holography.

(i) Material properties of the azobenzene-containing molecular glass: The photochromic material **1** described in this work is based on a 1,3,5-substituted cyclohexane central core with three azobenzene arms (see **figure 1**). The chromophoric arms are attached to the core by an esterification reaction similar as reported previously.[22] The required hydroxyl-functionalized azobenzene moieties are accessible by a common azo coupling reaction as described in basic literature. The material exhibits a stable amorphous phase with a glass transition temperature of 58 °C, which can either be achieved by cooling from the melt or filmforming processes such as spin-coating or doctor blading.

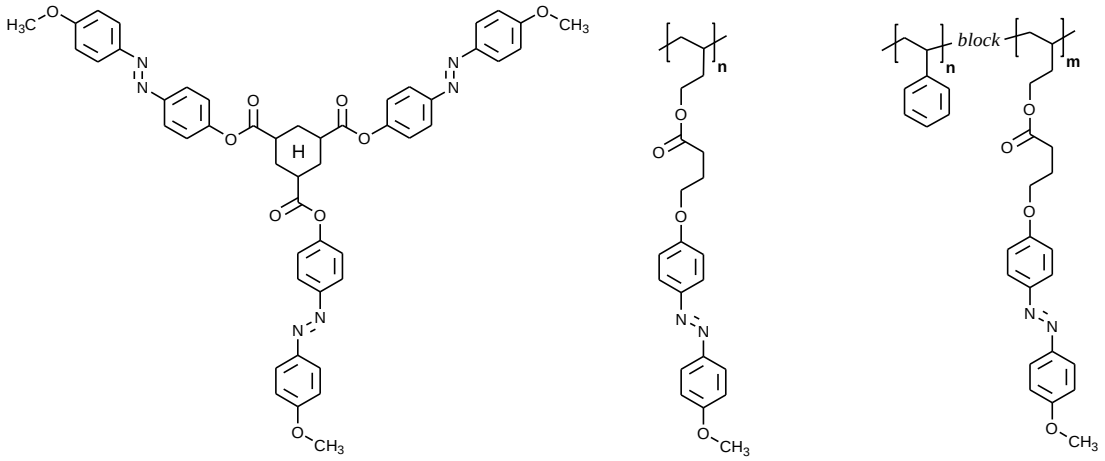

1 **2** **3**

Figure 1. Chemical structures of the utilized photoaddressable azobenzene-containing materials; molecular glass **1**, homopolymer **2** and blockcopolymer **3**.

Volume gratings were inscribed with a s:s polarization of two superimposed laser beams in transparent homogenous thin films of **1** with a thickness of 0.3 µm. The applied laser polarization is known to produce SRGs very ineffectively. Additionally the writing times were orders of magnitude shorter than the typical time to reach the maximum SRG height. Therefore, on the time-scale of the inscription a light-intensity grating in the volume is formed rather than a SRG. The photochromic molecular glass **1** exhibits a maximum refractive-index modulation n_{1max} of 0.007 and the time to reach the maximum refractive index modulation is 0.33 s. This is faster by a factor of 10 compared to block copolymers with similar optical density per µm.[14] The sensitivity of **1** was calculated according to Hesselink et al.[3] (see equation 1) to 1500 cm/J, which is a improvement by a factor of 5.

$$S = \frac{\frac{\partial\sqrt{\eta}}{\partial t}}{I_0 d_0} \qquad \textbf{(1)}$$

***η*:** *diffraction efficiency*

***I_0*:** *laser intensity*

***d_0*:** *thickness of the sample*

The sensitivity describes the slope of the holographic growth curve and is a parameter for the photo-physical response of the whole photochromic system. As can be seen from eq. 1, decreasing the writing time or increasing the refractive index modulation increases S ($\sqrt{\eta} \sim n_1$).

(ii) Holographic properties of binary blends of azobenzene-containing molecular glasses with polystyrene: In order to address the photophysical behavior of the azobenzene-containing molecular glasses in an inert polymer matrix, a concentration series of compound **1** in polystyrene (PS) was studied. For this purpose we diluted the molecular glass in commercially available polystyrene (BASF 165 H) by spin-coating blends from solution. All obtained thin films were amorphous and showed good optical quality as well as absence of undesired scattering. The concentration of **1** ranged from 6 to 50 wt%. As it can be seen in **figure 2**, the corresponding writing time to reach the maximum of refractive-index modulation strongly increases with decreasing azobenzene content and differs by more than two orders of magnitude in the investigated concentration range. Normalized refractive-index modulations of the blends with respect to the azobenzene content show that the value decreases with decreasing azobenzene content. Likewise, the stability of the inscribed gratings also decreases with a lower amount of molecular glass. Furthermore, the wavelength of the maximum of the π-π^*-transition shifts from 353 nm at 6 wt% to 348 nm at 50 wt% (see figure 2) and to 346 nm for pure films of molecular glass. The latter values are notably lower than in dilute solutions (351 nm). This slight hypsochromic shift at higher concentrations indicates a formation of H-aggregates between the azobenzene chromophores in the solid state, similar to observations in azobenzene-containing side-chain polymers.[16,27-29] The existence of aggregates, fast orientation processes and high refractive index modulations indicate the presence of beneficial cooperative effects, which are lost if the chromophores are diluted in an inactive matrix.

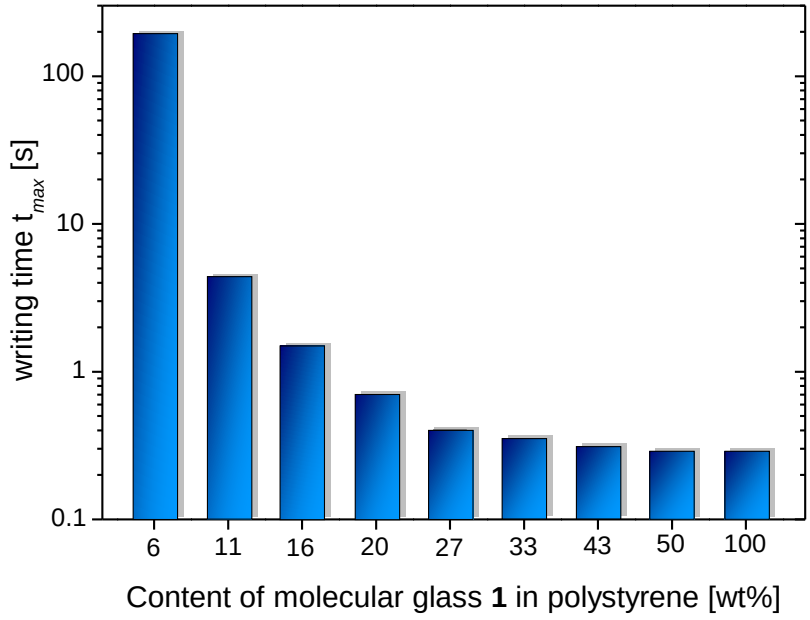

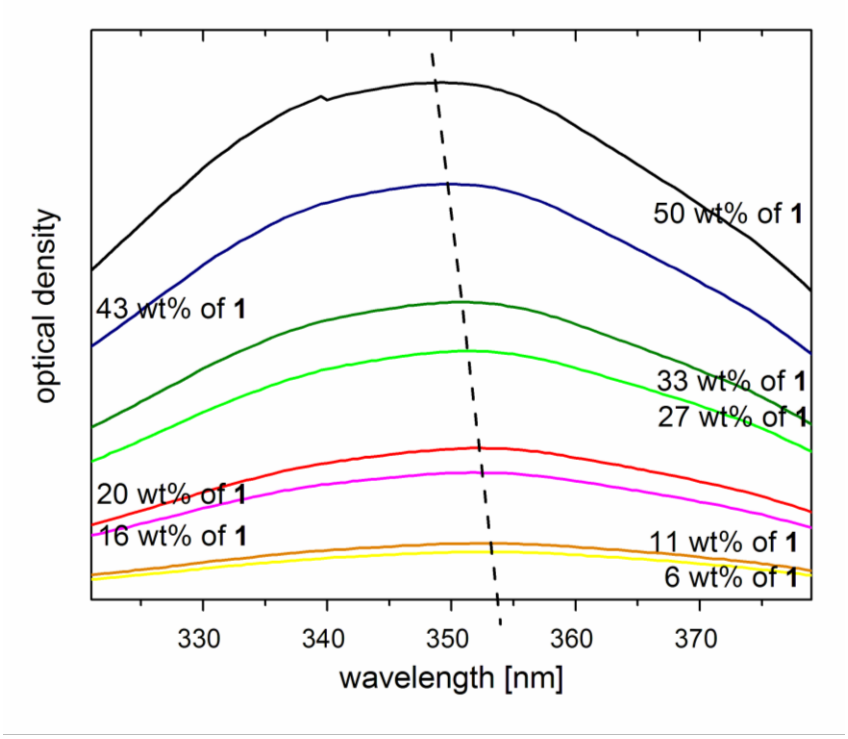

Figure 2. *Top:* Time to reach 90% of the maximum refractive-index modulation as a function of the concentration of the molecular glass **1** in PS. Note the semi-logarithmic representation. *Bottom:* UV-vis spectra of thin films in the investigated concentration range of the molecular glass **1** in PS (π-π*-transition). The dashed line is indicates the maximum of the π-π*-transition.

(iii) Holographic properties of binary blends of photoresponsive molecular glasses and azobenzene-containing homopolymers: In order to evaluate the photophysical properties of azobenzene–containing molecular glass **1** in the photoaddressable homopolymer **2**, thin films were prepared by doctor-blading from solution comprising different weight fractions of the molecular glass **1**, which ranges from 0 to 80 wt%. All obtained samples were amorphous and showed good optical quality as well as absence of undesired scattering. **Figure 3** shows the time t_{max} as a function of the content of compound **1**. With increasing content of **1** the writing time decreases and, consequently, the sensitivity increases, but there are subtle differences compared to the prior shown results with the inactive polymer blends. In contrast, a cooperative effect in these blends is always present, thus, it is reasonable to assume that the writing times lies between the slower photoaddressable polymer and the faster photoactive molecular glass. Already at 10 wt% of the molecular glass the writing time to achieve the maximum refractive index is significantly improved from approx. 6 sec to 3 sec, but at this concentration 90% of the polymer-linked chromophores excited. Thus one might assume that this is not only due to a faster orientation originating from the molecular glass alone but a substantially change of the photophysical behaviour in the photoaddressable system. This mutual interaction can be also seen for higher concentration, e.g., 20 wt%, where the writing time is slower than in the comparable homopolymer. Furthermore the growth curves do not indicate that there are single different processes which lead to the refractive index modulation.

Since it is known that photoaddressable polymer such as **2** can show a pronounced long-term stability of the inscribed gratings in contrast to photochromic molecular glasses, we investigated the stability of these gratings to evaluate the concentration where the gratings became unstable. Thus we studied the refractive-index modulation for 12 h after the writing laser was turned off. The pure photoaddressable polymer exhibits stable gratings whose n_1 is still slightly increasing even after 12 h due to post-development effects. All the blends up to 25 wt% of molecular glass still exhibit a positive slope of n_1 after 12 h, which means that the refractive-index modulation is long-term stable. In the blend with 25 wt% of molecular glass, compared to the pure

homopolymer, t_{max} decreases by more than a factor of 4 and the sensitivity increases by more than a factor of 3.

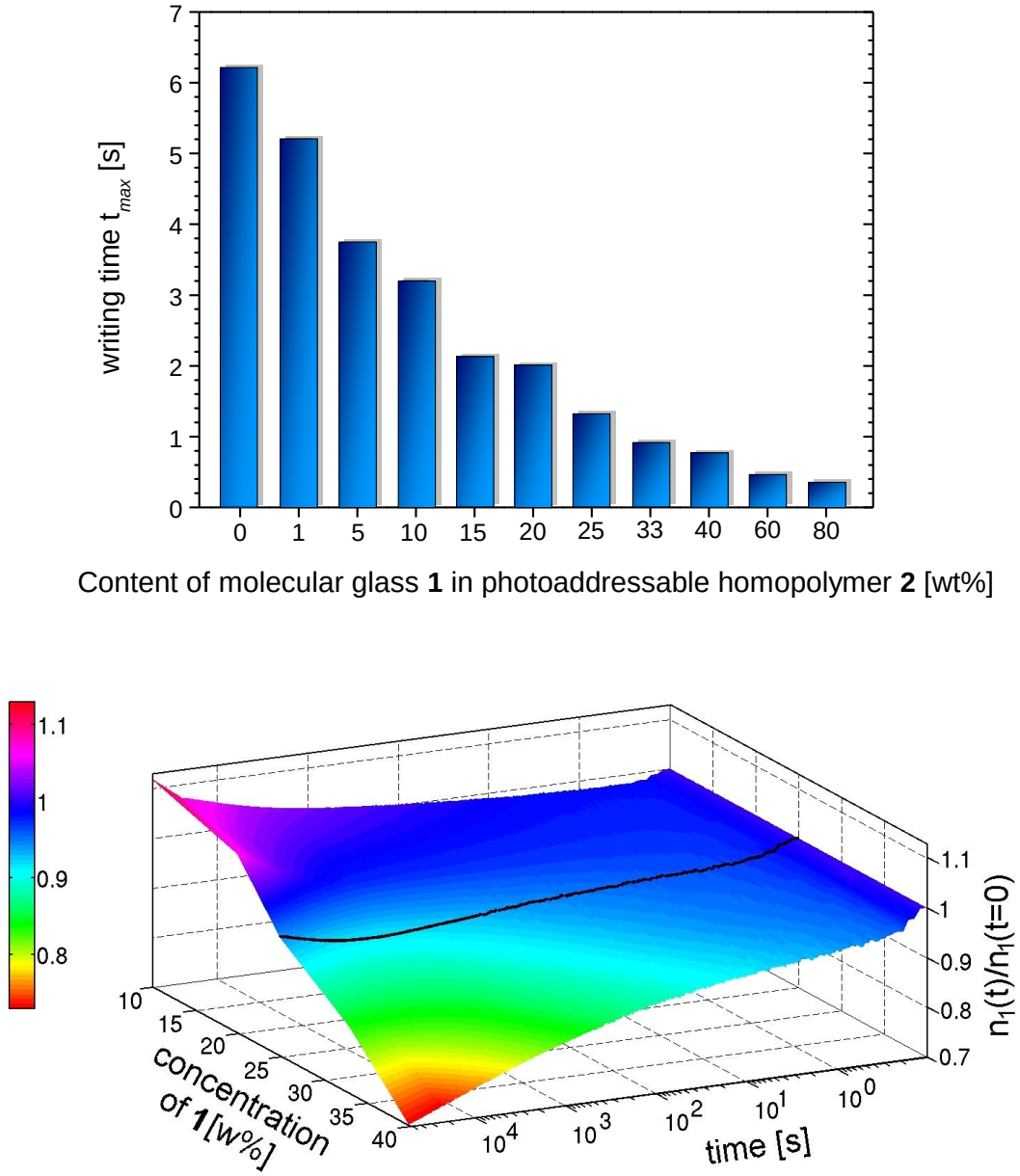

Figure 3. *Top:* Time to reach 90% of the maximum refractive-index modulation as a function of the concentration of the molecular glass **1** in photoaddressable homopolymer **2**. *Bottom:* Temporal evolution of the normalized refractive-index modulation of blends of the molecular glass **1** with a photoaddressable homopolymer **2** as a function of the content of **1**. The refractive index modulation is normalized to a value of one at the time zero when the writing laser is turned off. The black line indicates the blend with 25 wt% of molecular glass, which still exhibits a positive slope of n_1 after 12 h.

(iv) Holographic properties of binary blends of molecular glasses and azobenzene-containing block copolymers: Photoaddressable block copolymers are a suitable concept for controlling the optical density in mm-thick samples and thus enabling angular multiplexing.[17] Hence, it is a major goal to improve the recording sensitivity in such systems with the photochromic molecular glass. For this we have blended **1** with the photoaddressable block copolymer **3**. A series of thin films were prepared by doctor-blading whereby the concentration of **1** ranged from 0 to 10 wt%. All obtained samples were amorphous and showed good optical quality as well as absence of undesired scattering. As shown in **figure 4**, with increasing concentration of **1**, the time to reach the maximum refractive index change is decreased and, hence, the sensitivity increased. Already with a small content of 5 wt% molecular glass, the writing time is nearly halved and the sensitivity is more than doubled compared to pure **3**. As the azobenzene content increases due to addition of the molecular glass, the refractive-index modulation also does. However, the resulting increase of S is much smaller compared to the increase in sensitivity seen in our experiments. Furthermore the improved sensitivity is presumably not due to molecules of **1** located in the inert PS matrix of **3**, as t_{max} would be magnitudes greater at similar concentrations (see figure 2). From the data of the molecular glass blended with PS and with the homopolymer, one can estimate that around 45% of the molecules of **1** are located in the photoaddressable block of **3**. This is a factor of 2.5 more than one would expect from a statistical distribution. Obviously, the molecular glass preferably blends with the photoaddressable minority block rather than with the polystyrene matrix. This assumption is supported by a second measurement of the same samples after annealing at 170 °C for 3 hours. Far above the glass transition of polystyrene, the molecular glass starts to migrate into the photoaddressable block. This enrichment in the minority block can clearly be seen in **figure 4**, as the improvement of the holographic properties is even more pronounced after annealing. Judging from the data of **1** in PS and in the homopolymer, we can estimate that after the annealing step around 70% of the molecules of **1** are in the photoaddressable block. We assume that the the faster orienting chromophores of **1** lead to an increased rates of orientation in the photoaddressable segment of the block

copolymer caused by cooperative interactions. Therefore the maximum refractive index modulation is reached sooner and the sensitivity increases compared to the pure polymer.

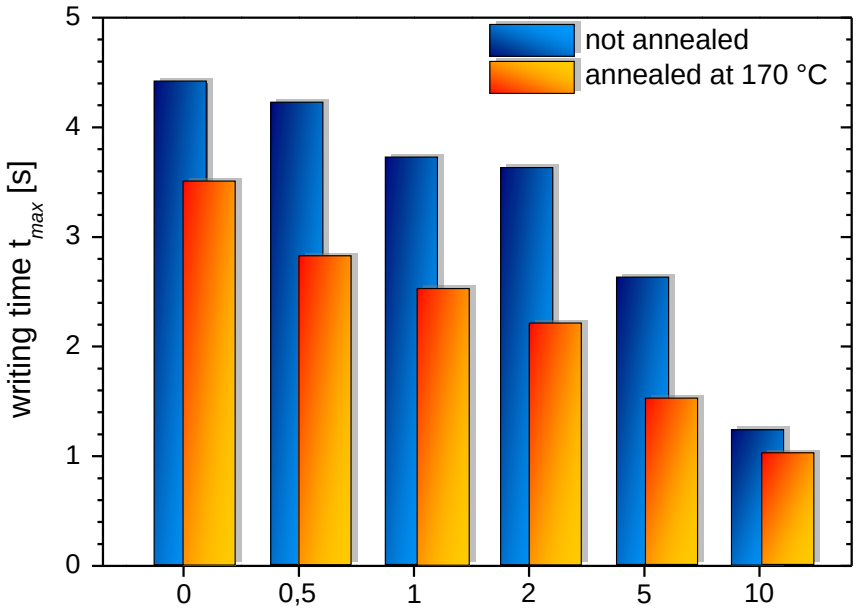

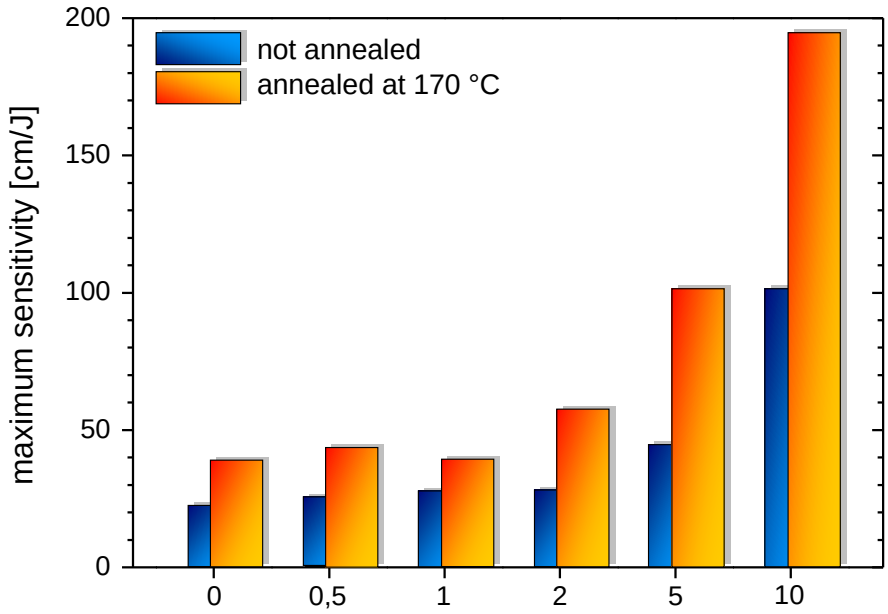

Figure 4. Holographic properties of blends of the molecular glass **1** with a photoaddressable block copolymer **3**. Writing time to 90 % of the maximum of the refractive-index modulation (*top*) and maximum sensitivity (*bottom*) are plotted as a function of the content of **1**. The dark columns correspond to not annealed samples, the light columns to samples annealed at 170 °C.

In this paper, a photoresponsive molecular glass is presented as blending material for azobenzene-containing polymers. By blending this photoresponsive molecular glass into a photoaddressable homopolymer we prove that the high stability of a polymer system can be combined with the faster response of a molecular glass to form a photoaddressable material which clearly exhibits a higher sensitivity and, in addition, has the superior long-term stability of polymers. By verifying that this concept is also suitable for photoaddressable block copolymer systems we demonstrate that photoresponsive molecular glasses are a promising candidate for enhancing the holographic recording sensitivity of rewritable materials for volume holography.

Experimental

Materials and Methods

The photochromic molecular glass **1** has been reported in detail elsewhere.[30]

*Molecular glass **1**:* The corresponding tris carboxylic acid chloride of 1,3,5-cyclohexanetricarboxylic acid (1 equiv.) is placed in a flame-dried Schlenck flask and dissolved in 150 ml toluene under argon atmosphere. A threefold molar excess of anhydrous triethylamine per acid chloride group and 1.1 equivalents of 4-(4-methoxy)phenylazo)phenol for each acid chloride group are added. The dark red solution is stirred for 24 h under reflux at 110 °C. The solution is filtered, washed with additional toluene, and thereafter the solvent is distilled off. The crude product is solved in THF and precipitated in EtOH. The precipitate is filtered with a frit and dried in high-vacuum. Remaining impurities are removed by a second precipitation in EtOH.

Polystyrene: Commerically available polystryene BASF 165 H from BASF SE.

*Photoaddressable Homopolymer **2**:* The utilized homopolymer **2** is an azobenzene side chain polymer with a poly(1,2-butadiene) backbone (M_n 20,000 g/mol, PDI 1.4) similar to literature.[16]

*Photoaddressable Block copolymer **3**:* The utilized blockcopolymer **3** is an AB-type block copolymer (M_n: 59,000 g/mol, PDI: 1.04, 17.5 wt% azobenzene) with polystyrene as majority block and a functionalized azobenzene side chain block with a poly(1,2-butadiene) backbone, similar to literature.[16]

Film preparation

Thin films for holographic experiments were prepared by spin-coating a filtered solution in THF comprising in total 4 wt% of molecular glass and polymer at 1000 rpm for 60 s on a glass slide. Subsequently the films were annealed at 70 °C for 3 h in order to remove residual solvent. Additionally, thin films were prepared by doctor blading a filtered 4 wt% solution in THF on a glass slide at 20 mm/s. The film thickness of all samples was determined with a Dektak (Veeco 3300ST auto remote control stage profiler) and varied from 0.3 to 2 µm. All samples showed good optical properties and absence of undesired scattering.

Holographic Setup

Volume gratings are inscribed at room temperature with the blue-green line (488 nm) of an argon ion laser with ss polarization.[30] The intensity of each beam is adjusted to 1 W/cm² and the grating period to 1 μm. A laser diode (12mW/cm^2) with s-polarization at 685 nm, which is outside the absorption band of the azobenzene chromophores, is used for monitoring the diffraction efficiency without affecting the writing process. The signals of the diffracted and the transmitted beam are measured with two photodiodes, and the diffraction efficiency is calculated from their quotient. The reading laser is modulated at 10 kHz and lock-in detection is used to reduce noise. The refractive index modulation is calculated according to Kogelnik.[31]

Literature

[1] M. Haw, *Nature* **2003**, *422*(6932), 556-558

[2] J. Ashley, M. P. Bernal, G. W. Burr, H. Coufal, H. Guenther, J. A. Hoffnagle, C. M. Jefferson, B. Marcus, R. M. Macfarlane, R. M. Shelby, G. T. Sincerbox, *IBM J. Res. Dev.* **2000**, *44*(3), 341-368

[3] L. Hesselink, S. S. Orlov, M. C. Bashaw, *Proc. of IEEE* **2004**, *92*(8), 1231-1280

[4] H. Ringsdorf, H. W. Schmidt, G. Baur, R. Kiefer, F. Windscheid, *Liq. Cryst.* **1986**, *1*(4), 319-25

[5] M. Eich, J. H. Wendorff, H. Ringsdorf, H. W. Schmidt, *Makromol. Chem.* **1985**, *186*(12), 2639-47

[6] S. J. Zilker, M. R. Huber, T. Bieringer, D. Haarer, *Appl. Phys. B* **1999**, *68*(5), 893-897

[7] S. J. Zilker, T. Bieringer, D. Haarer, R. S. Stein, J. W. Van Egmond, S. G. Kostromine, *Adv. Mater.* **1998**, *10*(11), 855-859

[8] R. Hagen, T. Bieringer, *Adv. Mater.* **2001**, *13*(23), 1805-1810

[9] A. Natansohn, P. Rochon, *Chem. Rev.* **2002**, *102*(11), 4139-4175

[10] X. Meng, A. Natansohn, P. Rochon, *Polymer* **1997**, *38*(11), 2677-2682

[11] X. Meng, A. Natansohn, C. Barrett, P. Rochon, *Macromolecules* **1996**, *29*(3), 946-52

[12] S. Hvilsted, F. Andruzzi, C. Kullia, H. W. Siesler, P. S. Ramanujam, *Macromolecules* **1995**, *28*, 2172-2183

[13] K. G. Yager, C. J. Barrett, *J. Photochem. Photobiol., A* **2006**, *182*(3), 250-261

[14] M. Haeckel, L. Kador, D. Kropp, C. Frenz, H.-W. Schmidt, *Adv. Funct. Mater.* **2005**, *15*(10), 1722-1727

[15] J. Minabe, T. Maruyama, S. Yasuda, K. Kawano, K. Hayashi, Y. Ogasawara, *Jpn. J. Appl. Phys.* **2004**, *43*(7B), 4964-4967

[16] C. Frenz, A. Fuchs, H.-W. Schmidt, U. Theissen, D. Haarer, *Macromolecular Chemistry and Physics* **2004**, *205*(9), 1246-1258

[17] M. Haeckel, L. Kador, D. Kropp, H.-W. Schmidt, *Adv. Mater.* **2007**, *19*(2), 227-231

[18] H. Nakano, T. Tanino, T. Takahashi, H. Ando, Y. Shirota, *J. Mater. Chem.* **2008**, *18*(2), 242-246

[19] A. Perschke, T. Fuhrmann, *Adv. Mater.* **2002**, *14*(11), 841-843

[20] C. Chun, M.-J. Kim, D. Vak, D. Y. Kim, *J. Mater. Chem.* **2003**, *13*(12), 2904-2909

[21] E. Ishow, R. Camacho-Aguilera, J. Guerin, A. Brosseau, K. Nakatani, *Adv. Funct. Mater.* **2009**, *19*(5), 796-804

[22] R. Walker, H. Audorff, L. Kador, H.-W. Schmidt, *Adv. Funct. Mater.* **2009**, *19*(16), 2630-2638

[23] M.-J. Kim, E.-M. Seo, D. Vak, D.-Y. Kim, *Chem. Mat.* **2003**, *15*(21), 4021-4027

[24] E. Ishow, B. Lebon, Y. He, X. Wang, L. Bouteiller, L. Galmiche, K. Nakatani, *Chem. Mater.* **2006**, *18*(5), 1261-1267

[25] A. Stracke, J. H. Wendorff, D. Goldmann, D. Janietz, *Liq. Cryst.* **2000**, *27*(8), 1049-1057

[26] Y. Shirota, *J. Mater. Chem.* **2005**, *15*(1), 75-93

[27] X. Tong, L. Cui, Y. Zhao, *Macromolecules* **2004**, *37*(9), 3101-3112

[28] U. Wiesner, N. Reynolds, C. Boeffel, H. W. Spiess, *Makromol. Chem., Rapid Commun.* **1991**, *12*(8), 457-64

[29] J. Stumpe, T. Fischer, H. Menzel, *Macromolecules* **1996**, *29*(8), 2831-42

[30] H. Audorff, R. Walker, L. Kador, H.-W. Schmidt, *submitted to Chem. – Eur. J*

[31] H. Audorff, R. Walker, L. Kador, H.-W. Schmidt, *J. Phys. Chem. B* **2009**, *113*, 3379-3384

[32] H. Kogelnik, *Bell System Tech. J.* **1969**, *48*(9), 2909-2947

Acknowledgements

Financial support by the German Science Foundation (DFG) within the framework of the Collaborative Research Centre (SFB 481) is gratefully acknowledged. The authors thank Dr. Klaus Kreger for many fruitful discussions and Christina Löffler for her support in the material synthesis.

4.6 Stable holographic volume gratings with novel photochromic bisazobenzene-based low molecular weight compounds

By *Roland Walker*, *Hubert Audorff*, *Lothar Kador,* and *Hans-Werner Schmidt**

[*] Prof. H.-W. Schmidt, R. Walker
University of Bayreuth, Macromolecular Chemistry I and
"Bayreuth Institute of Macromolecular Research"
D-95440 Bayreuth (Germany)
E-mail: hans-werner.schmidt@uni-bayreuth.de

Prof. L. Kador, H. Audorff
University of Bayreuth, "Bayreuth Institute of Macromolecular Research"
D-95440 Bayreuth (Germany)
E-mail: lothar.kador@uni-bayreuth.de

This paper is intended for publication in
Chemistry of Materials

Keywords: low molecular weight compounds, bisazobenzene, liquid crystalline, stable holographic gratings

A subject of current intense study are polymeric or low molecular weight materials based on azobenzene for use as smart light-responsive materials in various potential applications.[1,2] Commonly known is the ability of azobenzenes to reorient in the solid state upon light irradiation through multiple reversible *trans-cis-trans* photo-isomerization cycles. With polarized light, these motions continue until the chromophores are oriented perpendicular to the polarization plane of the incident light. This light-induced in-plane orientation was mainly explored in polymeric materials.[3-8] In contrast, photo-induced birefringence in photochromic low molecular-weight compounds have been studied far less extensively.[9-14] In holographic experiments, these materials are expected to show a faster build-up of the diffraction efficiency than polymers because of the absence of the polymer backbone and its entanglement.[14,15] However, they often exhibit a pronounced decay of the inscribed gratings. In view of an application, the inscription of long-term stable holographic gratings in such materials is highly desirable, however, this goal has to date only been seldom achieved. Recently, we have demonstrated that long-term stable holographic gratings can be obtained with photochromic low molecular weight spezies. In those, the azobenzene chromophores are decoupled from the central core by a spacer as well as the additional terminal dipolar groups attached to the chromophores. In initially amorphous films consisting of such compounds a liquid-crystalline phase[16] can be triggered by light, which stabilizes the holographic volume grating due to a cooperative effect.

In general, azobenzenes are well-known shape-anisotropic chromophores. If the mesogenic character is extended, e.g. in the case of bisazobenzene, they readily form liquid crystalline phases. To a large extent these units have been incorporated in polymer systems,[17-23] where different highly ordered liquid-crystalline phases were observed.[24-26] Due to their larger shape-anisotropy they potentially exhibit a higher refractive index modulation as common azobenzene moieties.[27,28]

In this study we present the synthesis and characterization of novel photochromic bisazobenzene-based low molecular-weight compounds. The goal of this work is to tailor photochromic materials which exhibit high refractive index modulations as well as a long-term stable photo-orientation. In

holographic experiments, it is demonstrated that long-term stability of holographic volume gratings could be achieved by the introduction of a liquid-crystalline phase. To the best knowledge of the authors, bisazobenzene chromophores have to this date not been introduced in small molecular materials to inscribe stable holographic gratings.

The photochromic materials described in this work are based on a triphenylamine central core with three bisazobenzene side groups (see **figure 1**, A). The synthesis of the triphenylamine core has been described elsewhere.[29] The hydroxyl-functionalized bisazobenzene chromophore for compound **1** was commercially available, whereas the chromophore for compound **2** is accessible by common azo coupling reactions. The chromophoric side groups are attached to the core by a threefold aryl-aryl esterification similar as reported previously.[29] The three-arm star-shaped compounds could be obtained in good yields, of approx. 55% after purification. Purity was determined by common analytical techniques such as thin layer chromatography, NMR and elemental analysis as well as size exclusion chromatography suitable for small molecular species (oligomeric SEC).

In view of holographic experiments thin film architectures with excellent optical quality and without the scattering of light required. Hence, one has to determine relevant parameters such as glass or film forming ability, the position of the T_g as well as the tendency to recrystallize. Molecular glasses, for example, are well-known glass formers, whereby amorphous film can be readily obtained by non-equilibrium processes, e.g. spin-coating or quenching of a melt. Alternatively, blending of the photochromic compounds with a small amount of a polymeric material can result in transparent thin films without significantly altering the photo-physical behaviour. Therefore, in addition to the investigation of the pure compounds, we have utilized, blends comprising the photochromic materials and 10 wt% of ULTEM©, which is a commercially available polyetherimide featuring a glass transition temperature of 215 °C.

A)

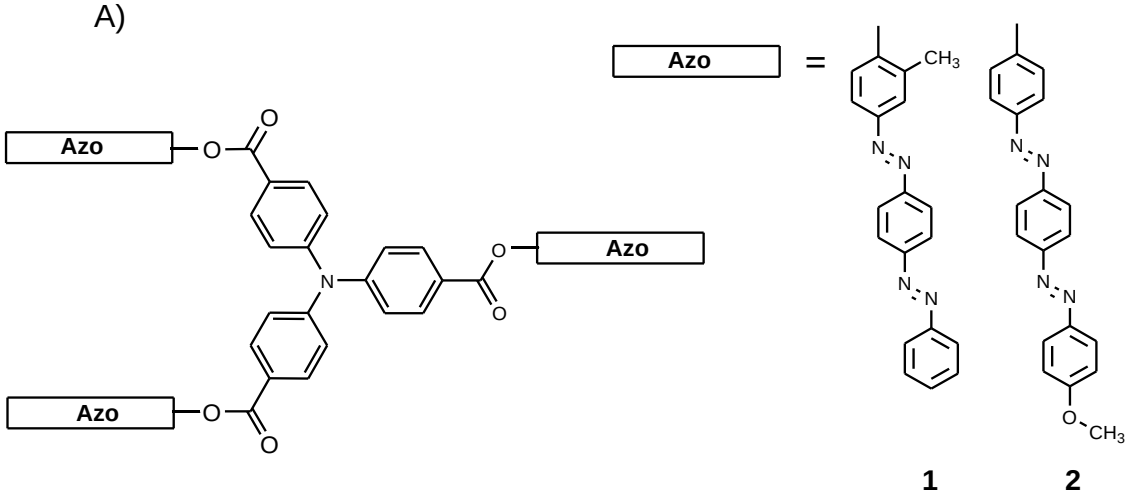

B)

material	first heating [a]		second heating [a]		
	T_m [°C]	T_{cryst} [°C]	T_g [°C]	$T_{recryst}$ [°C]	T_m [°C]
1	228	n.d.	107	n.d.	n.d.
1u	n.d.	n.d.	112	n.d.	n.d.
2	260	243[b]	106	n.d.	260[c]
2u	n.d.	n.d.	114	n.d.	n.d.

[a] determined by DSC with heating and cooling rates of 10 K/min under N_2, [b] transition from melt to liquid-crystalline phase [c] transition from liquid-crystalline phase to melt

Figure 1. A) Schematic representation of the photochromic azobenzene-containing materials **1** and **2**. B) Thermal properties of compounds **1** and **2**, as well as their corresponding blends with 10wt% of ULTEM© (**1u** and **2u**).

In order to evaluate the thermal properties of compounds **1** and **2** as well as their corresponding blends **1u** and **2u**, they were first investigated with differential scanning calorimetry (DSC) and thermogravimetric analysis (TGA). Relevant thermal data are given in **figure 1** (B). The decomposition temperature of the compounds **1** and **2** is about 300 °C which allows thermal treatment in a wide temperature range. Both pure materials possess a glass transition

temperature (T_g) of 107 and 106 °C respectively, so the change to the T_g caused by the methoxy substituent at the bisazobenzene moiety is only minor (see **figure 2**, A). Compound **1** forms a stable amorphous phase on moderate cooling rates of 10 K/min without crystallization on cooling the melt. In case of **2**, on cooling, a liquid-crystalline phase ($\Delta H_{LC \rightarrow I}$ = 3 kJ/mol) was found. On further cooling, the LC phase vitrifies than reaching the glass transition temperature. On subsequent heating cycles no crystallization was observed. Investigation of the blends revealed that the glass transition temperatures shifted slightly to higher values for **1u** and **2u** as it was expected since ULTEM© exhibits a higher T_g. On cooling no phase transition of the LC-phase was detected for **2u**. This demonstrates that the formation of the LC phase can be successfully suppressed by blending with 10 wt% of an amorphous polymer.

In addition, the existence of the liquid-crystalline phase is confirmed by polarizing microscopy investigations. 2 showed a mosaic-like texture which remains unchanging between RT and the clearing temperature (see **figure 2**, B). Furthermore, the LC phase was characterized by X-ray diffraction experiments at room temperature (see **figure 2**, C). At small angles two distinct peaks at 1,58° and 2,22° can be distinguished. A third, broader peak is apparent at 3,15°. Additionally, at larger angles a halo at ~10° can be seen. The three peaks are situated in relation of 1 : √2 : 2 to each other. These results let us assume that the LC phase is smectic. It is remarkable that the formation of a LC-Phase is determined by the presence of a terminal methoxygroup, as the examination of compound **1** showed only a halo at ~9° and no further peaks.

A)

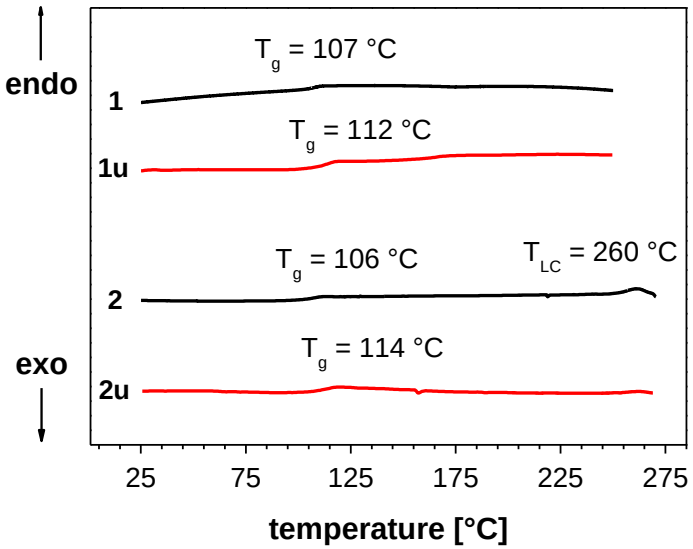

B)

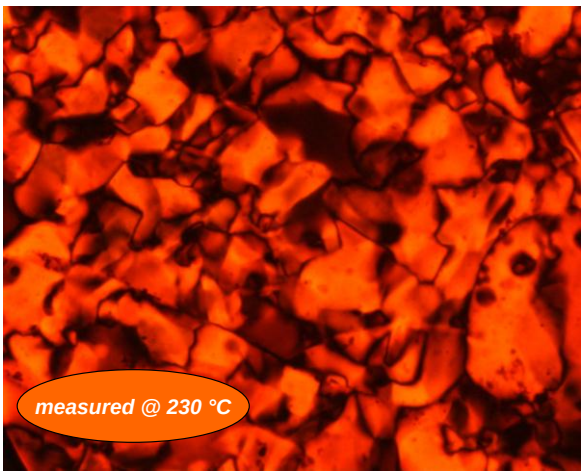

C)

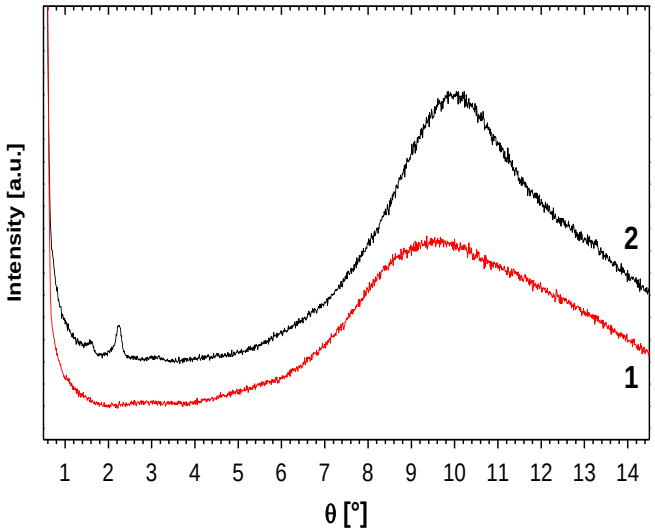

Figure 2. *A)* DSC scans of compounds **1** and **2** as well as the ULTEM© blends **1u** and **2u** (second heating; heating rate 10 K/min). *B)* Optical microscopy image taken at 230 °C on cooling from the melt (image taken between crossed polarizers). *C)* X-ray powder diffractograms of **1** and **2** respectively; measured at room temperature.

To determine basic optical properties of both compounds, UV-Vis spectroscopy were performed on 10^{-5} M solutions in $CHCl_3$. In the absorption spectra in the range of 250-650 nm two peaks can be distinguished for compound **1**. Both can be assigned to the azobenzene chromophore, e.g., an intense π-π* transition at 371 nm and a much weaker n-π* transition at approx. 440 nm. An absorption of the triphenylamine core could not be distinguished. By incorporation of the methoxy substituent (compound **2**) the π-π* transition is slightly redshifted to longer wavelength (π-π^*_{max} = 376 nm). n-π^*_{max} could not be determined due to an overlapping of the π-π* and n-π* peaks.

As thin films of pure compound **2** can not be amorphously obtained by quenching or spin-coating, the blends of both materials (**1u** and **2u**) were investigated in holographic experiments. After inscribing holographic gratings, both blends showed a photo-orientation which causes a refractive index modulation (n_1) between oriented and non-oriented domains of the intensity gratings (see **figure 3**). The maximal achievable n_1 were $33.3*10^{-3}$ and $43.5*10^{-3}$ (for **1u** and **2u** respectively). As presumed, these n_1 values are about five times higher as in comparable azobenzene-functionalized molecular glasses.[30] The writing times at 2 W/cm^2 to the maximum of the refractive index modulation are 8.8 s (**1u**) and 11.8 s (**2u**), respectively. After the writing laser was shut off (t = 0), the blend **1u** exhibits a decay of n_1 as commonly observed in such amorphous molecular materials.[10,14,30] In contrast, a long-term stable photo-orientation was observed for blend **2u**. Furthermore the blend exhibited a so-called "post-development" effect, i.e. an increase of n_1 after writing of the holographic gratings exceeding the originally inscribed n_1. This long term stable photo-orientation arises from a latent liquid-crystalline phase in the blend, as proposed for other small molecular materials.[31]

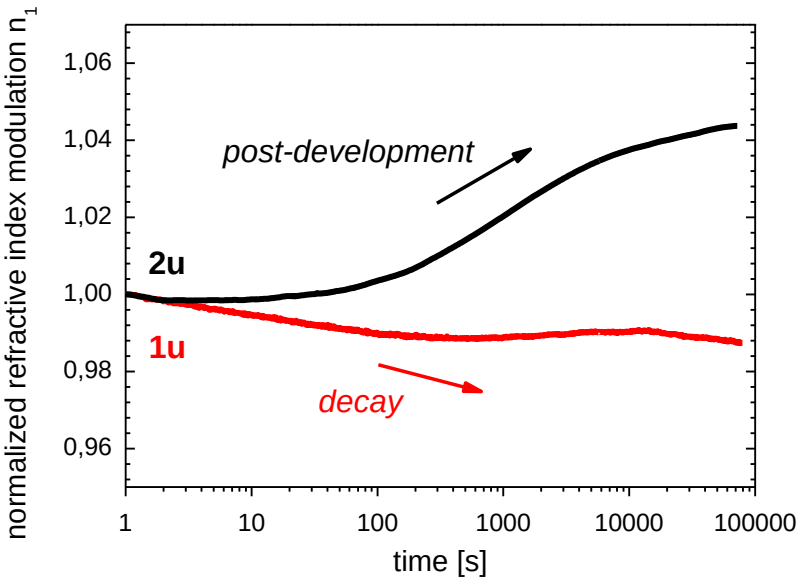

Figure 3. Temporal evolution of the normalized refractive index modulation (norm. to t = 1s) of volume phase gratings inscribed in films of **1u** and **2u**. The writing laser was turned off at t = 0. The general trend of evolution of the refractive index modulation is depicted by the arrows. Note the logarithmic time scale.

In this communication, novel photochromic materials based on a triphenylamine core and three bisazobenzene moieties have been successfully synthesized, characterized and analyzed with respect to their photo-physical response in holographic experiments. A terminal methoxygroup in the bisazobenzene chromophore leads to a liquid-crystalline phase in three-arm starshaped photochromic material. Holographic volume gratings with comparable high refractive index modulation and a pronounced long-term stability could be inscribed in initially amorphous thin films. To the knowledge of the authors this phenomenon has not yet been reported for low molecular-weight compounds functionalized with bisazobenzene chromophores. This photo-physical property makes such materials interesting candidates for inscription of holographic volume gratings.

Experimental

Details on the synthesis, materials and utilized methods can be found in the supplementary information.

Literature

[1] Y. Zhao, T. Ikeda, *Smart light-responsive materials* **2009**, Wiley, Hoboken, NJ

[2] H. Audorff, K. Kreger, R. Walker, D. Haarer, L. Kador, H. W. Schmidt, *Holographic gratings and data storage in azobenzene-containing block copolymers and molecular glasses* **2010**, Advances in polymer science, Vol 228, Springer, Berlin

[3] S. J. Zilker, T. Bieringer, D. Haarer, R. S. Stein, J. W. Van Egmond, S. G. Kostromine, *Adv. Mater.* **1998**, *10*(11), 855-859

[4] A. Natansohn, P. Rochon, *Chem. Rev.* **2002**, *102*(11), 4139-4175

[5] X. Meng, A. Natansohn, C. Barrett, P. Rochon, *Macromolecules* **1996**, *29*(3), 946-52

[6] S. Gimeno, P. Forcen, L. Oriol, M. Pinol, C. Sanchez, F. J. Rodriguez, R. Alcala, K. Jankova, S. Hvilsted, *Eur. Polym. J.* **2009**, *45*(1), 262-271

[7] M. Haeckel, L. Kador, D. Kropp, C. Frenz, H.-W. Schmidt, *Adv. Funct. Mater.* **2005**, *15*(10), 1722-1727

[8] M. Haeckel, L. Kador, D. Kropp, H.-W. Schmidt, *Adv. Mater.* **2007**, *19*(2), 227-231

[9] Y. Shirota, *J. Mater. Chem.* **2005**, *15*(1), 75-93

[10] C. Chun, M.-J. Kim, D. Vak, D. Y. Kim, *J. Mater. Chem.* **2003**, *13*(12), 2904-2909

[11] T. Fuhrmann, T. Tsutsui, *Chem. Mater.* **1999**, *11*(8), 2226-2232

[12] E. Ishow, B. Lebon, Y. He, X. Wang, L. Bouteiller, L. Galmiche, K. Nakatani, *Chem. Mater.* **2006**, *18*(5), 1261-1267

[13] A. Stracke, J. H. Wendorff, D. Goldmann, D. Janietz, B. Stiller, *Adv. Mater.* **2000**, *12*(4), 282-285

[14] M.-J. Kim, E.-M. Seo, D. Vak, D.-Y. Kim, *Chem. Mat.* **2003**, *15*(21), 4021-4027

[15] H. Ando, T. Tanino, H. Nakano, Y. Shirota, *Mater. Chem. Phys.* **2009**, *113*(1), 376-381

[16] K. Kreger, P. Wolfer, H. Audorff, L. Kador, N. Stingelin-Stutzmann, P. Smith, H.-W. Schmidt, *J. Am. Chem. Soc.*, *132*(2), 509-516

[17] M. Jin, Q. X. Yang, R. Lu, T. H. Xu, Y. Y. Zhao, *J. Polym. Sci., Part A: Polym. Chem.* **2004**, *42*(17), 4237-4247

[18] L. Angiolini, T. Benelli, L. Giorgini, F. Mauriello, E. Salatelli, R. Bozio, A. Dauru, D. Pedron, *Eur. Polym. J.* **2007**, *43*(8), 3550-3561

[19] B. Sun, X. Zhu, J. Zhu, Z. Cheng, Z. Zhang, *Macromol. Chem. Phys.* **2007**, *208*(10), 1101-1109

[20] J. Wang, L. Zhang, Y. Niu, Z. Liang, Y. Chen, Y. Huang, H. Wang, W. Lin, *Polym. Int.* **2003**, *52*(7), 1165-1168

[21] S. Wu, F. Zeng, S. Yao, Z. Tong, W. She, D. Luo, *Macromolecules* **2003**, *36*(25), 9292-9294

[22] T. Fukuda, J. Y. Kim, D. Barada, T. Senzaki, K. Yase, *J. Photochem. Photobiol., A* **2006**, *182*(3), 262-268

[23] Z. Zhang, Y. Hu, Y. Luo, Q. Zhang, W. Huang, G. Zou, *Opt. Commun.* **2009**, *282*(16), 3282-3285

[24] T. Fukuda, J. Y. Kim, D. Barada, K. Yase, *J. Photochem. Photobiol., A* **2006**, *183*(3), 273-279

[25] C. Cojocariu, P. Rochon, *Macromolecules* **2005**, *38*(23), 9526-9538

[26] Z. Zheng, L. Wang, Z. Su, J. Xu, J. Yang, Q. Zhang, *J. Photochem. Photobiol., A* **2007**, *185*(2-3), 338-344

[27] H. Wang, Y. Huang, Z. Liu, F. Zhao, W. Lin, J. Wang, Z. Liang, *Appl. Phys. Lett.* **2003**, *82*(20), 3394-3396

[28] X. Meng, A. Natansohn, P. Rochon, *Polymer* **1997**, *38*(11), 2677-2682

[29] R. Walker, H. Audorff, L. Kador, H.-W. Schmidt, *Adv. Funct. Mater.* **2009**, *19*(16), 2630-2638

[30] H. Audorff, R. Walker, L. Kador, H.-W. Schmidt, *submitted to Chem.--Eur. J.*

[31] K. Kreger, P. Wolfer, H. Audorff, L. Kador, N. Stingelin-Stutzmann, P. Smith, H.-W. Schmidt, *J. Am. Chem. Soc.* **2010**, *132*(2), 509-516

Acknowledgements

Financial support by the German Science Foundation (DFG) within the framework of the Collaborative Research Centre (SFB 481) is gratefully acknowledged. The authors thank Dr. Klaus Kreger for many helpful discussions and Christina Löffler for her assistance in the preparation of the utilized compounds.

Supplemental information

Methods

All starting materials not specifically mentioned were commercially available and were used without further purification. Dry toluene was refluxed over potassium. All synthesized compounds were identified by ^{1}H-NMR spectroscopy with a BRUKER AC250 spectrometer (250 MHz). To confirm purity, SEC measurements were employed utilizing a WATERS model 515 HPLC-pump with a UV-detector at 254 nm (WATERS model 486) and a Differential RI-detector (WATERS model 410). The column set-up consists of a guard column (PSS: SDV-gel; length 5 cm, diameter 0.8 cm, particle size 5 µm, pores size 100 Å) and two separation columns (PL: PL-gel; length 60 cm, diameter 0,8 cm, particle size 5µm, pores size 100 Å). Stabilized THF at a constant flow rate of 0.5 ml/min was used as eluent. Characterization of the thermal properties by DSC measurements with a PERKIN-ELMER DSC7 (standard heating rate: 10 K/min) using approx. 10 mg of the compounds in 40 µl pans. Verification of the data obtained from the DSC was done in an optical microscope with crossed polarizers (NIKON DIAPHOT 300) on a heating table (METTLER FP82 with METTLER FP 80 control unit). UV/Vis absorption spectra of the compounds were recorded in the range from 250 nm to 650 nm with HITACHI U-3000 spectral photometer. Elemental analysis was carried out with an EURO EA 3000 analyzer (HEKATECH). X-ray diffractograms were measured with a HUBER GUNIER-DIFFRAKTOMETER 6000 with a HUBER QUARZ-MONOCHROMATOR 611 and a Cu-anode ($CuK_{\alpha 1}$-radiation, λ = 1.54051 Å; SEIFERT x-ray generator), HUBER SMC 9000 stepping motor controller, HUBER HTC 9634 temperature controller.

Synthesis of the photochromic materials

General preparation method (GPM 1): Ester coupling of tris carboxylic acids

The corresponding tris carboxylic acid chloride (1 equiv.) is placed in a flame-dried Schlenck flask and dissolved in 150 ml toluene under argon atmosphere. A threefold molar excess of anhydrous triethylamine per acid chloride group and 1.1 equivalents of the corresponding azo compound for each acid chloride group are added. The dark red solution is stirred for 24 h under reflux at 110 °C. The solution is filtered, washed with additional toluene, and thereafter the solvent is distilled off. The crude product is solved in THF and precipitated in EtOH. The precipitate is filtered with a frit and dried in high-vacuum. Remaining impurities are removed by a second precipitation in EtOH.

Materials

4,4',4''-Tris [4-carbo(2-methyl-4-((4-(phenylazo)phenyl)azo)phenoxyphenyl]-amine **1**:

4,4',4''-Tris-[(4-carboxylchloride)phenyl]amine (1.00 g, 2.3 mmol) is coupled with (2-Methyl-4-((4-(phenylazo)phenyl)azo)phenol (2.40 g, 7.6 mmol) according to GPM 1 yielding 1.61 g (55 %) of the title compound as orange powder. ^{1}H-NMR (250°MHz, $CDCl_3$, δ): 2.40 (s, 9H, CH_3), 7.32 (d, *J* = 3°Hz, 6H, Ar-H), 7.34 (d, *J* = 3°Hz, 3H, Ar-H), 7.49-7.56 (m, 9H, Ar-H), 7.89-7.94 (m, 6H, Ar-H), 7.95 (dd, *J* = 3°Hz, *J* = 1°Hz, 3H, Ar-H), 7.96 (d, *J* = 3°Hz, 3H, Ar-H), 8.07-8.11 (m, 12H, Ar-H), 8.22 (d, *J* = 3°Hz, 6H, Ar-H), elem. anal. calcd. for $C_{78}H_{57}N_{13}O_6$: C 73.63, H 4.52, N 14.31; found: C 73.13, H 4.44, N 14.15.

4,4',4''-Tris [4-carbo(4-(4-((4-methoxy)phenylazo)phenyl)azo)phenoxyphenyl]-amine **2**:

4,4',4''-Tris-[(4-carboxylchloride)phenyl]amine (0.22 g, 0.5 mmol) is coupled with 4-(4-((4-Methoxy)phenylazo)phenyl)azophenol (0.57 g, 1.7 mmol) according to GPM 1 yielding 0.35 g (53 %) of the title compound as orange powder. ^{1}H-NMR (250°MHz, $CDCl_3$, δ): 3.94 (s, 9H, CH_3), 7.06 (d, *J* = 3°Hz, 6H, Ar-H), 7.32 (d, *J* = 3°Hz, 3H, Ar-H), 7.44 (d, *J* = 3°Hz, 6H, Ar-H), 8.00 (d, *J* = 3°Hz, 6H, Ar-H), 8.04-8.11 (m, 18H, Ar-H), 8.24 (d, *J* = 3°Hz, 6H, Ar-H), elem. anal. calcd. for $C_{78}H_{57}N_{13}O_9$: C 70.95, H 4.35, N 13.79; found: C 70.99, H 4.80, N 14.41.

Film preparation

Samples for the holographic experiments were prepared by spin-coating a filtered 2 wt.-% $CHCl_3$ solution containing the photochromic material and the polymer in their respective contents at 1000 rpm for 60s onto a commercially available glass slide. The films were dried at 70 °C for 4 hours to remove residual solvent. The film thickness of the different samples were determined with a Dektak (Veeco 3300ST auto remote control stage profiler) and varied from 200 nm to 300 nm. All samples showed good optical properties and absence of light scattering.

Holographic Setup

A typical holographic set-up was used for the experiments. The gratings were inscribed with the blue-green line (488 nm) of an Argon-ion-laser. A beam splitter generates two coherent beams which are superimposed in the plane of the sample. Their diameter was about 1.4 mm; the intensity of each beam was adjusted to 1 W/cm². The state of polarization of each writing beam was adjusted separately by $\lambda/2$ or $\lambda/4$ plates. The angles of incidence with respect to the surface normal are ±14°, resulting in a grating period of 1 μm. A laser diode at 685 nm, which is outside the absorption band of the azobenzene moiety, was used for monitoring the diffraction efficiency *in situ* without affecting the writing process. The power of the transmitted and the diffracted beam was measured with two photodiodes, whose signals yield the diffraction efficiency. For improving the signal-to-noise ratio, the laser diode was modulated at 10 kHz and lock-in detection was used.

LIST OF PUBLICATIONS AND PRESENTATIONS

Publications and manuscripts of this thesis

1. Walker, R.; Audorff, H.; Kador, L.; Schmidt, H.-W., *Synthesis and Structure–Property Relations of a Series of Photochromic Molecular Glasses for Controlled and Efficient Formation of Surface Relief Nanostructures*, ***Adv. Funct. Mater.***, *19*(16), 2630-2638 (2009)

2. Audorff, H.; Walker, R.; Kador, L.; Schmidt, H.-W., *Polarization Dependence of the Formation of Surface Relief Gratings in Azobenzene-Containing Molecular Glasses*, ***J. Phys. Chem. B***, *113*(11), 3379-3384 (2009)

3. Audorff, H.; Walker, R.; Kador, L.; Schmidt, H.-W., Holographic investigations of azobenzene-containing low molecular weight compounds in pure materials and binary blends with polystyrene, ***submitted to Chem. – Eur. J.***

4. Walker, R.; Audorff, H.; Kador, L.; Schmidt, H.-W., *Improving the Holographic Recording Sensitivity of Photoaddressable Azobenzene-Containing Polymers with Photochromic Molecular glasses*, ***intended for Adv. Mater.***

5. Walker, R.; Audorff, H.; Kador, L.; Schmidt, H.-W., *Stable Holographic Volume Gratings with Novel Photochromic Bisazobenzene-Based Low Molecular Weight Compounds,* ***intended for Chem. Mater.***

Book chapters

Audorff, H.; Kreger, K.; Walker, R.; Haarer, D.; Kador, L.; Schmidt, H.-W., *Holographic Gratings and Data Storage in Azobenzene-Containing Block copolymers and Molecular Glasses*, ***Advances in Polymer Science***, *228*, 59-121 (2010)

Additional publications

1. Lu, Y.; Mei, Y.; Walker, R.; Ballauff, M.; Drechsler, M., *"Nano-tree"-type Spherical Polymer Brushes as Templates for Metallic Nanoparticles*, ***Polymer***, *47*, 4985-4995 (2006)

2. Kreger, K.; Löffler, C.; Walker, R.; Wirth, N.; Bingemann, D.; Audorff, H.; Rössler, E.; Kador, L.; Schmidt, H.-W., *Dynamic Behavior of the Minority Phase of Photoaddressable Block Copolymers*, ***Macromol. Chem. Phys.***, *208*(14), 1530-1541 (2007)

3. Audorff, H.; Walker, R.; Kador, L.; Schmidt, H.-W., *Holographic Studies of Azobenzene-Containing Low-Molecular-Weight Organic Glasses*, ***Proc. of SPIE***, *7233*, 72330O (2009)

4. Walker, R.; Audorff, H.; Kador, L.; Schmidt, H.-W., *Optimization of Photochromic Response of Photoaddressable Polymers with Azobenzene-Containing Molecular Glasses*, ***Proc. of SPIE***, *7358*, 735803 (2009)

5. Walker, R.; Audorff, H.; Kador, L.; Schmidt, H.-W., *Blends of Azobenzene-Containing Polymers and Molecular Glasses as Stable Rewritable Holographic Storage Materials*, ***Proc. of SPIE***, *7619*, 76190H (2010)

6. Audorff, H.; Walker, R.; Kador, L.; Schmidt, H.-W., *Blends of Azobenzene-Containing Diblockcopolymers and Molecular Glasses for Holographic Data Storage*, ***Proc. of SPIE***, *7730*, 77300X (2010)

Contributed talks

1. *Optimization of Photochromic Response of Photoaddressable Polymers with Azobenzene-Containing Molecular Glasses*; SPIE Europe Optics + Opto-electronics 2009; Prague, Czech Republic; 20. – 23. April 2009

2. *Polymer Blends with Azobenzene-Containing Blockcopolymers and Azobenzene-Containing Molecular Glasses as Stable Rewritable Volume Holographic Media*; 8th International Conference on Advanced Polymers via Macromolecular Engineering; Dresden, Germany; 4. – 7. October 2009

3. *Blends of Azobenzene-Containing Polymers and Molecular Glasses as Stable Rewritable Holographic Storage Materials*; SPIE Photonics West 2010; San Francisco, United States of America; 23. - 28. January 2010

Poster contributions

1. *Photochromic Response of Photoaddressable Polymer Blends with Azobenzene-Containing Molecular Glasses*; Frontiers in Polymer Science 2009; Mainz, Germany; 7. – 9. June 2009

2. *Optimization of Photochromic Response of Photoaddressable Polymers with Azobenzene-Containing Molecular Glasses*; Bayreuther Polymer Symposium 2009; Bayreuth, Germany; 13. – 15. September 2009

3. *Photochromic Azobenzene-Containing Molecular Glasses*; Closing Symposium of SFB 481; Weingarten, Germany; 10. – 11. June 2010

4. *Controlled and Efficient Formation of Surface Relief Gratings in Novel Azobenzene-Containing Molecular Glasses*; 3rd EuCheMS Chemistry Congress 2010; Nuremberg, Germany; 29. August – 2. September 2010

DANKSAGUNG

Als aller Erstes möchte ich meinem Doktorvater Herrn Prof. Dr. Hans-Werner Schmidt aufs aller Herzlichste danken! Für ein äusserst interessantes und gleichzeitig anwendungsbezogenes Arbeitsthema, für die Bereitstellung eines gut sortierten Arbeitsplatzes und für die Möglichkeit, dort meine Forschung zu verrichten. Darüber hinaus für sein Vertrauen, dass es mir erlaubte eigene Ideen und Herangehensweisen zu verwirklichen. Und zum Schluss natürlich für die Unterstützung und Motivation, die er mir bei der Durchführung dieser Arbeit zukommen lies und für die zahlreichen wissenschaftlichen Diskussionen, von denen ich viel lernen und profitieren konnte.

Besonderer Dank gilt Herrn Dr. Klaus Kreger, der mir zunächst bei meiner Diplomarbeit mit Rat und Tat zur Seite stand, und später während der Durchführung meiner Doktorarbeit ein immer hilfsbereiter Ansprechpartner war. Besonders gewinnbringend für mich waren seine konstruktive Kritik, sowie sein tatkräftiges und unermüdliches Engagement bei der Korrektur meiner Manuskripte.

Ebenfalls besonderer Dank geht an meine Kooperationspartner am „Bayreuther Institut für Makromolekülforschung“ für die enge und sehr erfolgreiche Zusammenarbeit. Ich danke Herrn Prof. Dr. Lothar Kador, den ich als freundlichen und stets hilfsbereiten Menschen kennenlernen durfte, für die Bereitstellung der benötigten Gerätschaften und seine zahlreichen Anregungen in wissenschaftlichen Diskussionen.

Aufs aller Herzlichste möchte ich Herrn Hubert Audorff danken, ohne den diese Arbeit in ihrer jetzigen Form gar nicht möglich gewesen wäre. Danke für die Durchführung aller holographischen Messungen, für alle physikalischen Berechnungen und für die unzähligen Diskussionen über Experimente, Manuskripte und Materialien. In der gemeinsamen Arbeit mit Hubert hat sich für mich deutlich gezeigt, welches Potential sich aus einer Zusammenarbeit zwischen Physikern und Chemikern entfalten kann, wenn sie nur ihre unterschiedlichen Sicht- und Herrangehensweisen gewinnbringend vereinen. Hubert, wir können stolz sein auf die Arbeit, die wir zusammen verrichtet haben!

Mein Dank geht an Frau Christina Löffler für ihre Hilfe mit den kleinen und größeren Problemen des Laboralltags und für ihre Unterstützung bei diversen Synthesen.

Für die Finanzierung dieser Arbeit danke ich der Deutschen Forschungsgemeinschaft (Sonderforschungsbereich 481), Teilprojekt B2 „Komplexe Makromolekül- und Hybrid-Systeme in inneren und äußeren Feldern“.

Ein grosser Dank geht auch an meine Laborkollegen, die mit ihrer offenen, freundlichen und lustigen Art, ein wunderbares und reibungsloses Zusammenarbeiten ermöglicht haben. Viel Glück für eure eigene Promotion!

Desweiteren danke ich allen Mitarbeitern des Lehrstuhls MC I für eine freundliche und angenehme Arbeitsathmosphäre und zudem für eine stets präsente Hilfsbereitschaft. Dankend hervorheben möchte ich unsere Sekretärin Frau Petra Weiss, ohne deren Hilfe ich mich in machen bürokratischen Wirrungen verstrickt hätte.

Ich danke auch den vielen Helfern der Universität Bayreuth, die doch so essentiell wichtig sind: die Glasbläser, die Werkstätten, die Poststelle, die Verwaltung, die Bibliotheken und natürlich die Mensa.

Während meines Studiums in Bayreuth habe ich hier viele Freunde und Bekannte gefunden, denen ich allen meinen tiefsten Dank für all die schönen gemeinsamen Stunden aussprechen möchte! Hier alle aufzuzählen würde jedoch den Rahmen dieser kleinen Danksagung sicherlich sprengen. Deshalb möchte ich mich darauf beschränken die Gründungsmitglieder der Chemiker Spass Gesellschaft CSG e.V. besonders hervorzuheben. Ihr habt mich hier so unglaublich nett aufgenommen und ich fühle mich Euch allen in tiefer Freundschaft verbunden. Meine damalige Entscheidung nach Bayreuth zu wechseln habe ich niemals bereut!

Zum Schluss möchte ich mich aufs Herzlichste bei den allerwichtigsten Personen in meinem Leben bedanken: meiner Familie! Vielen Dank, dass Ihr mir immer zur Seite standet, vielen Dank für Eure Liebe und vielen Dank für Eure bedingungslose Unterstützung! Ohne Euch wäre mein Studium und diese darausfolgende Arbeit nicht möglich gewesen.

Erklärung

Hiermit erkläre ich, daß ich die vorliegende Arbeit selbständig verfaßt und keine weiteren als die von mir angegebenen Quellen und Hilfsmittel benutzt habe.
Ferner erkläre ich, daß ich weder anderweitig mit oder ohne Erfolg versucht habe eine Dissertation einzureichen, noch mich einer Doktorprüfung zu unterziehen.

Bayreuth, den

Roland Walker